1. AGENCY USE ONLY (Leave blank)	2. REPORT DATE	3. REPORT TYPE AND DATES COVERED
	1992	THESIS/DISSERTATION

4. TITLE AND SUBTITLE
The Role of Conditional Symmetric Instability in the Development of Moderate To Heavy Frozen Precipitation Bands

5. FUNDING NUMBERS

6. AUTHOR(S)
Thomas Eugene Lambert, Captain

7. PERFORMING ORGANIZATION NAME(S) AND ADDRESS(ES)
AFIT Student Attending: Saint Louis University

8. PERFORMING ORGANIZATION REPORT NUMBER
AFIT/CI/CIA- 92-100

9. SPONSORING / MONITORING AGENCY NAME(S) AND ADDRESS(ES)
AFIT/CI
Wright-Patterson AFB OH 45433-6583

10. SPONSORING / MONITORING AGENCY REPORT NUMBER

11. SUPPLEMENTARY NOTES

12a. DISTRIBUTION / AVAILABILITY STATEMENT
Approved for Public Release IAW 190-1
Distributed Unlimited
ERNEST A. HAYGOOD, Captain, USAF
Executive Officer

12b. DISTRIBUTION CODE

13. ABSTRACT *(Maximum 200 words)*

14. SUBJECT TERMS	15. NUMBER OF PAGES 114
	16. PRICE CODE

17. SECURITY CLASSIFICATION OF REPORT	18. SECURITY CLASSIFICATION OF THIS PAGE	19. SECURITY CLASSIFICATION OF ABSTRACT	20. LIMITATION OF ABSTRACT

THE ROLE OF CONDITIONAL SYMMETRIC INSTABILITY IN THE DEVELOPMENT OF MODERATE TO HEAVY FROZEN PRECIPITATION BANDS

Thomas Eugene Lambert, B.S.

A Thesis Presented to the Faculty of the Graduate School of Saint Louis University in Partial Fulfillment of the Requirements for the Degree of Master of Science (Research)

1992

THE ROLE OF CONDITIONAL SYMMETRIC INSTABILITY IN THE DEVELOPMENT OF MODERATE TO HEAVY FROZEN PRECIPITATION BANDS

Thomas Eugene Lambert, B.S.

A Digest Presented to the Faculty of the Graduate School of Saint Louis University in Partial Fulfillment of the Requirements for the Degree of Master of Science (Research)

1992

DIGEST

The relationship between conditional symmetric instability (CSI), slantwise convection, and heavy frozen precipitation in winter type extratropical cyclones (ETCs) is analyzed for several cases where thunder and frozen precipitation were reported. Analysis of the atmosphere's vertical temperature, humidity, and wind field structure was used to identify areas of CSI and the atmospheric conditions that may serve as precursors to the development of CSI. Vertical cross sections showing areas of CSI were used to provide insight into when and where slantwise convection could be expected.

A correlation was found between vertical motion, vertical wind shear, the equivalent potential temperature (theta-e) field, and areas of CSI, slantwise convection, and heavy frozen precipitation. Regions of moderate to strong upward vertical motion, strong vertical wind shear, and small increases or even decreases in theta-e with height are the regions where CSI tends to develop in winter type ETCs. Areas of CSI were present in all cases where thunder and frozen precipitation were reported. CSI creates conditions favorable for the development of slantwise convection and the heavy frozen precipitation it sometimes produces.

Analysis was completed on two winter type ETCs that produced snow but no convection, to determine how the temperature and wind structure of these storms were different from the those that produced convection. It was found that these storms did not have any areas of CSI associated with them.

The cases in this study support the hypothesis that there is a direct relationship between areas of CSI, associated with winter type ETCs, slantwise convection, and the thunder and heavy frozen precipitation (usually snow) produced by the convection.

THE ROLE OF CONDITIONAL SYMMETRIC INSTABILITY IN THE DEVELOPMENT OF MODERATE TO HEAVY FROZEN PRECIPITATION BANDS

Thomas Eugene Lambert, B.S.

A Thesis Presented to the Faculty of the Graduate School of Saint Louis University in Partial Fulfillment of the Requirements for the Degree of Master of Science (Research)

1992

COMMITTEE IN CHARGE OF CANDIDACY:

Associate Professor James T. Moore,
Chairperson and Advisor

Professor Albert J. Pallmann

Professor Gandikota V. Rao

ACKNOWLEDGEMENTS

First, I would like to thank God who is the head of my life, for without him, none of this would be possible. I would like to express my deep appreciation to my friend and advisor, Dr. James T. Moore for his support, guidance, and encouragement during the completion of this thesis. I would also like to thank Dr. Gandikota V. Rao and Dr. Albert J. Pallmann for their assistance as members of my research committee. Also, I thank the United States Air Force for giving me the opportunity to attend graduate school. Thanks to Mike Crowder for his photographic support. A special thanks to fellow students: Tim, Mike, Chris, Andrea, and Sepi for all their support.

A final thanks goes to my wife, Suzanne, for without her support and understanding I would not have been able to complete this degree program.

TABLE OF CONTENTS

LIST OF FIGURES

1. INTRODUCTION

Every year heavy frozen precipitation (usually snow) produced by winter type extratropical cyclones (ETCs) paralyzes many regions of the United States including large urban areas. For example between the 13th and 16th of December 1987, a winter type ETC produced an extensive band of heavy snowfall (> 6 inches) from Texas to Michigan. Total snowfall accumulation was over 22 inches in some areas. At the peak of the storm, early morning on the 15th, much of northern and central Illinois experienced a combination of thunder, snow, sleet, and some freezing rain. The storm knocked out power to over 165,000 customers in the Chicago metropolitan area, shut down operations at O'Hare International Airport for several hours, and closed many primary and secondary roads. This is one example of the impact a strong winter type ETC and the convective frozen precipitation they may produce can have on an area.

1.1 Scientific Problem

A current problem in operational meteorology is forecasting the organization and intensity of precipitation associated with winter type extratropical cyclones (ETCs). This problem exists

because the precipitation bands often occur on the mesoscale and their intensity is affected by mesoscale processes, while the forecaster is constrained to use synoptic scale data to produce the forecast. Due to the limited data available, an operational meteorologist can only develop forecasting methods or guidelines based on synoptic scale data.

Heavy frozen precipitation may be associated with a type of mesoscale convection known as slantwise convection and may produce thunderstorms with snow often called thundersnow. This is convection that occurs in a slantwise direction, therefore it has both a vertical and a horizontal component. Analyzing the atmosphere for conditional symmetric instability (CSI) or conditional symmetric stability (CSS) is a method of determining its susceptibility to slantwise convection as demonstrated by Emanuel (1983a) and Sanders and Bosart (1985a). The scientific problem addressed in this thesis is to determine whether or not there is a relationship between the existence of CSI and the occurrence of slantwise convection. CSI and CSS are used when the atmosphere is assumed to be or actually is saturated with respect to water vapor. CSI can be determined using synoptic scale data and is related to vertical profiles of temperature,

humidity, and wind velocity. The temperature and humidity analysis is accomplished using the vertical profile of equivalent potential temperature (theta-e) and the wind velocity is analyzed using synoptic scale rawinsonde data. The terms symmetric instability or symmetric stability are used when determining the susceptibility of an unsaturated atmosphere to slantwise convection and vertical profiles of potential temperature (theta) are used for temperature and humidity analysis.

1.2 Research Objective

The objective of this thesis is to show that CSI, associated with winter ETCs, can be used to help identify when and where slantwise convection, and the thunder and heavy frozen precipitation (usually thundersnow) it produces, will occur. In an attempt to accomplish this objective, a comprehensive study of several winter type ETCs was made. The study included winter type ETCs that did and did not produce thunderstorms and heavy frozen precipitation. A comparison was made between the cases where there was convection (thunderstorms) and those cases where there was no convection, to determine if CSI was present and establish the role CSI plays in slantwise convection. In addition, an

attempt was made to identify atmospheric parameters such as areas of CSI or other diagnostic atmospheric parameters that can be used as a precursor to predict when and where the slantwise convection and heavy frozen precipitation will occur. Finally, an attempt was made to formulate quantitative criteria that need to be satisfied to identify areas where CSI and slantwise convection are likely to develop.

2. BACKGROUND LITERATURE

2.1 Background Information on Conditional Symmetric Instability (CSI)

The traditional Norwegian frontal model displays an organized, narrow line of showers associated with the cold front and a broad shield of relatively light precipitation ahead of the warm front. However, meteorologists often see mesoscale bands of precipitation associated with ETCs that do not fit this model. Sometimes these mesoscale bands of precipitation can be explained by local topographic effects or by secondary vertical circulations induced by frontogenetical zones. It has been suggested that sometimes the mesoscale precipitation may be the result of slantwise convection occurring in regions of conditional symmetric instability. Bennetts and Hoskins (1979) and Emanuel (1983a) allude to CSI as an explanation for precipitation band formation.

Symmetric stability or instability is the result of a combination of horizontal (inertial versus centrifugal) and vertical (buoyancy versus gravitational) forces. Although the atmosphere may be stable to both purely vertical and purely horizontal motions, it may be unstable to certain slantwise motion. The term, symmetric, comes from the fact that there is a compensating downward

slantwise motion in response to the upward slantwise motion. Bennetts and Hoskins (1979) showed that although there is a compensating downward slantwise motion, these downdrafts tend to be spread over a broader area and are weaker than the upward slantwise motions. To assess symmetric instability a parcel is forced both horizontally and vertically. The horizontal instability is based on inertial instability and is evaluated through investigation of accelerations that act on the parcel when it becomes displaced from its geostrophically balanced flow. As described in Holton (1979), consider the motion of an individual fluid parcel in a steady, geostrophically balanced, purely meridional flow, neglecting vertical motion and buoyancy effects. The simplifying assumption of a purely meridional flow was made to allow the geostrophically balanced flow to be oriented so that the positive y-direction was to the north and the positive x-direction was to the east. In the general case, for any given flow, the direction in which the base state flow (averaged over the 850-300 mb layer) moves is defined as the positive y-direction. This direction is parallel to the 850-300 mb thickness pattern. The x-direction is

defined as the direction normal to the base state flow. To determine the horizontal stability of the parcel, we evaluate whether the parcel will continue to be displaced (inertial or horizontal instability) or return to its original position (inertial or horizontal stability). Vertical stability can be viewed in the traditional manner using parcel theory. The parcel moves dry adiabatically if it is unsaturated with respect to water vapor or moist adiabatically if saturated. The parcel's temperature is then compared to that of the environment at any given point to determine if it is stable or unstable with respect to the environment. If the parcel temperature is greater than the environmental temperature, it is unstable and the displacement will continue. If the parcel temperature is less than the environmental temperature, it is stable and the parcel will return to its original position.

According to Lilly (1986), the process of evaluating the CSI of a parcel involves the determination of both the inertial (horizontal) and buoyant (vertical) stability of the parcel. To evaluate inertial stability a quantity called absolute momentum (M) must be defined. As noted in

Emanuel (1983a), a steady, geostrophically balanced flow is assumed and M is defined as:

$$M = Vg + fx = \text{environmental M value} \quad (1)$$

where Vg = environmental geostrophic wind, f = Coriolis parameter, and x = displacement in the x direction (normal to Vg). To further explain the evaluation of CSI some other parameters are defined as in Lilly (1986):

$$M' = v' + fx = \text{parcel M value} \quad (2)$$

where v' = parcel wind speed

$$M'' = M' - M \quad (3)$$

M'' = difference between the parcel M value and the environmental M value. It can be shown that:

$$du/dt = fM'' \quad (4)$$

Thus, if du/dt > 0 then the parcel acceleration is to the east. If du/dt < 0 then the parcel acceleration is to the west.

As described in Lilly (1986) the criteria for conditional symmetric instability (CSI) is:

$$\delta z/\delta x|_{\text{theta-e}} > \delta z/\delta x|_{M} \qquad (5)$$

SLOPE OF THE THETA-E SURFACES>SLOPE OF THE M SURFACES

If the theta-e surfaces are more vertical than the M surfaces then the atmosphere is conditionally symmetrically unstable.

The criteria for conditional symmetric stability (CSS) is:

$$\delta z/\delta x|_{\text{theta-e}} < \delta z/\delta x|_{M} \qquad (6)$$

SLOPE OF THE THETA-E SURFACES<SLOPE OF THE M SURFACES

If the theta-e surfaces are less vertical than the M surfaces then the atmosphere is conditionally symmetrically stable.

If the air is not saturated then potential temperature (theta) is used instead of equivalent potential temperature (theta-e) and a comparison is made between the slopes of the theta surfaces and the slopes of the M surfaces.

The criteria for symmetric instability in a steady, geostrophic, purely meridional flow is as follows:

$$\delta z/\delta x|_{theta} > \delta z/\delta x|_{M} \qquad (7)$$

SLOPE OF THE THETA SURFACES > SLOPE OF THE M SURFACES

The criteria for symmetric stability for the conditions listed previously is as follows:

$$\delta z/\delta x|_{theta} < \delta z/\delta x|_{M} \qquad (8)$$

SLOPE OF THE THETA SURFACES < SLOPE OF THE M SURFACES

Figure 1 is an illustration of CSI and CSS from Sanders and Bosart (1985a). It shows a schematic vertical cross section normal to a steady geostrophically balanced flow. This means the cross section is also normal to the 850-300 mb thermal wind or the 850-300 mb thickness pattern. The speed of this flow, Vg, is chosen to increase with elevation and to be independent of x, the horizontal direction in the plane of the cross section. Also, it is assumed that the air is everywhere saturated. A stratification was chosen in which the equivalent potential temperature of the base state increases upward and thermal wind balance is assumed. For parcel A, a leftward displacement produces an excess of parcel absolute momentum (M') over the

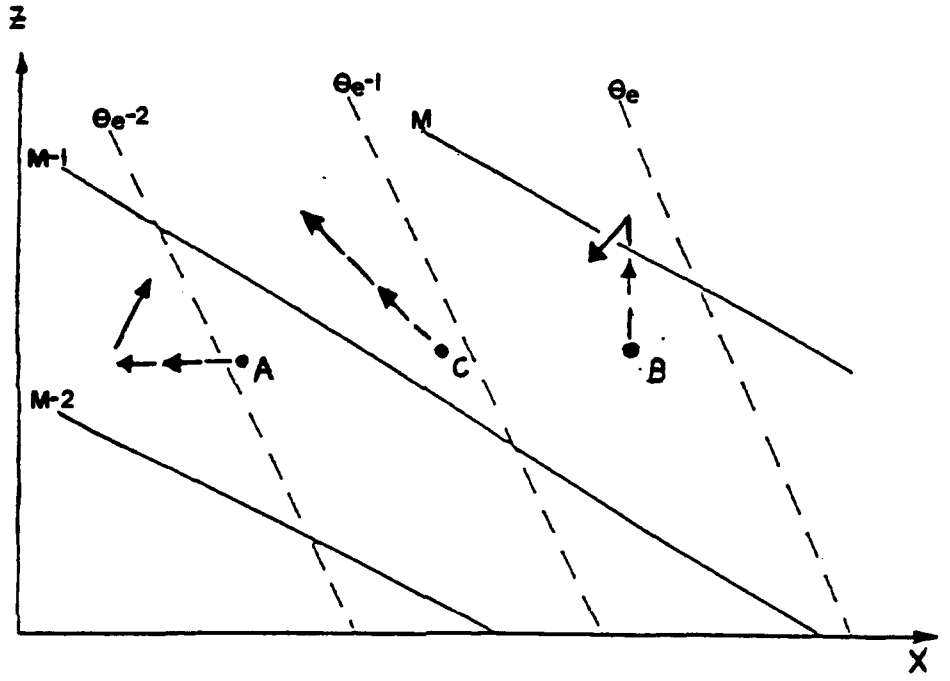

Fig. 1 Schematic vertical cross section of equivalent potential temperature and absolute momentum illustrating conditional symmetric instability. Isopleths of absolute momentum of the basic flow, M, are solid lines. Dashed lines represent equivalent potential temperature (θ_e). Dashed lines from lettered points show parcel displacements and accelerations (adapted from Sanders and Bosart (1985a)).

environmental absolute momentum (M). Therefore M'' = M' - M is > 0 and from (4) du/dt > 0. The horizontal acceleration is to the right, and acts to restore the parcel to its initial position. In this case the displaced parcel is positively buoyant since theta-e' > theta-e where theta-e' is the equivalent potential temperature of the parcel and theta-e is the equivalent potential temperature of the environment. The resulting upward acceleration does not mitigate the horizontal acceleration to the right and does not continue upward because the atmosphere is convectively stable, theta-e increases with height. The parcel will eventually return to its point of origin.

The illustration for parcel B also shows vertical stability. For the displaced parcel, theta-e' < theta-e so the vertical component of acceleration is downward. In this case, M'' < 0 and from (4) du/dt < 0 so the horizontal acceleration of the parcel is to the left. However, the horizontal acceleration does not affect the stable downward acceleration, and the horizontal acceleration quickly lessens since the fluid is inertially stable. As the parcel moves to the left there will be an acceleration to the right as the parcel's absolute momentum (M') will be greater than the environmental absolute momentum (M). So the downward motion is

opposite to its initial impulse and the inertially stable environment will eventually force parcel B back to its original position and therefore parcel B is stable.

Parcel C is given an initial acceleration to the left and up. The displacement has a slope between the M and theta-e isopleths. In this case theta-e' > theta-e and therefore the parcel accelerates upward, the same vertical direction as its initial displacement. Also M' < M, therefore according to (4) du/dt < 0, so the parcel accelerates in the same horizontal direction as its initial displacement. The slantwise displacement of parcel C in this case is unstable. Once the acceleration is initiated it will continue. From this case, we see that slantwise convection requires the slope of the theta-e surfaces to be greater (more vertical) than the slope of the M surfaces as described in (5). Emanuel (1983b) described CSI this way: if there are areas where following the M surface upward, the equivalent potential temperature decreases in a saturated environment then potential slantwise instability exists. In cases where the air is not saturated, theta is used in place of theta-e and the terms used to describe the stability or instability are symmetric stability or symmetric instability, respectively. For the atmosphere to be symmetrically

unstable the slope of the theta surfaces must be greater (more vertical) than the slope of the M surfaces, as described in (7).

Martin et al. (1991) used a different equation to define CSI or CSS. This definition begins with an expression for equivalent potential vorticity as follows:

$$EPV \approx -\eta \cdot \text{grad}\theta_e \qquad (9)$$

where η = 3-D absolute vorticity vector, grad is the gradient operator in x,y,p coordinates. Neglecting y-variations and the contributions to absolute vorticity from terms involving omega = dp/dt and using M as defined previously, the following equation can be obtained:

$$EPV = ((\delta M/\delta p \ \delta\theta_e/\delta x) - (\delta M/\delta x \ \delta\theta_e/\delta p)) \qquad (10)$$

EPV can be used as a diagnostic tool to analyze areas of CSI. Areas where EPV values are < 0 indicate areas of CSI and areas where EPV values are > 0 indicate areas of CSS. This will be explained in more detail in section 3.3.4 of this thesis.

2.2 Literature Review

Sanders and Bosart (1985a) studied a cyclone moving northeastward off the coast of the northeastern United States on 11-12 February 1983. This storm produced a band of heavy snow (up to 64 cm) from Washington D.C. to Boston. Frontogenetical forcing and conditional symmetric instability were discussed as possible explanations for the intense precipitation. Rawinsonde data was used to analyze the conditional symmetric instability of the storm. It was concluded that an updraft associated with the storm over Dulles International Airport was a concentrated response to large-scale frontogenetical forcing and low conditional symmetric stability over the area.

Moore and Blakley (1988) studied a low pressure system that moved through the lower Mississippi Valley and into western Tennessee from 30-31 January 1982. Embedded convection associated with this system occurred over east-central Missouri and west-central Illinois including the St. Louis Metropolitan area producing a narrow band with snow totals over 25 cm. Frontogenetical forcing together with CSI were discussed as possible physical explanations for the intense precipitation. Using rawinsonde data to calculate vertical cross sections of absolute

momentum (M) and equivalent potential temperature, it was determined that CSI existed in the low and middle levels over the cold frontal zone in central Illinois in the region of the updraft of a direct thermal circulation. This region of CSI and the associated slantwise convection is believed to have increased the intensity of the updraft and decreased the scale of the phenomena, contributing to the heavy snowfall.

Gyakum (1987) studied a modest (generally < 1 cm melted), yet, unforecast snowfall that occurred on 10 December 1982 in a mesoscale band (50 to 200 km wide) from the Ohio Valley states eastward to western New York. The precipitation was not associated with a surface cyclone or an obvious surface front. The CSI of the regions where there was snowfall was assessed. Neutral or unstable conditions existed through a deep layer in an area nearly coincident with the cloud and precipitation bands from Green Bay to Nashville. An area of CSI over and to the north of Buffalo corresponded well to the easternmost section of the precipitation band. This study showed the importance of CSI to precipitation evolution in a synoptically weak environment.

Rueter and Yau (1990) studied seven precipitation bands during the Canadian Atlantic Storms Program (CASP) to assess the importance of CSI and slantwise convection in producing precipitation.

The atmosphere was shown to contain shallow layers of air that had slight CSI and were susceptible to slantwise convection, particularly in areas of pronounced vertical wind shear. In the lower part of the atmosphere it appeared that CSI was often released leading to heavy precipitation which was sometimes organized into multiple bands. The results showed that there appeared to be a relationship between the formation of multiple precipitation bands, CSI, and slantwise convection. Their observations were inadequate to allow a clear distinction between slantwise convection and the response of the atmosphere to baroclinic and frontogenetical forcing.

Martin et al. (1991) studied a rainband of moderate intensity, which occurred on 26 January 1986 over the eastern Carolinas. They evaluated the CSI of the atmosphere in the area of the rainband using equivalent potential vorticity (EPV). They concluded that the rainband formed in the updraft portion of a thermodynamically direct vertical circulation about an upper-level frontal zone in an area of CSI. The release of CSI is presumed to have been responsible for the dimensions of the mesoscale precipitation band which was 20-40 km wide and its orientation was parallel to the vertical wind shear vector.

Scofield and Robinson (1990) studied two snow events, 15 December 1989 and 14-15 December 1987. In this paper the term instability burst (IB) is used and defined as a thrust of maximum atmospheric destabilization into an area. One of the causes of the IB is related to the 850 or 700 mb theta-e advection pattern and this will be evaluated for several cases in this thesis. The role of the 850 and 700 mb theta-e advection will be explained in more detail later in this section. It was stated that the instability burst (IB) is one of the primary mechanisms for producing heavy precipitation. IB's are best detected using a combination of satellite imagery, instability analysis, and numerical model forecasts. IB's are identified as developing subsynoptic scale wave patterns, baroclinic leaf type patterns or convective cloud areas or bands embedded in the ETC cloud pattern. Scofield and Robinson explained how the 850 mb equivalent potential temperature advection and satellite imagery can be used to analyze and NOWCAST heavy snow. It is the advection of equivalent potential temperature that will affect the CSI of an area and relates this method of analysis to what is described in this thesis. Scofield and Robinson state that heavy snow can be expected with the following positive 850 or

700 mb equivalent potential temperature advection patterns:

- Equivalent potential temperature advection ridge axes
- Near areas of maximum equivalent potential temperature advection
- Within areas of equivalent potential temperature advection gradients north of the ridge axis
- Occasionally, north of the ridge axis, but within areas of weaker equivalent potential temperature advection when an upper level system is passing over the area

Snow areas must then be adjusted using heavy snow signatures seen in the satellite imagery and lifting mechanisms shown by the models.

Beckman (1987) established general interpretation techniques which relate heavy snow areas (10 cm or more in 12 hours) to infrared (IR) and visible geostationary satellite imagery. He demonstrated how the satellite imagery can be used to formulate rules to aid in predicting development and progression of the heavy snow. Several factors such as the dynamic strength of the system, speed of movement, and structure of the moist layer control the total amount of snow that a storm produces. Convective clouds, especially with thunder, are

significant when moving into the snow threat area. Experience has shown that the three step analysis method developed by Beckman is a useful approach to assess the threat of heavy snow. This method brings together the latest observations, the current numerical guidance, and the latest satellite imagery to obtain the best estimate of the heavy snow threat. Once the initial threat is assessed, the forecaster, knowing the relationship between heavy snow and satellite imagery, can predict the future trends in heavy snow for the forecast period of interest. This procedure could be used in conjunction with an evaluation of CSI to improve forecasts of heavy snow associated with convection.

3. DATA PROCESSING AND PROCEDURES

The data processing and procedures (methodology) used to accomplish the objective of this thesis began with upper air and surface data from across the United States. An objective analysis was performed on the data to produce fields of gridded data for several parameters. The next step in the methodology was to use the analyzed data to calculate derived fields that allowed identification of areas of CSI. Fields of vertical motion (kinematic omegas), vertical wind shear, and absolute momentum (M) values were calculated over the areas of interest. Then, using vertical profiles of theta-e and absolute momentum, areas of CSI, which are also areas where EPV < 0, could be located. Surface observations were then used to determine if areas where CSI existed were also areas where slantwise convection occurred. The occurrence of slantwise convection was confirmed by observations of thunder and frozen precipitation. Completion of the entire methodology for several cases led to accomplishment of the research objective which was to show that CSI can be used to identify when and where slantwise convection, and

the associated thunder and heavy precipitation will develop.

3.1 Data Sets

At Saint Louis University, data from the standard daily rawinsonde network and surface observation stations across the United States, southern Canada, and northern Mexico were received from the Domestic Data Service Plus (DDS+) and stored on tape. Upper air data for 102 stations were collected with a station spacing of 400 km and 12 hour temporal separation. Height, temperature, dewpoint temperature, and u, v wind data were used at 50 mb increments from 900-100 mb to create objectively analyzed fields. Soundings created from this data were used to diagnose areas of stability and the vertical wind profile at a station. An isentropic data set was created from the pressure coordinate data set using Duquet's (1964) method to compute those parameters required for isentropic analysis. Sounding data were vertically interpolated to potential temperature levels from 270 K to 370 K with a 2 K interval.

The surface data consist of approximately 624 stations with a station spacing of 150 km and 1 hour temporal separation. Temperature, dewpoint

temperature, pressure, and u, v wind components were used to create objectively analyzed fields.

Satellite imagery was provided by Dr. Roderick Scofield of the National Environmental Satellite Data and Information Service (NESDIS) and was used to depict regions of cloudiness, precipitation, storm intensity and propagation.

3.2 Objective Analysis

To prepare the objective analysis fields for this study the Barnes (1973) technique was utilized for surface and upper air data. Upper air objectively analyzed fields of u, v, temperature, dewpoint temperature, potential temperature, and equivalent potential temperature were interpolated to a 27 X 18 grid with a 190.5 km grid spacing at 17 levels, covering the same area as the rawinsonde network. Barnes parameters of c = 82000.0 km^2 and gamma = 0.20 were used to resolve 37% of the 2-delta waves of 800 km.

For the surface, objectively analyzed fields of temperature, dewpoint temperature, u, v, and potential temperature were interpolated to a 53 x 35 grid with 95.25 km spacing utilizing the Barnes (1973) objective analysis scheme.

For the surface, Barnes parameters of c = 22,000 km^2 and gamma = .4 were used to resolve 27% of the 2-delta waves of 500 km.

3.3 Computational Procedures

3.3.1 Vertical Motion

The vertical motion was computed on pressure surfaces using the kinematic method, which is based on the integration of the continuity equation in the vertical (Holton, 1979, p. 72). There are several advantages to the kinematic method, but the major disadvantage arises from using the observed winds to calculate divergence. A small error in the wind components can cause a large error in the horizontal divergence fields (Holton, 1979, p.73). These errors can accumulate in the vertical as the horizontal divergence is integrated. The O'Brien (1970) linear adjustment scheme is used to correct the errors and adjust the vertical motion pattern to predetermined values (set = 0) at the boundaries of the atmosphere (surface and 100 mb). The divergence is computed on pressure surfaces 50 mb apart, from 900 mb to 100 mb. The grid is the same as the one used for the isentropic surfaces, as are the Barnes parameters.

3.3.2 Vertical Wind Shear

The vertical wind shear is computed at each station where there is sounding data available. Weisman and Klemp (1986) used an algorithm that sums up the density weighted u and v wind components for each level from the surface to 500 m above the surface and from the surface to 6000 m above the surface. The linearized shear is equal to the difference between the resultant mean wind vectors over the two layers divided by the vertical distance of 5500 m. This provides an indication of the strength of the wind shear in the lower portion of the atmosphere which is also where CSI is most often found.

3.3.3 Absolute Momentum

To begin the definition of absolute momentum (M) we assume a water vapor saturated steady, geostrophically balanced, purely meridional flow. Following Emanuel (1983a) we consider the disposition of a parcel of air which is initially at rest at z = 0. The stability of this parcel will be examined after it has been displaced a finite distance in the x-z plane. Perturbation pressure

forces and turbulent mixing of the parcel with the environment will be neglected. This creates negligible errors in the calculation of absolute momentum because these effects are important on scales of motion several orders of magnitude smaller than those examined in this thesis. Under the conditions previously described, it can be shown that the quantity M, where M = Vg + fx, is conserved following the motion of the parcel. In this thesis absolute momentum was calculated in the following manner. Objectively analyzed fields of u and v wind, temperature, dewpoint temperature, potential temperature, and equivalent potential temperature were produced from rawinsonde data interpolated to a 27 X 18 grid at 17 levels using the Barnes (1973) objective analysis technique. Rawinsonde data was used to calculate the 850-300 mb thickness pattern for the area of interest. Then the location for the vertical cross section was chosen so that it was normal to the 850-300 mb pattern and passed through the area of interest. In all the cases in this thesis the origin of the vertical cross section was the northwestern most point of the cross section and the values of x increased to the southeast. The origin for each cross section was chosen such that the cross section was normal to the flow (averaged over the 850-300 mb layer) and passed through the

area of interest for each case. The areas of interest for this study were regions where heavy frozen precipitation (usually snow) and convection occurred. Determination of whether convection occurred or not was based on surface observations of thunder. To calculate values of M along the vertical cross section the gridded u and v wind data were interpolated in the vertical to specific pressure levels used by the program that plots the vertical cross section of M. Then the wind data were interpolated horizontally to the cross section and values of M were calculated at 20 points along the cross section on 21 different levels, creating a 20 X 21 grid in the x-z plane along the cross section chosen.

3.3.4 Conditional Symmetric Instability (CSI) and Equivalent Potential Vorticity (EPV)

The conditional symmetric instability of the atmosphere involves a combination of horizontal (inertial versus centrifugal) and vertical (buoyancy versus gravitational) forces. To access conditional symmetric instability the parcel must be forced both horizontally and vertically. The horizontal stability of the parcel is evaluated by the quantity absolute momentum (M) described in (1). In the case

of CSI the vertical stability is determined using equivalent potential temperature. The determination of the CSI of the atmosphere involves both M and equivalent potential temperature. The procedure for calculating the vertical profile of M was explained previously. The procedure to calculate the vertical profile of the equivalent potential temperature requires some additional explanation. The process is very similar to that described for M except that values of the equivalent potential temperature are used instead of M. The equivalent potential temperature values are interpolated from the grid to the cross section using the same procedures used for M. This yields a vertical profile of the equivalent potential temperature along the cross section chosen. The equivalent potential temperature profile is plotted along with the M profile on a single cross section.

The analysis of the CSI of the atmosphere along the vertical cross section is determined by the relative slopes of the equivalent potential temperature and the M surfaces. If the slopes of the equivalent potential temperature surfaces are greater (more vertical) than the slopes of the M surfaces in an area, then that area is conditionally symmetrically unstable as shown in (5). If the slopes of the equivalent potential temperature

surfaces are less (more horizontal) than the slopes of the M surfaces, then that area is conditionally symmetrically stable.

If the air is not saturated then potential temperature is used instead of equivalent potential temperature. The atmosphere is said to be symmetrically unstable if the slopes of the potential temperature surfaces are greater than the slope of the M surface and symmetrically stable if the slopes of the potential temperature surfaces are less than the slopes of the M surfaces. This is shown in (7) and (8), respectively.

Martin et al. (1991) defined the quantity Equivalent Potential Vorticity (EPV) as described in (10). EPV is a very effective tool to use when analyzing the conditional symmetric instability (CSI) or conditional symmetric stability (CSS) of the atmosphere. EPV will be defined in this thesis as follows:

$$EPV = g\,((\delta M/\delta p\ \ \delta\theta_e/\delta x) - (\delta M/\delta x\ \ \delta\theta_e/\delta p)) \qquad (12)$$

term A term B term C term D

term 1 = term A x term B term 2 = term C x term D

where g = gravity = 9.806 m s^{-2}. The equation is multiplied by g so that the units of EPV will be the same as potential vorticity units (PVU) in the SI (unit system), 1 X 10^{-6} m^2 K s^{-1} kg^{-1}. EPV can be

used to determine if CSI exists in an area. If EPV <0 then the atmosphere is conditionally symmetrically unstable. If EPV >0 then the atmosphere is conditionally symmetrically stable. A term by term explanation of (12) will help explain the relationship between EPV to CSI. Term 1 is defined as term A multiplied by term B and term 2 is defined as term C multiplied by term D.

Term A represents the change in absolute momentum with pressure and is generally < 0 below the level of the jet stream. From (1) we see that M is directly proportional to Vg, and under normal atmospheric conditions Vg increases as pressure decreases up to the jet stream level. It follows that term A will be < 0 below the jet stream under these conditions. As the vertical wind shear increases, due to increasing Vg with height, term A will become smaller (more negative) and the slopes of the M surfaces will decrease (M surfaces become more horizontal). This increases the opportunity for CSI because CSI exists in areas where the slope of equivalent potential temperature surfaces are greater (more vertical) than M surfaces.

Term B is generally > 0 as a result of the definition of M, where M = Vg + fx and x is defined as the displacement in the x direction (normal to Vg). This requires that the cross section must be

taken normal to the geostrophic wind which means it is normal to the 850-300 mb thickness pattern and the thermal wind pattern. This creates cross sections where the positive x direction points toward warmer air and since equivalent potential temperature surfaces slope down toward warmer air term B will be > 0. Therefore, the net result of term A multiplied by term B will be a negative number made more negative by larger values of term B or smaller (more negative) values of term A.

The value of term C is usually > 0 for several reasons. Since M is defined as M = Vg + fx and the terms Vg and fx are the same order of magnitude, the value of fx will *increase* as x increases resulting in larger values of M and term C will be > 0. An exception to this would be if there was a very strong Vg decrease in the positive x direction. This may overpower the increase in M values caused by increasing values of fx and cause term C to become < 0. In most cases the gradient of Vg in the x direction is not strong to cause term C to be < 0.

Term D is a measure of the convective stability/instability of the atmosphere. If term D is < 0 the atmosphere is convectively stable. If term D = 0 the atmosphere is convectively neutral and if term D is > 0 the atmosphere is convectively unstable. The effect of term D on the value of EPV

is evaluated for each of the three alternatives listed above. In each case term 1 (term A multiplied by term B) is assumed to be negative and term C is assumed positive, this is usually true.

Case 1: term D < 0 , the atmosphere is convectively stable, making term 2 negative. When term 2 is subtracted from term 1 in (12) the net result is to increase the value of EPV and decrease chances for CSI.

Case 2: term D = 0, the atmosphere is convectively neutral. This results in term 2 = 0 and therefore term 2 doesn't affect the overall value of EPV.

Case 3: term D > 0, the atmosphere is convectively unstable. This results in term 2 being positive and when term 2 is subtracted from term 1 the net result is that EPV becomes more negative and increases chances for CSI.

3.4 Error Estimations

The calculation of values for vertical motion (kinematic omegas), vertical wind shear, and absolute momentum (M) are all derived from rawinsonde data. The rawinsonde data, however, is plagued by systematic and random errors. Belt and Fuelberg (1982) stated that objective analysis and

smoothing procedures (e.g. Barnes, 1973; O'Brien, 1970) reduce the effects of data errors, however, they do not remove the problem.

A statistical study to determine the effects of random rawinsonde data error on computational results was published by Belt and Fuelberg in 1982. This study showed that below 500 mb correlations between calculated values for vertical motion (kinematic omegas) using actual data and 10 cases of randomly perturbed data were generally above 0.95. In my thesis all kinematic omega values used were for levels at or below 500 mb. The same procedure used by Belt and Fuelberg (1982) to calculate kinematic omegas was used in this thesis. Therefore, there is a high degree of confidence that the vertical motion data used here is not affected significantly by random rawinsonde errors.

Another source of error in rawinsonde data is the drift of the rawinsonde balloon away from the station due to the horizontal winds encountered as the balloon rises. The drift error arises because the observational data from the balloon is assumed to be representative of the atmosphere directly over the launch site when the balloon is actually making measurements at some distance downstream from the launch site. A rawinsonde ascent rate of 5 m s^{-1} was assumed. The case with the greatest average

windspeed in the 850-300 mb layer was used to calculate a worst case scenario to determine how far downstream the balloon would have drifted by the time it reached the 300 mb level. The 300 mb level was chosen because data above this level was not important in this thesis. The horizontal distance between the launch site and the balloon when it reached 300 mb, in this worst case scenario, was 60 km. This error is within acceptable limits when using synoptic scale data with a station spacing of 400 km, as was done in this thesis.

Another source of error was in interpolation of values from grid points to the cross sections used in this thesis. Values of several quantities such as: absolute momentum, theta-e, CSI, and EPV were interpolated to the cross sections using a bilinear interpolation scheme. The interpolation created only small errors that resulted in only minor smoothing of the data.

4. RESULTS

4.1 Case 1: 15 December 1987

4.1.1 Synoptic Overview

A long wave trough developed over the southwestern United States and Mexico on 14 December 1987 (Fig. 2a). On 15 December the trough lifted out and began to move rapidly into the central plains and mid-Mississippi Valley (Fig. 2b).

At 1200 UTC 14 December 1987 there was a weak surface low centered over south-central Texas. This low moved rapidly to the northeast and by 0000 UTC 15 December 1987 was centered over central Arkansas and with a central pressure of 999 mb. A cold front extended southward from the low pressure center and passed through north central Louisiana then it passed just south of Galveston Bay and on to the southern tip of Texas. A warm front stretched from the low center across extreme northwest Tennessee and along the Tennessee, Kentucky border as shown in Fig. 3. During the next 12 hours the storm moved from Arkansas to northeastern Illinois and the low deepened 20 mb. The progression of the surface low is shown in Fig. 4. This storm produced heavy snow from Texas to Michigan (Fig. 5) and there were many

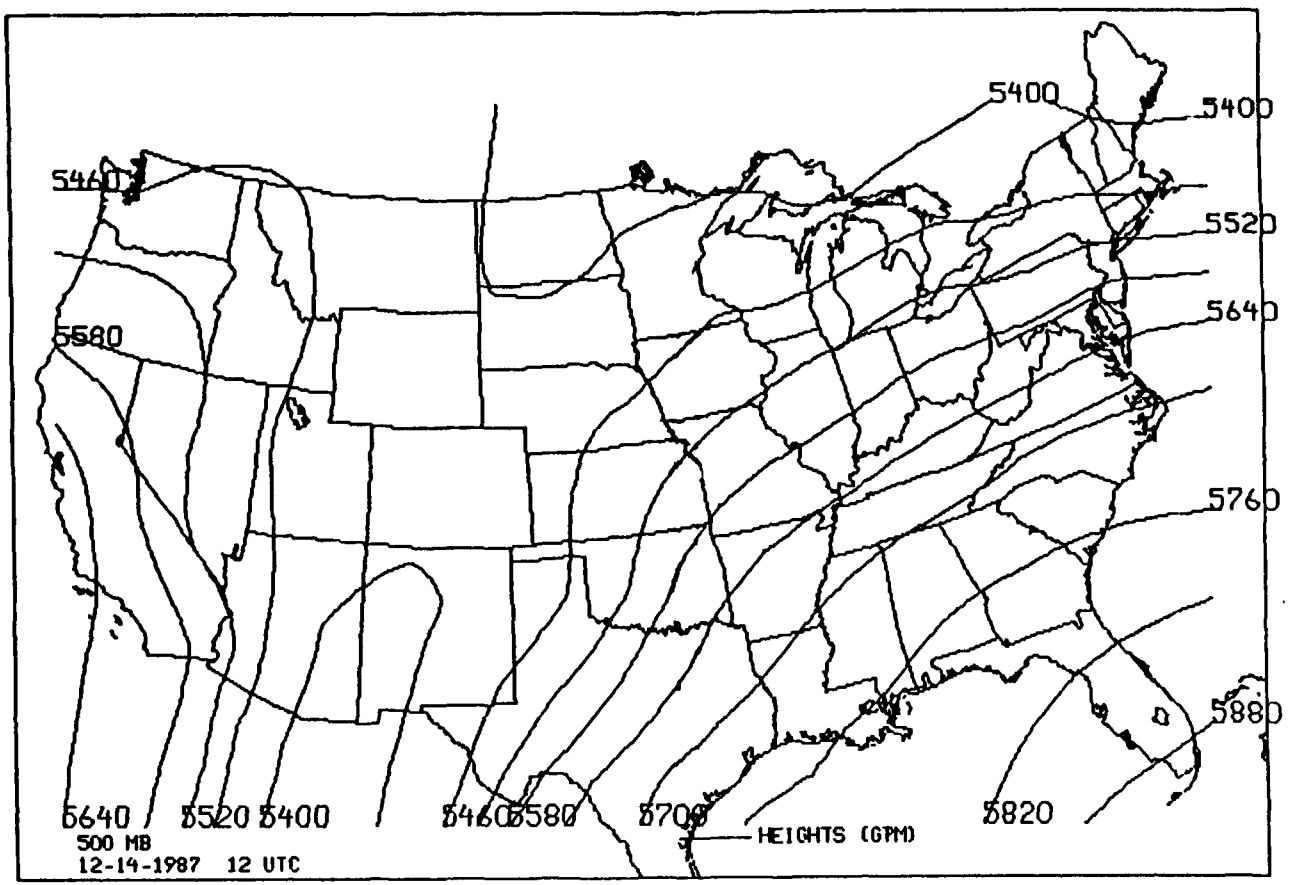

Fig. 2a 500 mb chart for 1200 UTC 14 December 1987. Height in geopotential meters (gpm).

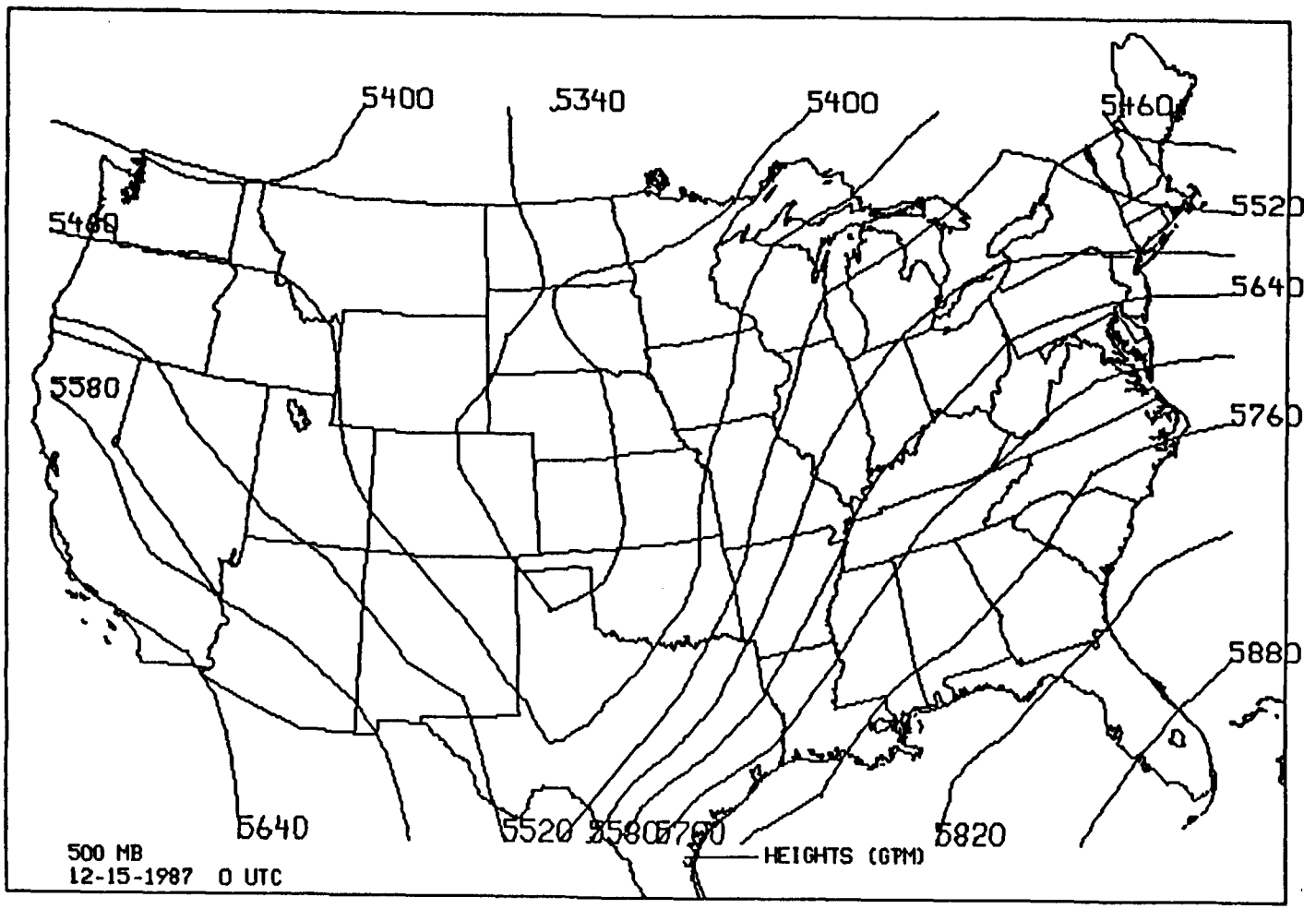

Fig. 2b Same as Fig. 2a, except for 0000 UTC 15 December 1987.

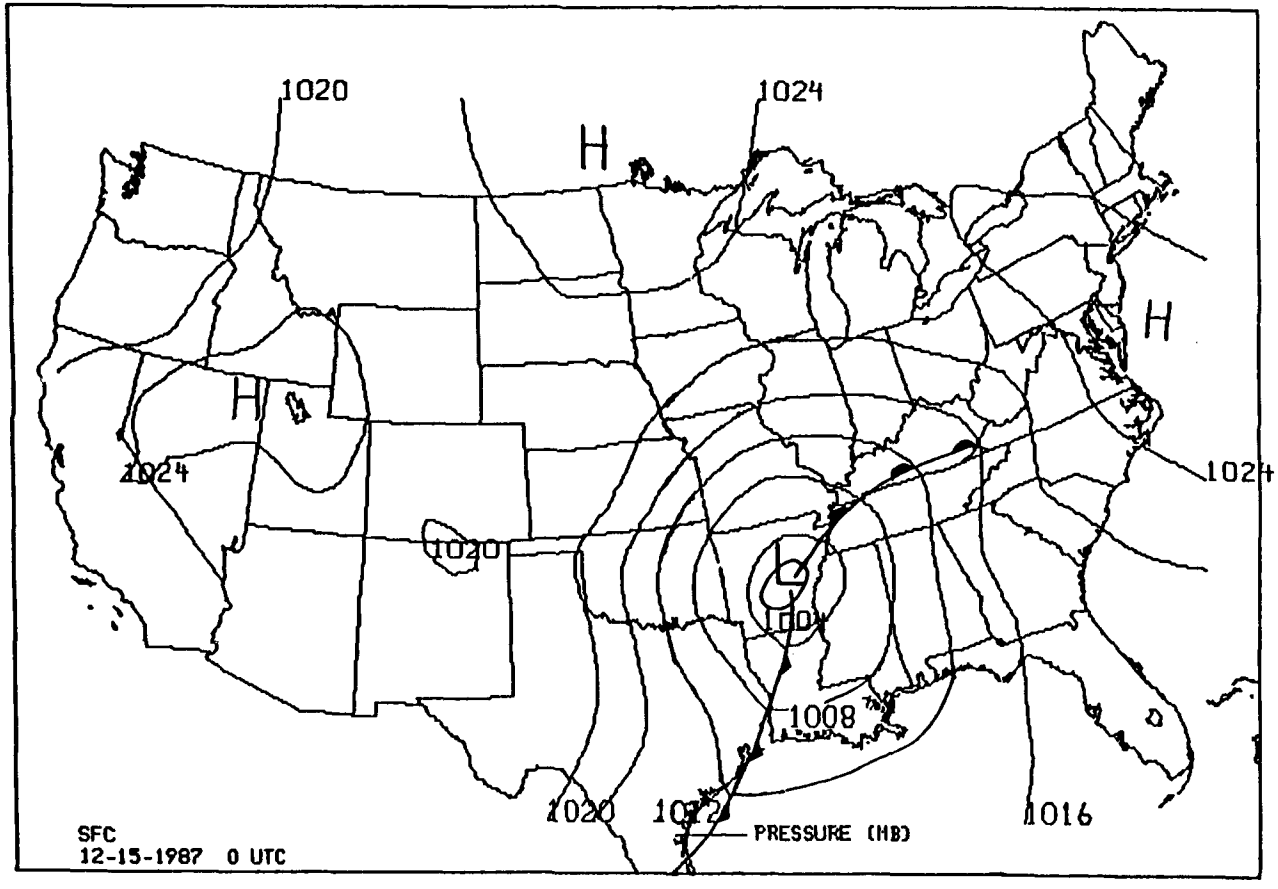

Fig. 3 Surface analysis for 0000 UTC 15 December 1987. Pressure in millibars.

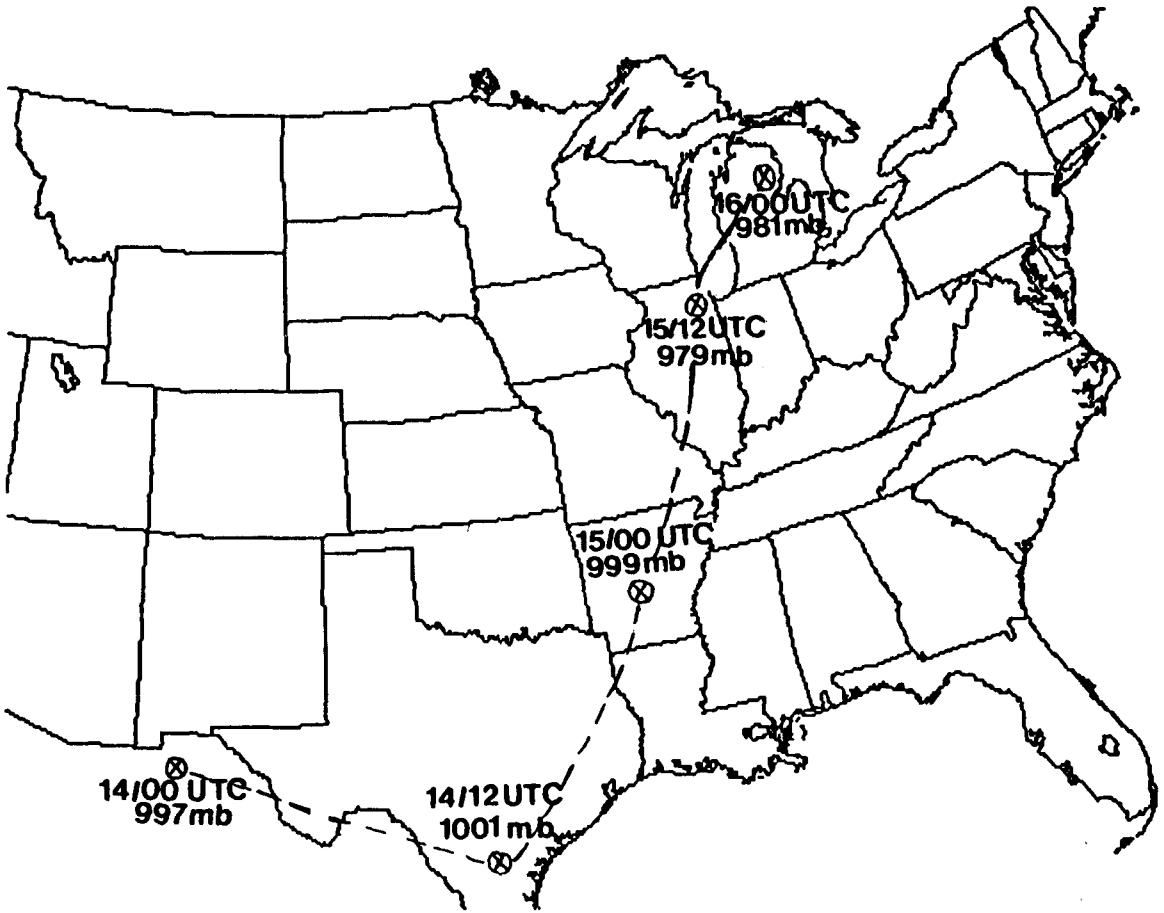

Fig. 4 The position of the surface low in time from 0000 UTC 14 December 1987 to 0000 UTC 16 December 1987.

Fig. 5 Snowfall totals (inches) over the central United States from 13 to 16 December 1987 (Storm Data, December 1987).

reports of thunder and frozen precipitation (mostly snow) associated with this storm.

4.1.2 Vertical Motion

To detect regions favorable for the contribution of macroscale dynamics to the mesoscale environment, kinematic omegas were diagnosed to depict the region of upward/downward vertical motions (UVM/DVM hereafter).

At 1200 UTC 14 December 1987, there was a region of UVM at 850 mb with an UVM maximum located over eastern Texas and extending into south-central Oklahoma (Fig. 6). There were similar features, but with stronger UVM, at 700 mb (not shown) and 500 mb (Fig. 7).

By 0000 UTC, this center of UVM had propagated northeastward in conjunction with the movement of the low pressure system. Maximum values of UVM were located in the vicinity of the Oklahoma, Arkansas, and Texas border area extending into southwestern Missouri with increased intensity at both the 850 mb (Fig. 8) and 500 mb (Fig. 9) levels. This area of strong UVM was located in the region where thunder and frozen precipitation was reported. Several stations, including Joplin, MO (JLN), Springfield, MO (SGF), and Harrison, AR (HRO) reported thunder

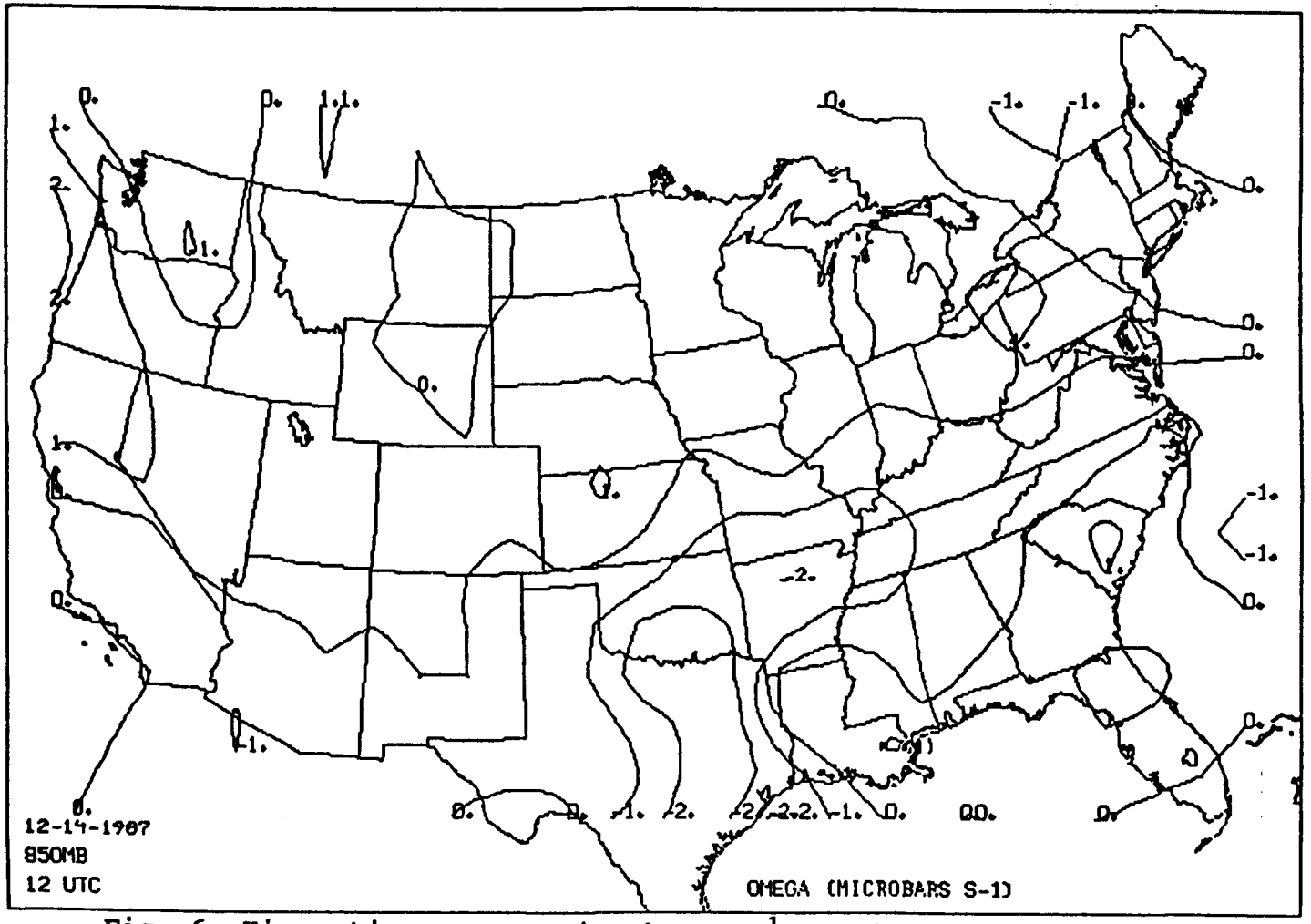

Fig. 6 Kinematic omegas (microbars s^{-1}) at 850 mb for 1200 UTC 14 December 1987.

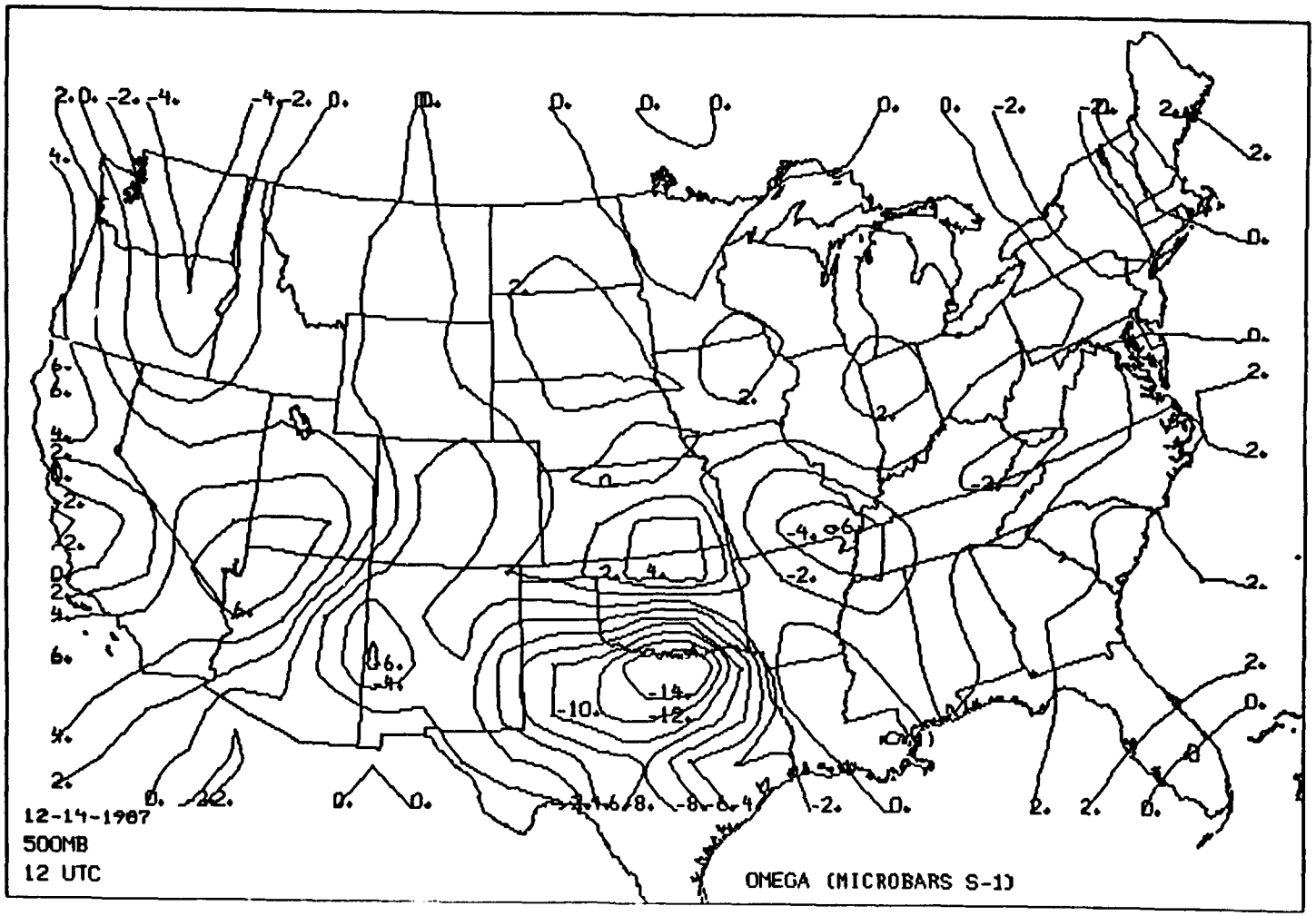

Fig. 7 Same as Fig. 6, except at 500 mb.

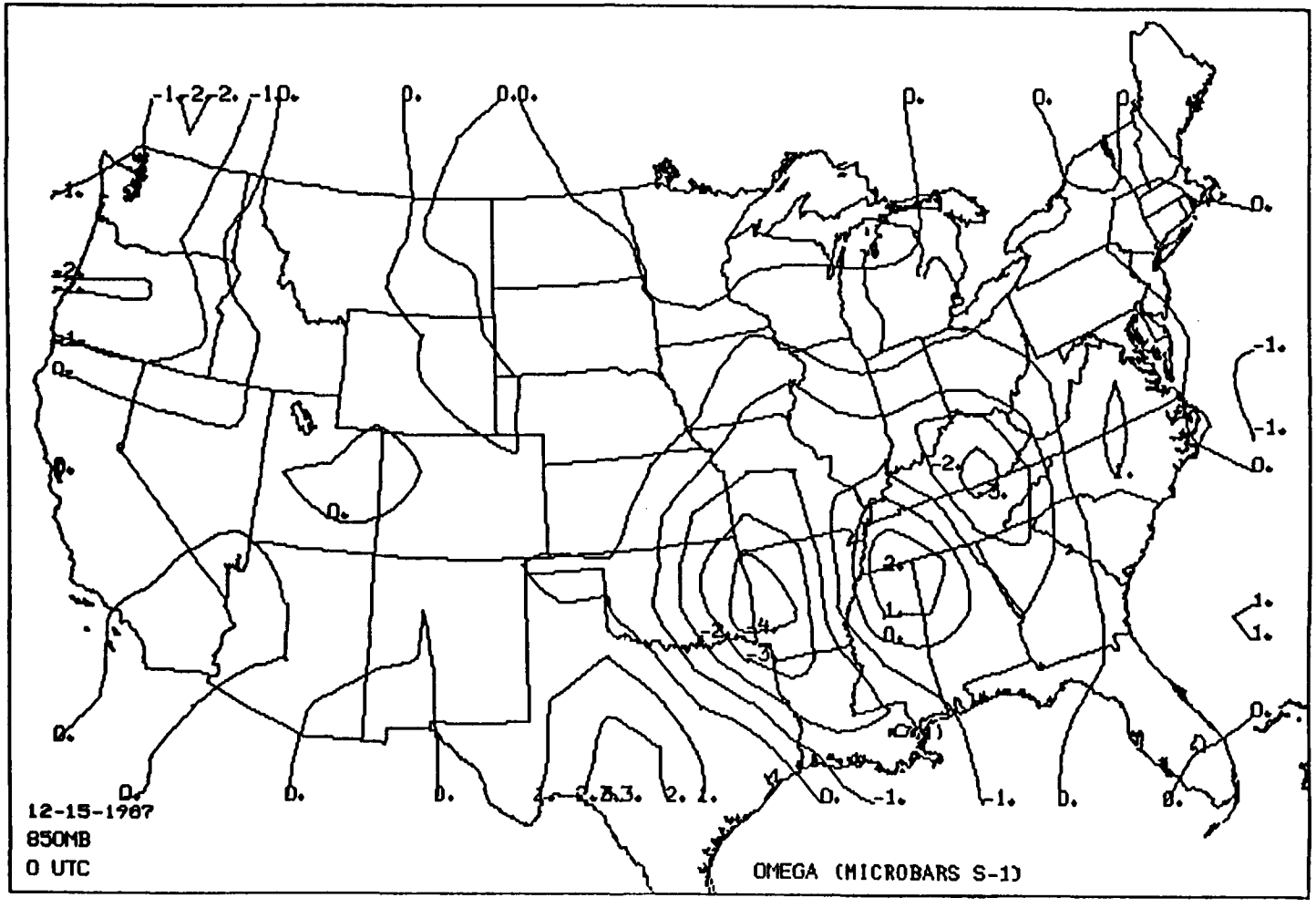

Fig. 8 Same as Fig. 6, except for 0000 UTC 15 December 1987.

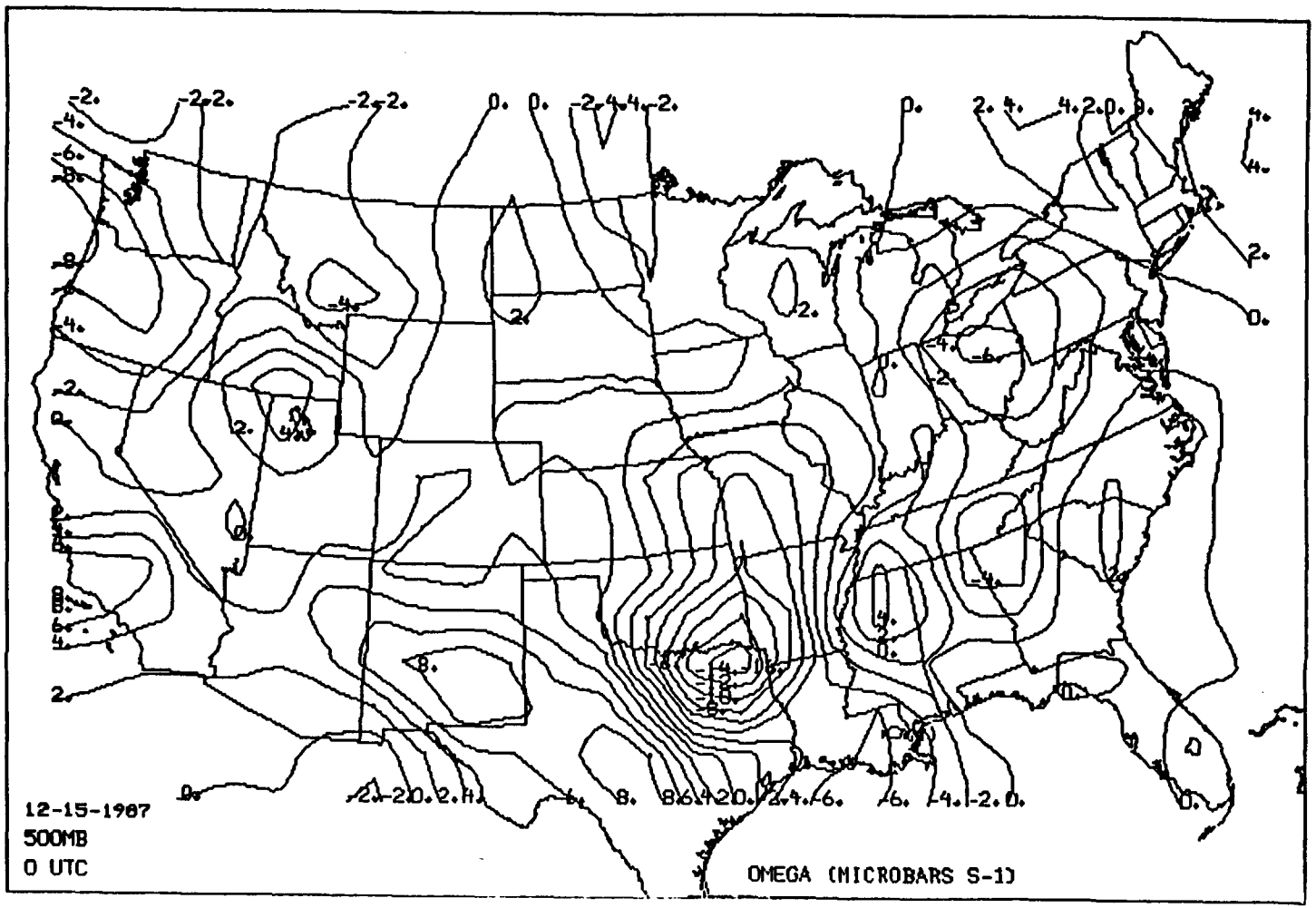

Fig. 9 Same Fig. 8, except at 500 mb.

and frozen precipitation between 2300 UTC 14 December 1987 and 0300 UTC 15 December 1987.

4.1.3 Vertical Wind Shear and Absolute Momentum

Vertical wind shear, as described in section 3.3.2, and the vertical distribution of absolute momentum (M), as described in (1), are very closely related. The stronger the vertical wind shear, the more horizontal the M surfaces. CSI occurs when the slope of the theta-e surfaces > the slope of the M surfaces. Therefore, as the vertical wind shear increases, and the slope of the M surfaces decreases, the chances for CSI increase. At 0000 UTC on 15 December 1987, the vertical wind shear at Monett, MO (UMN) was 9.4 m s^{-1} km^{-1} and greater than 8 m s^{-1} km^{-1} over southwest Missouri and northwest Arkansas, the region where the thunder and frozen precipitation occurred. These values of vertical wind shear are large and show the role strong vertical wind shear can play in producing areas of CSI making conditions favorable for slantwise convection.

4.1.4 Conditional Symmetric Instability and Equivalent Potential Vorticity

To assess the role of CSI, a set of vertical cross sections normal to the 850-300 mb thickness lines were prepared. The x-axis of the cross section is directed toward the warmer air. The first type of cross section contains isopleths of M (solid lines) at increments of 10 m s^{-1} and isopleths of theta-e (dashed lines) at increments of 4 K. Areas where the slopes of theta-e surfaces are greater than the slopes of M surfaces are areas of CSI. A second type of cross section depicts areas of CSI along the cross section in terms of equivalent potential vorticity (EPV) as described in (12). Regions where the value of EPV < 0 are regions of CSI and are therefore susceptible to slantwise convection.

Fig. 10 shows the 850-300 mb thickness pattern for 0000 UTC 15 December 1987 and the location of the cross sections labeled A-B and C-D, used for this case. Also shown in this figure are the locations and three letter identifiers for stations that reported thunder and frozen precipitation and the times (UTC) that the thunder and frozen precipitation occurred. The following stations reported thunder and frozen precipitation:

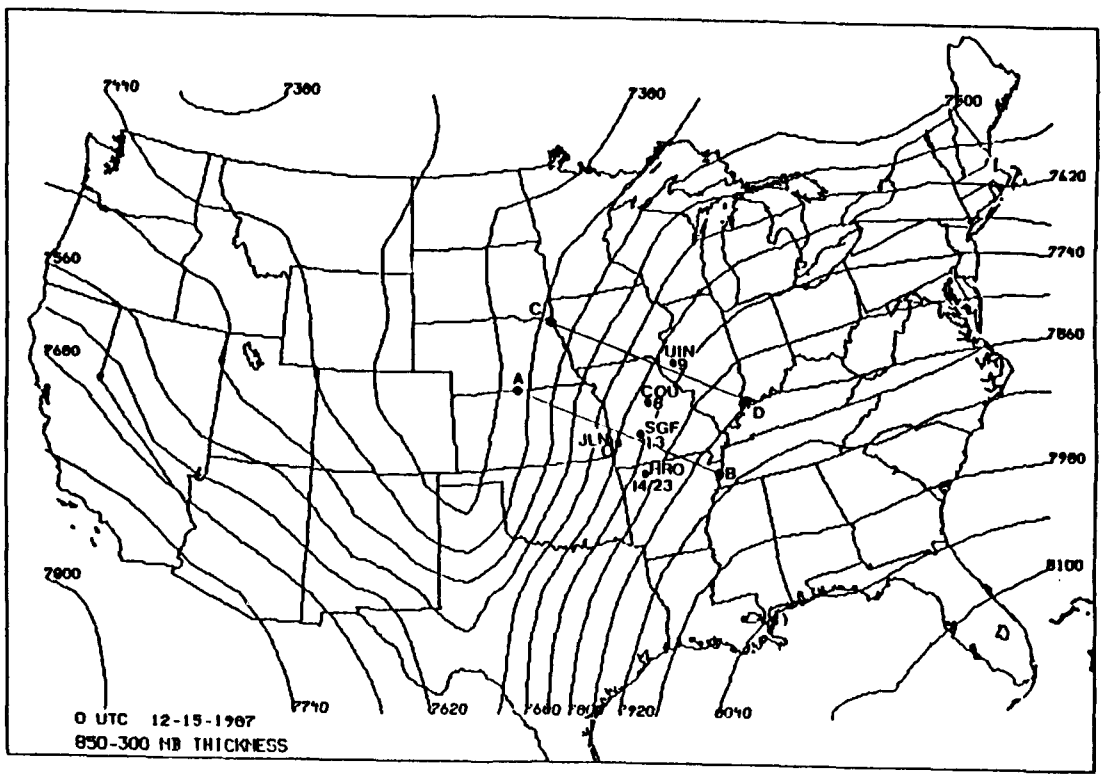

Fig. 10 850-300 mb thickness chart for 0000 UTC 15 December 1987 in units of gpm. The positions of the cross sections are indicated by the lines, labeled with letters, between points. Other filled circles are locations of thunder and frozen precipitation reports with their three letter identifier and the time (UTC) that thunder and frozen precipitation occurred.

Harrison, AR (HRO), Joplin, MO (JLN), Springfield, MO (SGF), Columbia, MO (COU), and Quincy, IL (UIN). Cross section A-B intersects an area over southwestern Missouri where there was thunder and frozen precipitation.

Figure 11 is a vertical cross section of theta-e and M surfaces along line A-B. The vertical distribution of theta-e is partially the result of theta-e advection. Scofield and Robinson (1990) explained how theta-e advection at the 850 and 700 mb levels could be used to improve forecasts for heavy snow. They studied the 14-15 December 1987 central U.S. snowstorm and determined that for the 12 hour period ending at 0000 UTC 15 December 1987 heavy snow occurred in an area that had a strong gradient of positive 850 mb theta-e advection at 1200 UTC 14 December 1987. Analysis of the 0000 UTC 15 December 1987 850 mb theta-e advection pattern (Fig. 12) in this thesis showed there was heavy snow and reports of thundersnow or thunder and frozen precipitation within a region of strong positive 850 mb theta-e advection in this case also. A possible explanation for this relationship is that strong low level positive advection of theta-e acts to decrease the stability of the atmosphere above the level of advection. This advection may be sufficient to create conditions of CSI making the atmosphere

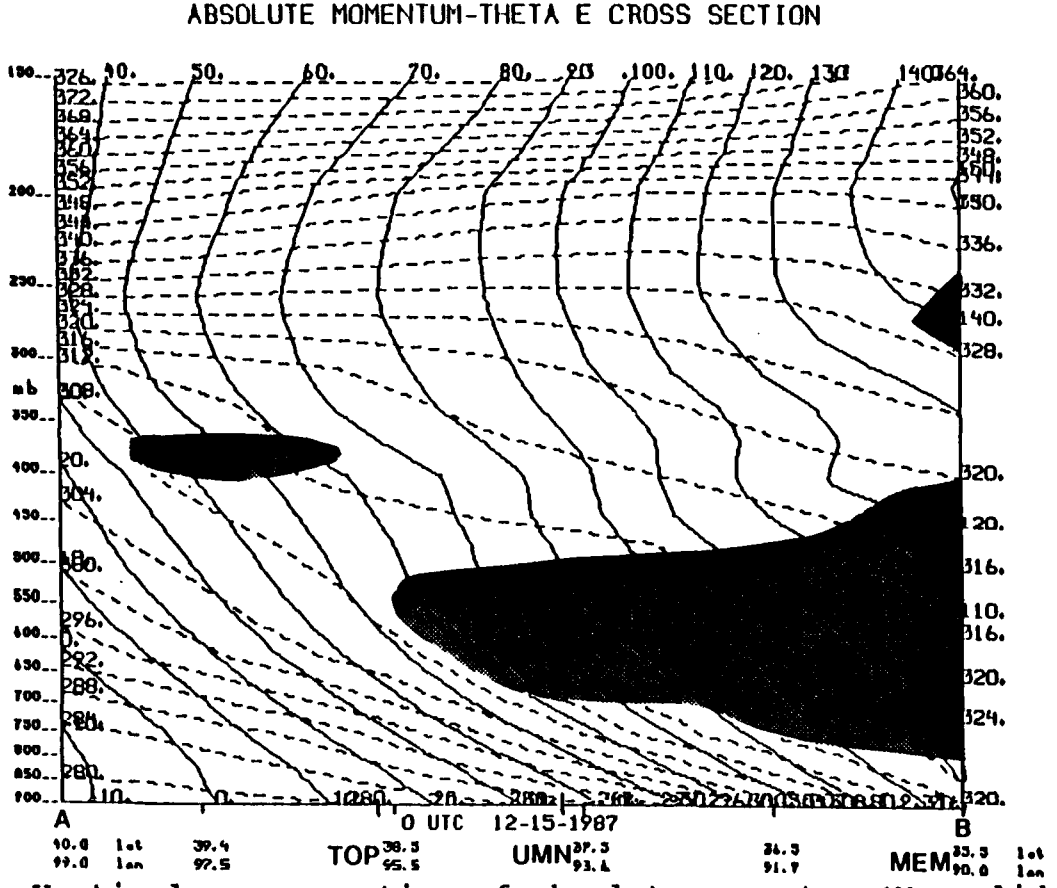

Fig. 11 Vertical cross section of absolute momentum (M, solid lines in m s^{-1}) and equivalent potential temperature (theta-e, dashed lines in K) along line A-B for 0000 UTC 15 December 1987. Shaded regions indicate areas of conditional symmetric instability.

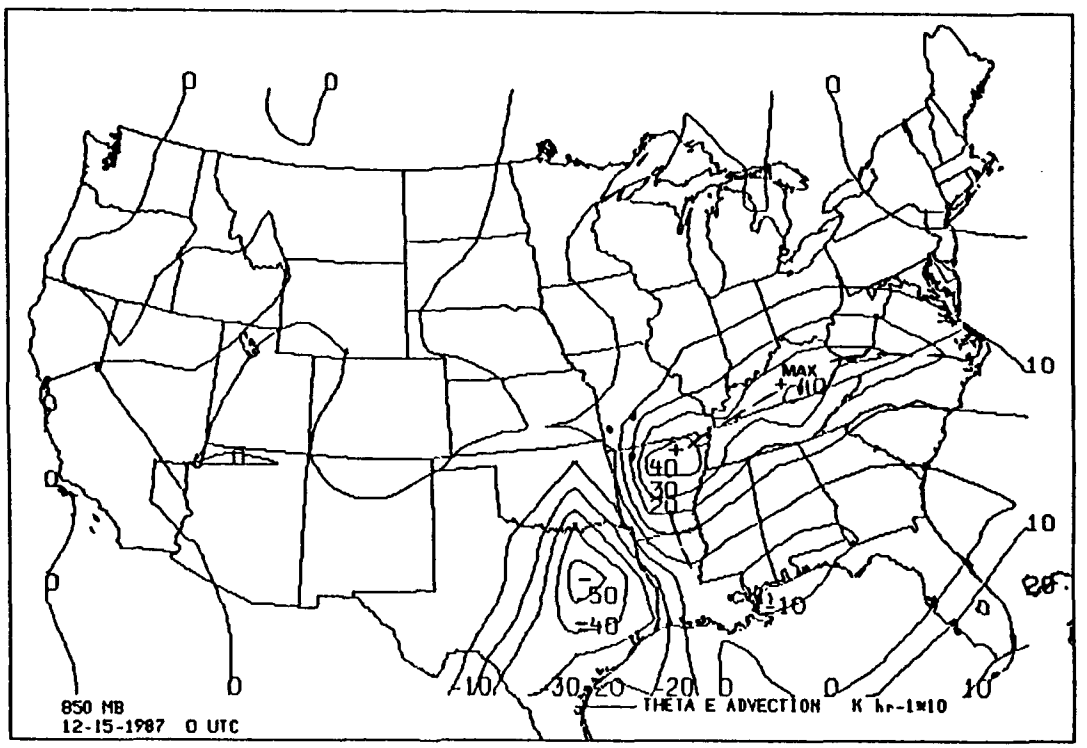

Fig. 12 Equivalent potential temperature advection in units of K hr^{-1} X 10 at 850 mb for 0000 UTC 15 December 1987.

susceptible to slantwise convection. If the advection is strong enough it may create a layer of convective instability (a decrease in theta-e with height).

Analysis of the distribution of theta-e in Fig. 11 reveals that there is an area of CSI (shaded) in the lower to middle troposphere that extends from Monett, MO (UMN) eastward to Memphis, TN (MEM). Figure 13 is an analysis of equivalent potential vorticity (EPV) along cross section A-B. The areas of CSI are areas where the values of EPV are < 0 and are indicated by the shaded areas. Within the large area of CSI in Fig. 13 convection did occur. There were two reports of thundersnow and two of thunder and freezing rain in this area within three hours of 0000 UTC 15 December 1987. Total snowfall from the storm in the area around Joplin, MO (JLN) and Springfield, MO (SGF), two stations that reported thundersnow, ranged from 6 to 12 inches. In this case, CSI was present, and convection did occur within the large area of CSI contributing to the heavy snowfall over parts of southwestern Missouri.

A cross section was also analyzed along the line labeled C-D in Fig. 10. This cross section begins near Sioux City, IA (SUX), passes through Quincy, IL (UIN) and ends near Evansville, IN (EVV). Figure 14 shows an area of CSI near the 625 mb level

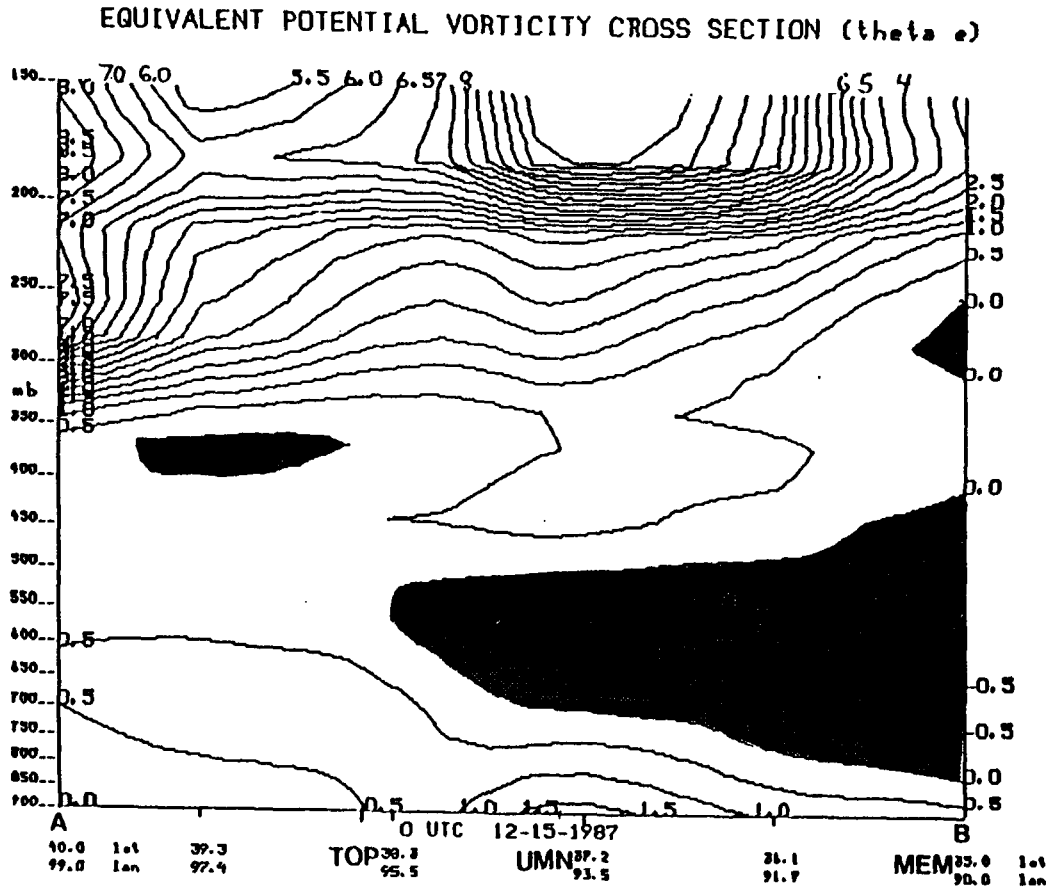

Fig. 13 Vertical cross section of equivalent potential vorticity in units of 1 X 10^{-6} m^2 K s^{-1} kg^{-1} along line A-B for 0000 UTC 15 December 1987. Shaded regions indicate areas where EPV < 0 (areas of conditional symmetric instability).

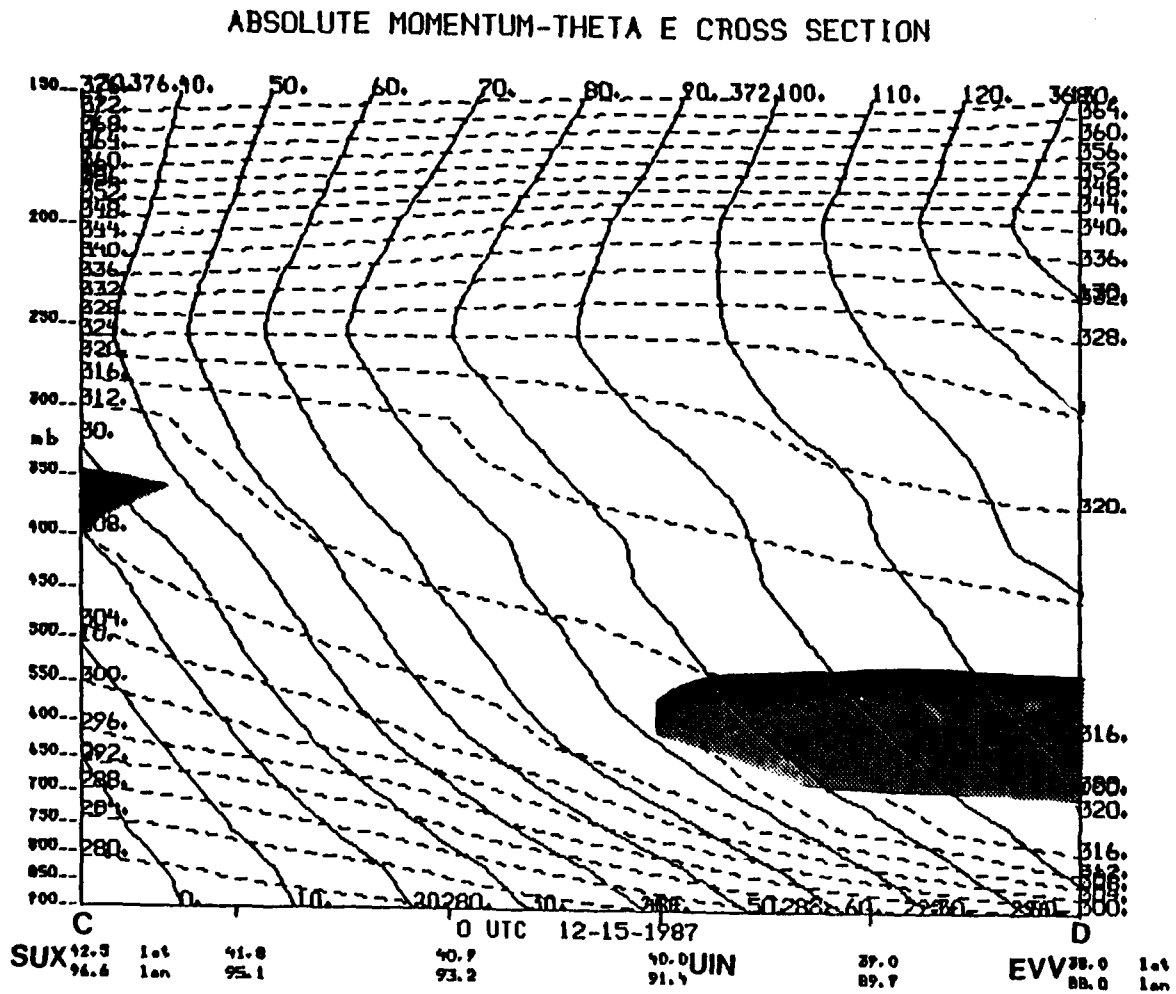

Fig. 14 Same as Fig. 11, except along line C-D.

that is shaded and below this is a region of weak CSS. Figure 15 is a vertical cross section of EPV along line C-D and the shaded regions where EPV < 0 delineate where CSI is present. No thunder and frozen precipitation was reported for areas near cross section C-D until 0800 UTC 15 December 1987. At 0000 UTC the upward vertical velocities over the area was relatively weak > -2 microbars/s at 850 mb (Fig. 8) and approximately +3 microbars/s at 500 mb (Fig. 9). Although there was an area of CSI there was not significant UVM to initiate the slantwise convection. As the low pressure system intensified and moved northeastward the vertical velocities over west-central Illinois increased and thundersnow was reported at 0800 UTC 15 December 1987 at Columbia, MO (COU) and at 0900 UTC 15 December 1987 at Quincy, IL (UIN). This indicates that the CSI was present but slantwise convection did not occur until a significant initiating force was present to trigger the slantwise convection and produce thundersnow.

4.2 Case 2: 4 March 1990

4.2.1 Synoptic Overview

At 1200 UTC 4 March 1989 there was a deep trough extending from the northern plains to the

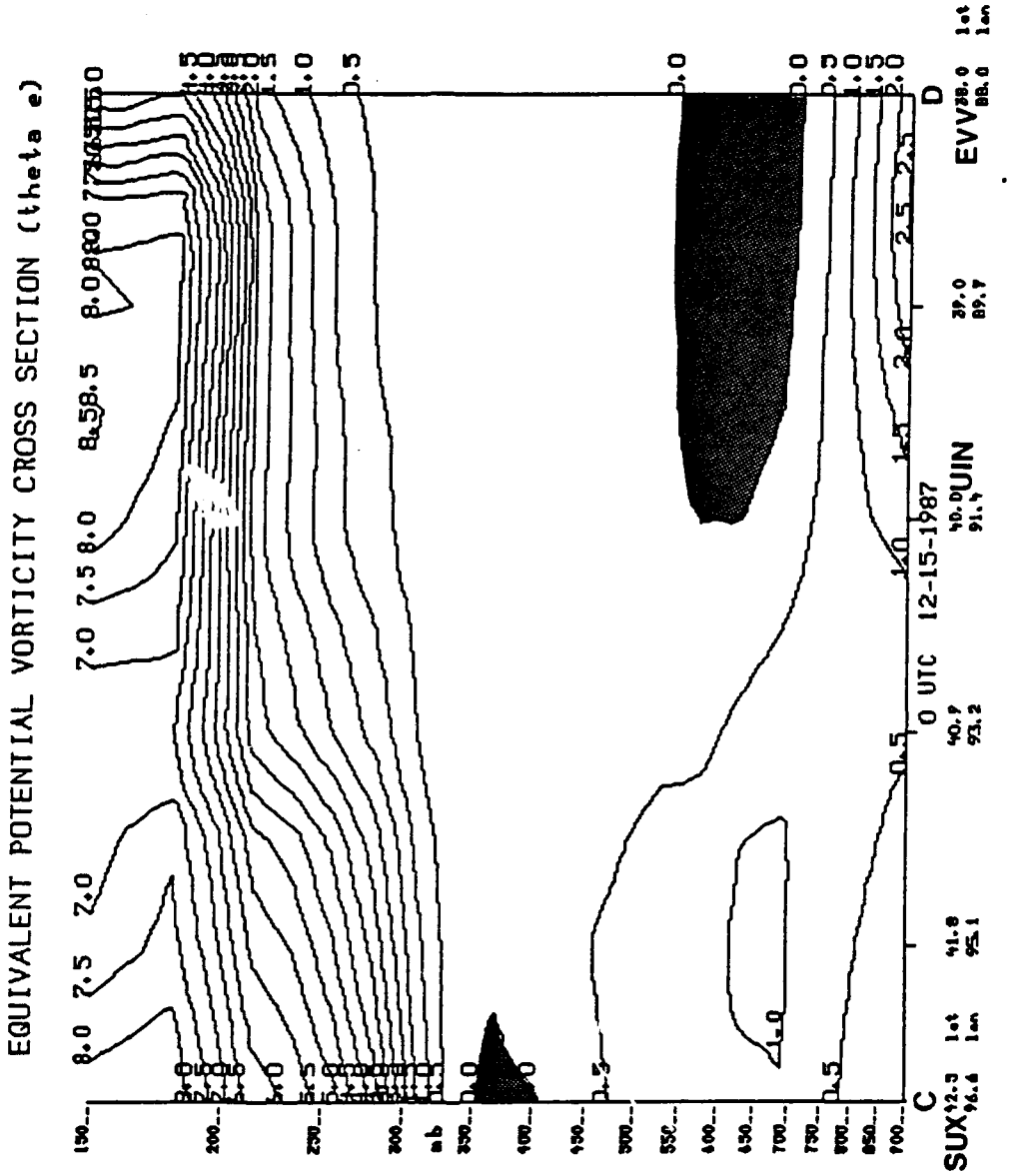

Fig. 15 Same as Fig. 13, except along line C-D.

southern Rocky Mountains. A 500 mb low was centered over New Mexico creating a pattern of southwest to northeast flow over much of the United States east of the Rockies (Fig. 16). At the surface there was an area of low pressure centered west of Chicago, IL with a cold front extending southward to near Little Rock, AR. From there it became a warm front extending to a weak low pressure center over the extreme northeast corner of Texas. A cold front extended from this low to just north of San Antonio, TX then east of El Paso (see Fig. 17). The area of interest in this case extended from near Dallas, TX across eastern Oklahoma and northwestern Arkansas into southern Missouri. There were 13 reports of thunder and frozen precipitation (freezing rain or ice pellets) between 1200 UTC 4 March 1989 and 1700 UTC 4 March 1989 over the area of interest in this case (see Fig. 18).

Infrared (IR) Geostationary Operational Environmental Satellite (GOES) imagery from 1601 UTC 4 March 1989 (Fig. 19a) shows an area of cold cloud tops with temperatures ranging from -42°C to -52°C over the area where thunder and frozen precipitation was reported in this case. GOES IR imagery from 1701 UTC 4 March 1989 (Fig. 19b) shows that this same area of cold cloud tops expanded in size, and over northwest Texas became colder with temperatures

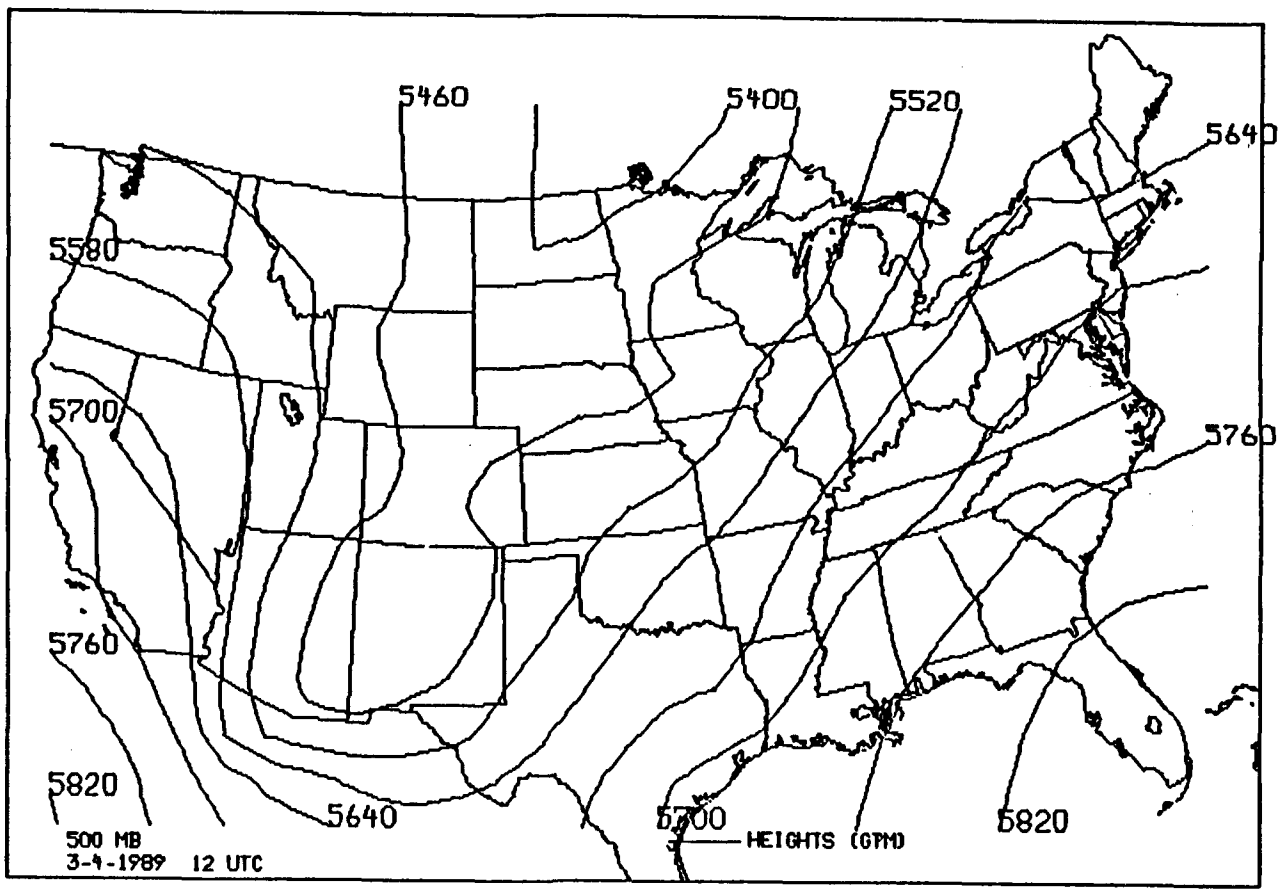

Fig. 16 Same as Fig. 2a, except for 1200 UTC 4 March 1989.

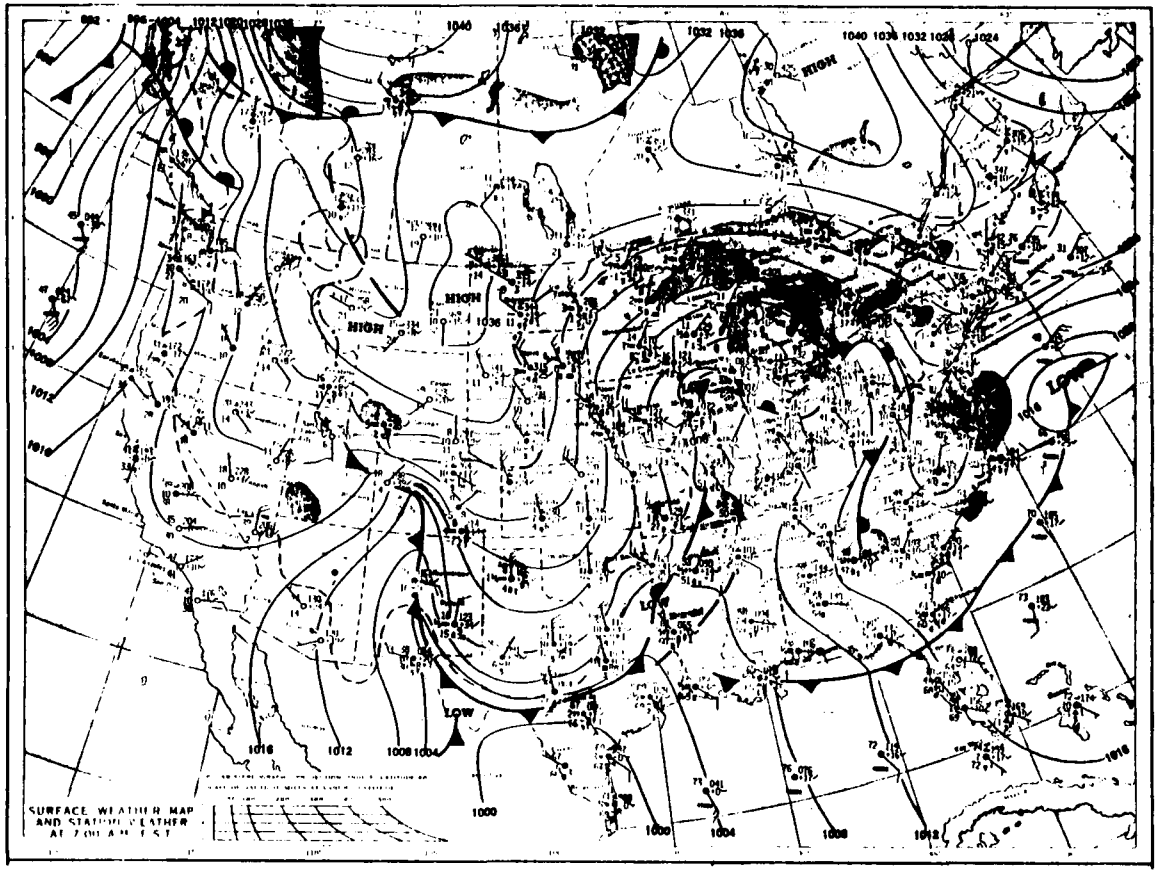

Fig. 17 Same as Fig. 3, except for 1200 UTC 4 March 1989. (Daily Weather Maps, March 1989)

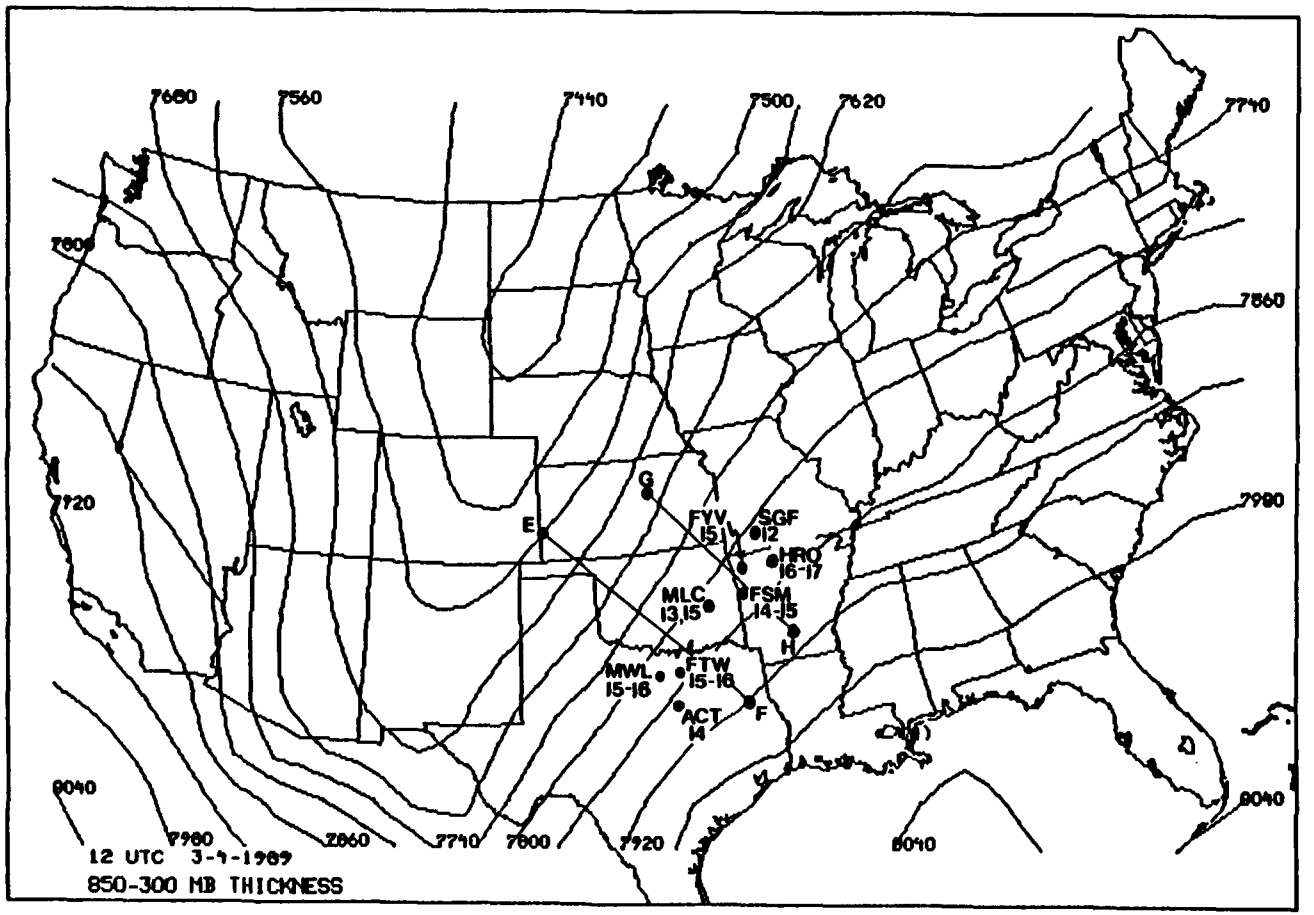

Fig. 18 Same as Fig. 10, except for 1200 UTC 4 March 1989.

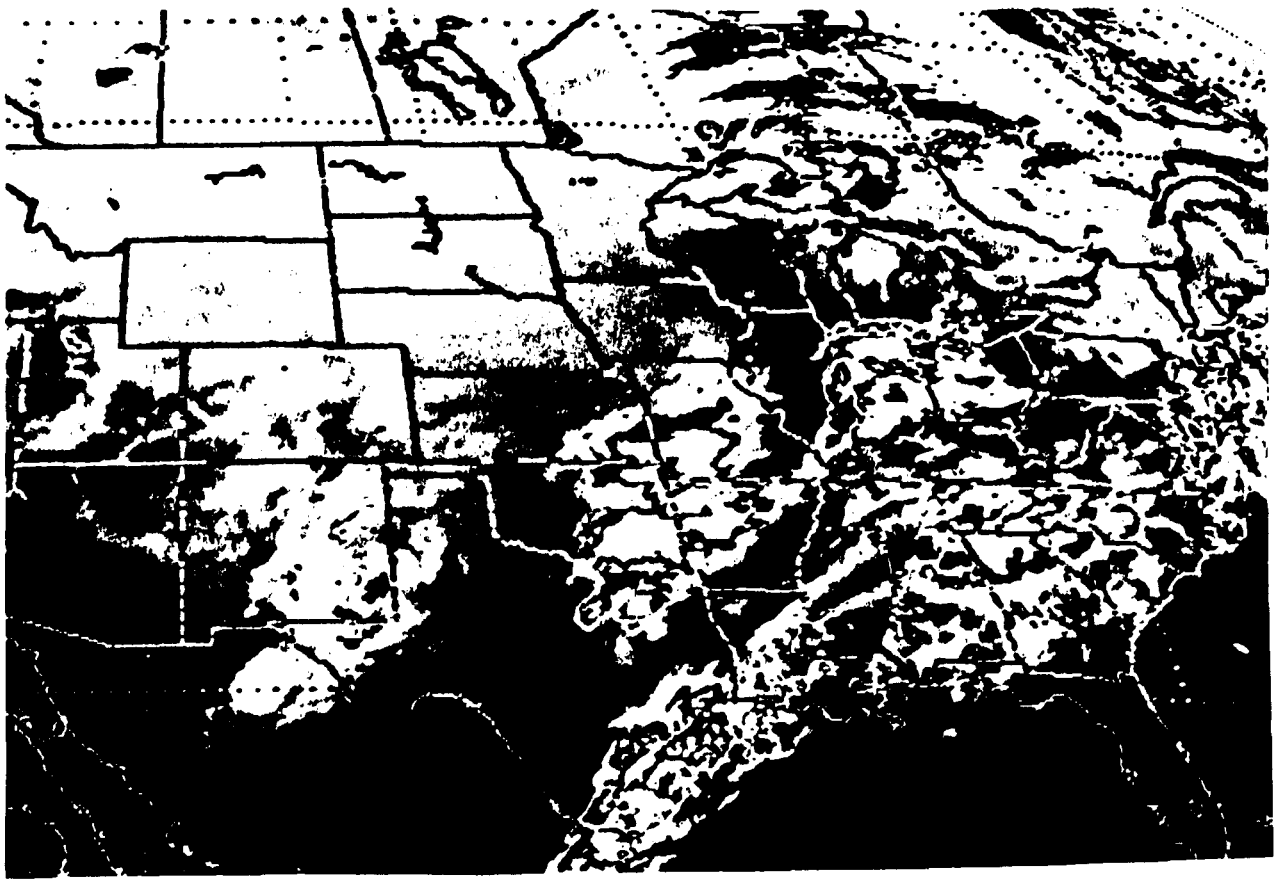

Fig. 19a Satellite imagery using the MB enhancement curve for 1601 UTC 4 March 1989.

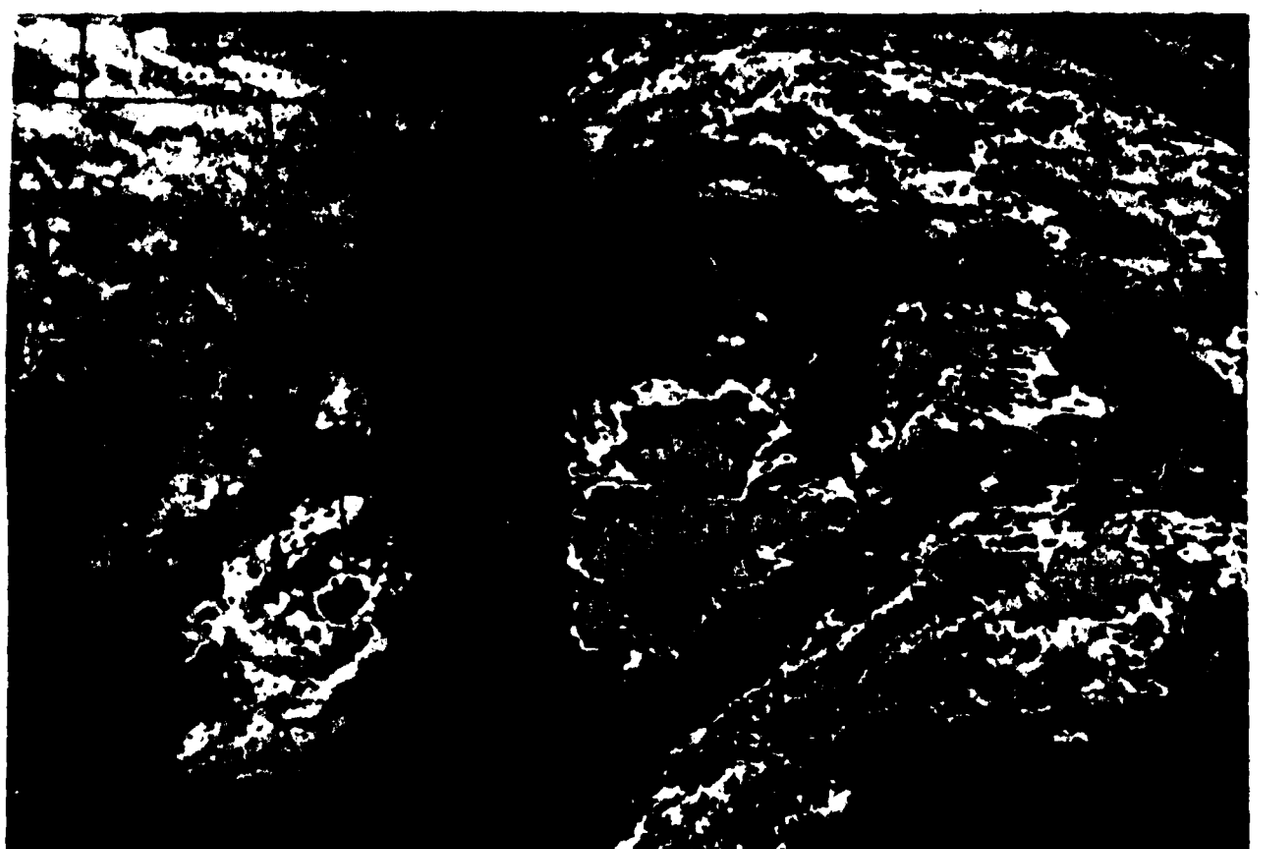

Fig. 19b Same as Fig. 19a, except for 1701 UTC.

ranging from -55°C to -60°C. Beckman (1987) described how IR satellite imagery can be used as a tool to predict the development and progression of heavy snow. He explained that decreases in IR cloud top temperatures and increases in the size of cold cloud top areas are indications of areas where heavy snow can be expected. GOES IR satellite imagery from 0331 UTC March 1989 to 1801 UTC 4 March 1989 (not shown) did show that the cloud top temperatures decreased and the area of cold cloud tops (-42°C to -52°C) increased over the region where the thunder and frozen precipitation occurred. In this case, both of these parameters would have provided an indication of where there was CSI and convection and therefore where the heaviest snow accumulations would occur.

4.2.2 Vertical Motion

At 1200 UTC 4 March 1990 the 850 mb kinematic omega field showed weak UVM over the area of interest with values near -1 microbars/s (Fig. 20a). At the 700 mb level the UVM increased over the area of interest. As shown in Fig. 20b, the values of omega ranged from -1 to -4 microbars/s over the area where thunder and frozen precipitation was reported. The analysis shows that there was a significant

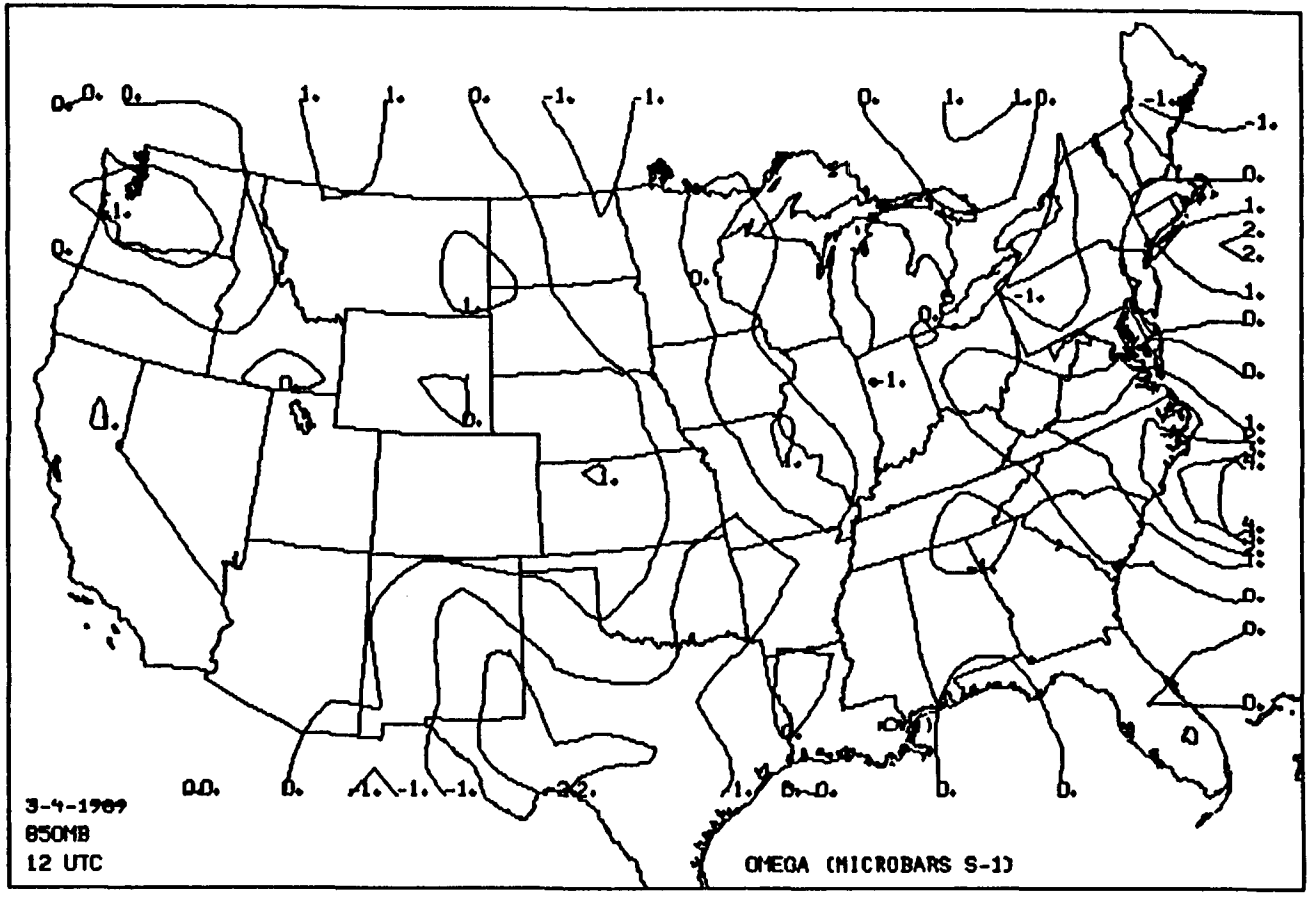

Fig. 20a Same as Fig. 6, except for 1200 UTC 4 March 1989.

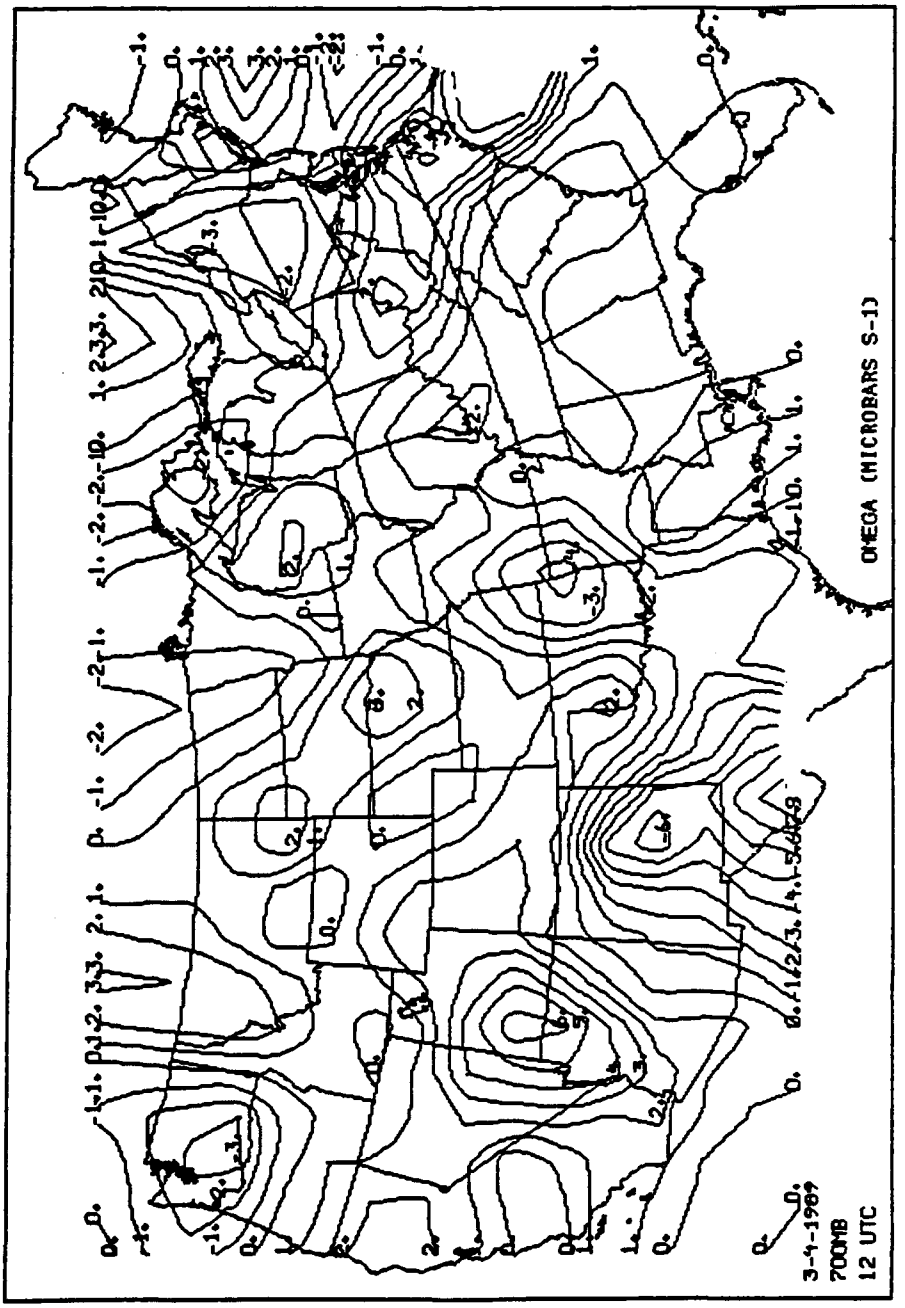

Fig. 20b Same as Fig. 20a, except at 700 mb.

amount of UVM below 700 mb to possibly initiate slantwise convection.

4.2.3 Vertical Wind Shear and Absolute Momentum

At 1200 UTC 4 March 1989 there was strong vertical wind shear over most of the area of interest. The largest value of vertical wind shear was 9.5 m s^{-1} km^{-1} at Stephenville, TX (SEP). At Oklahoma City, OK (OKC) it was 7.7 m s^{-1} km^{-1} and over the entire area of interest the value was greater than 5.0 m s^{-1} km^{-1}. This strong vertical wind shear coincides with a decrease in the slope of the absolute momentum (M) surfaces and increase the opportunity for CSI.

4.2.4 Conditional Symmetric Instability and Equivalent Potential Vorticity

To access the role of CSI a set of vertical cross sections normal to the 850-300 mb thickness were prepared. For this case two cross sections were used and are labeled E-F and G-H as shown in Fig. 18. Also shown in Fig. 18 are the location and three letter identifier for stations reporting thunder and frozen precipitation and the times (UTC) that the thunder was reported. These stations are:

Springfield, MO (SGF), Fayetteville, AR (FYV), Harrison, AR (HRO), Fort Smith, AR (FSM), McAlester, OK (MLC), Fort Worth, TX (FTW), Mineral Wells, TX (MWL), and Waco, TX (ACT).

The distribution of theta-e along the cross sections is affected by the advection of theta-e. As described previously, the 850 or 700 mb theta-e advection may be used as a tool to forecast heavy snow. In this case the rules for using 850 or 700 mb theta-e advection to help forecast heavy snow were limited. There are several reasons for the limited use of this forecast method in this case. First, this case did not involve snow during the time period studied, although, 12 hours later significant amounts of snow did occur with this system over the area of interest. Snow accumulations over 12 inches were reported over northeastern Oklahoma and southwestern Missouri. Also, the precipitation was associated with a strong arctic front and it occurred in the cold air behind the front. Therefore, the 850 mb theta-e advection pattern shows negative 850 mb theta-e advection in the region where the thunder and frozen precipitation occurred (see Fig. 21a). This is in contrast to the pattern of positive 850 mb theta-e advection that can be used to forecast heavy snow as described by Scofield and Robinson (1990). The 700

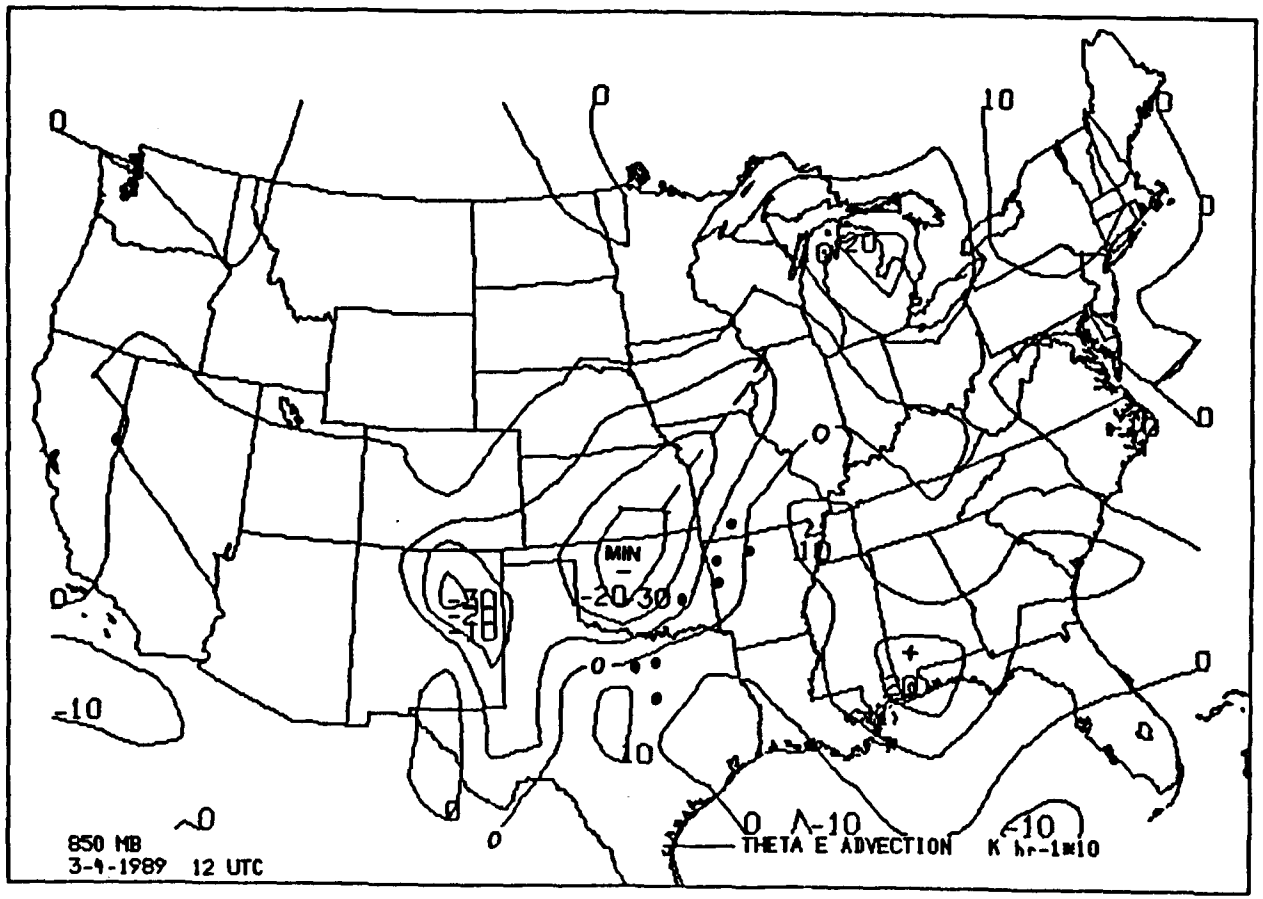

Fig. 21a Same as Fig. 12, except for 1200 UTC 4 March 1989.

mb theta-e advection pattern (Fig. 21b) did show a weak positive theta-e advection maximum and some of the thunder and frozen precipitation occurred near the maximum which is one of the areas favorable for heavy snow as described in Scofield and Robinson (1990).

Figure 22 shows the vertical cross section of M and theta-e along line E-F. Analysis of Fig. 22 shows that the atmosphere is convectively unstable in a layer from 700 to 550 mb with areas of convective stability but CSI above and below this layer in several areas. The regions of CSI are shown by the shading in Fig. 22. A cross section of EPV along line E-F is shown in Fig. 23 and two large areas of CSI are shaded. These areas of CSI were located in the region where thunder and frozen precipitation was reported. Therefore, there was convection occurring over an area where there was CSI.

A second cross section was chosen along line G-H as shown in Fig. 18. Once again the cross section of M and theta-e shows a large area of CSI indicated by the shaded region in Fig. 24. The cross section of EPV in Fig. 25 also shows the CSI confined primarily below the 550 mb level with the depth of this CSI increasing toward H which is the southeast endpoint of the cross section. There were several

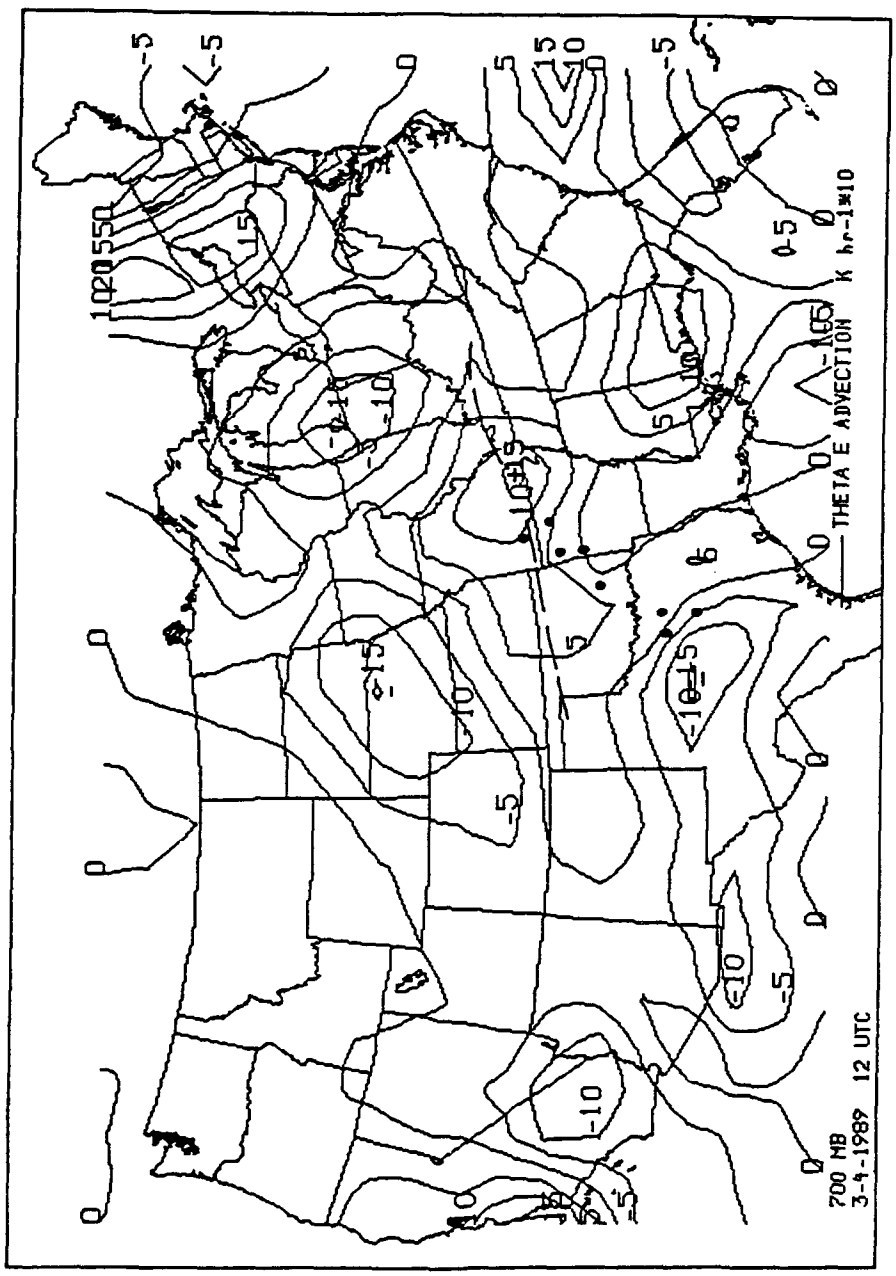

Fig. 21b Same as Fig. 21a, except for 700 mb.

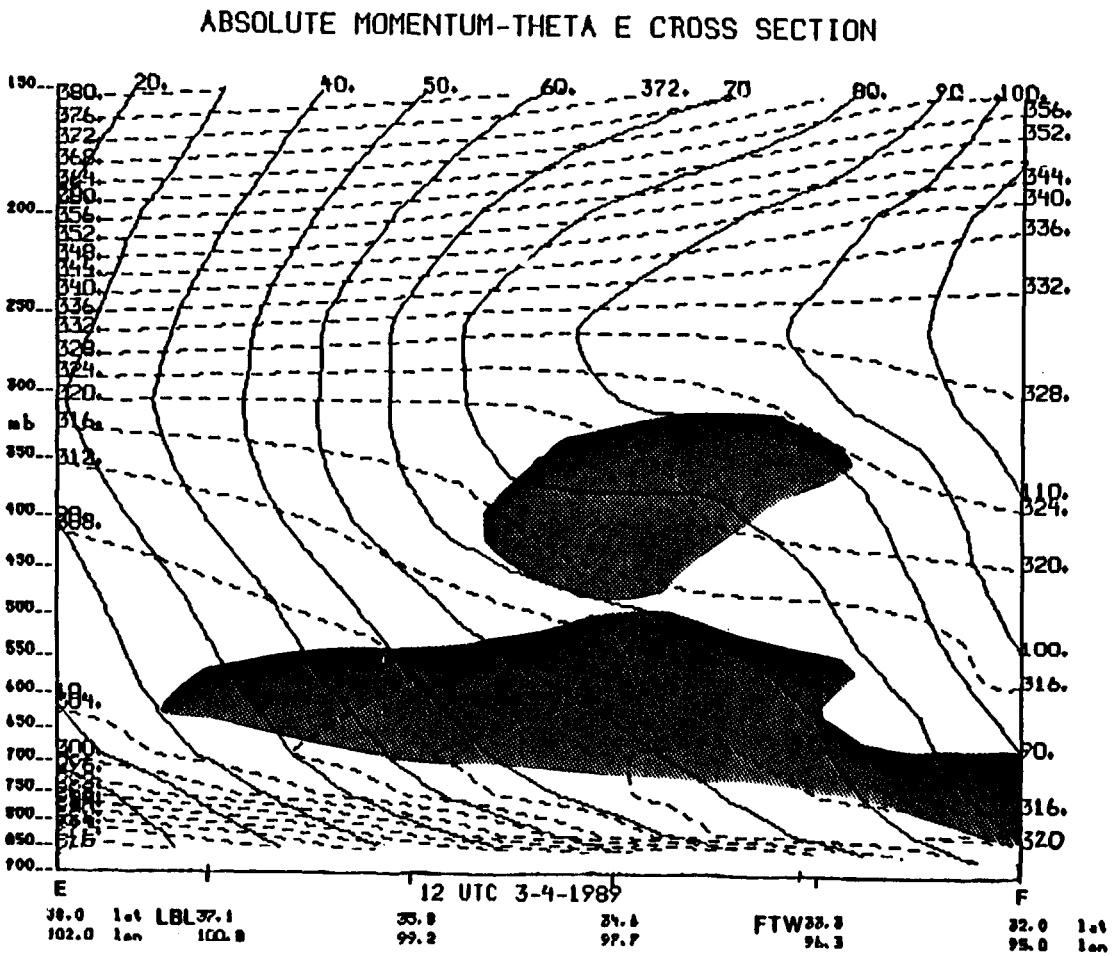

Fig. 22 Same as Fig. 11, except along line E-F for 1200 UTC 4 March 1989.

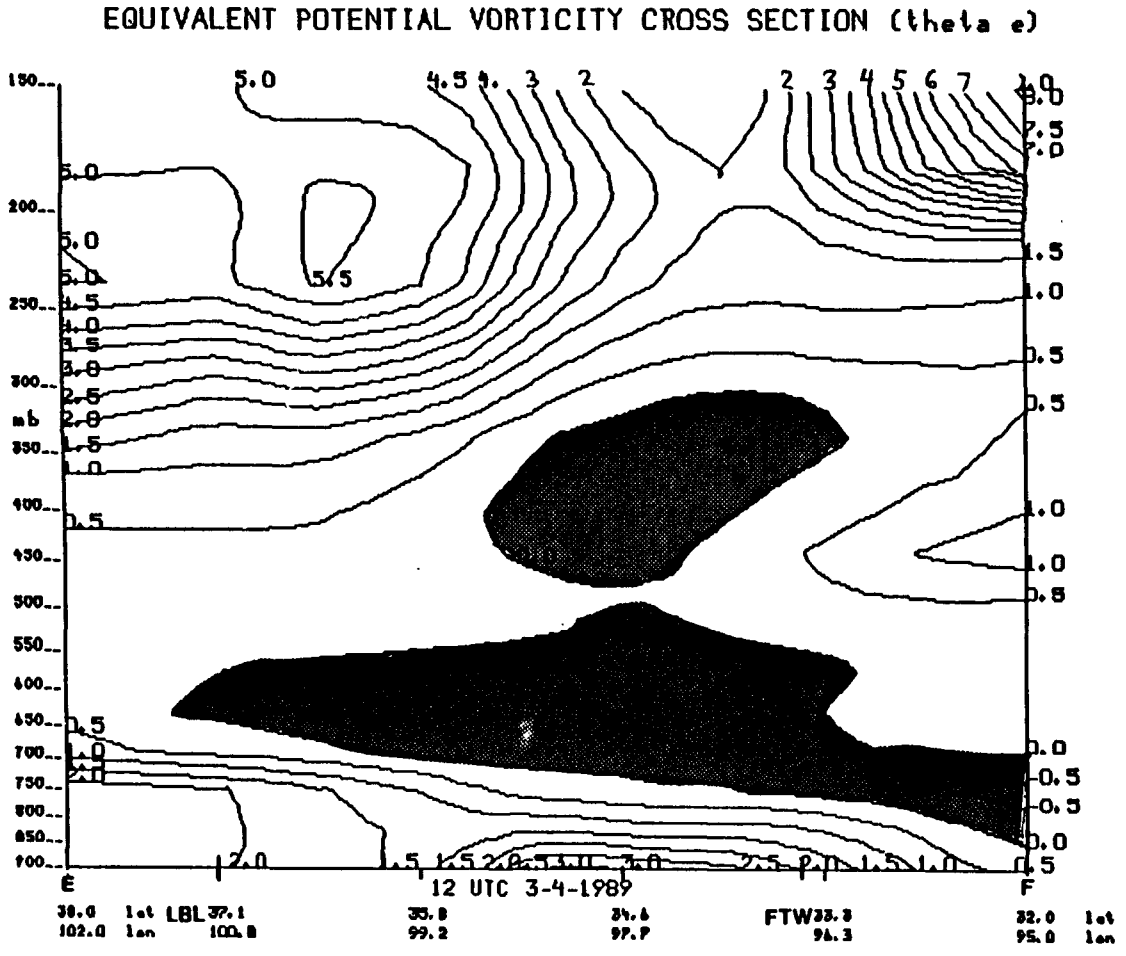

Fig. 23 Same as Fig. 13, except along line E-F for 1200 UTC 4 March 1989.

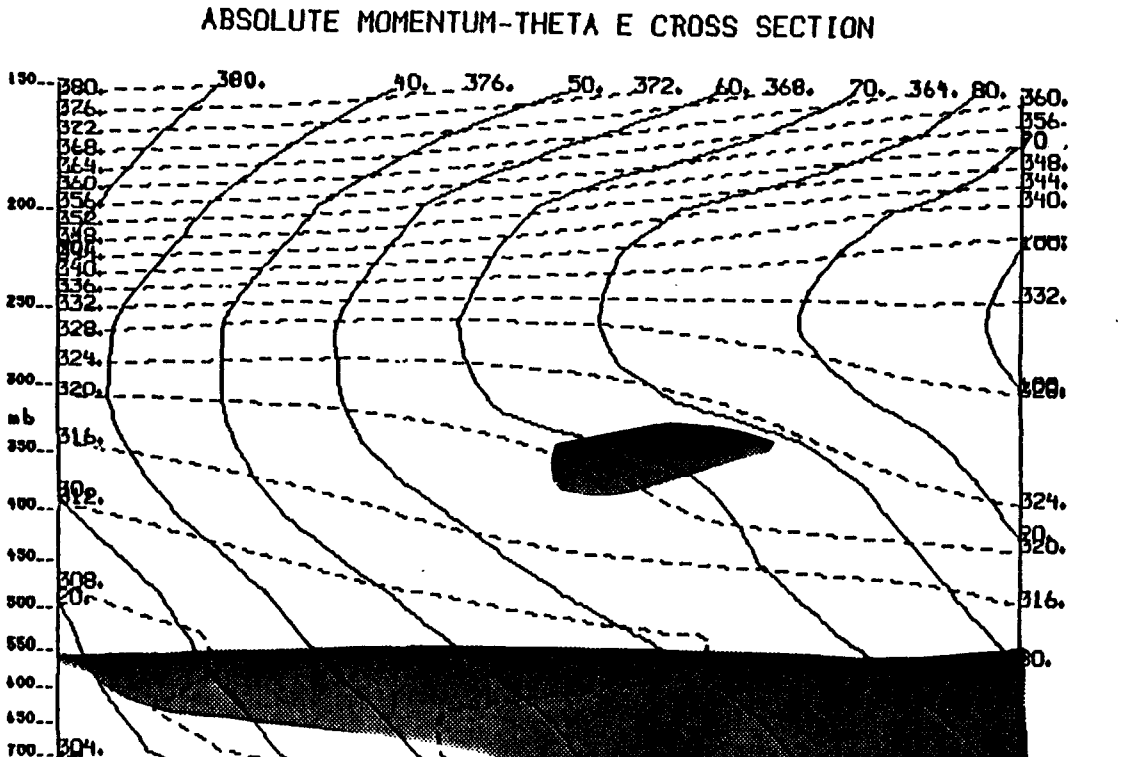

Fig. 24 Same as Fig. 22, except along line G-H.

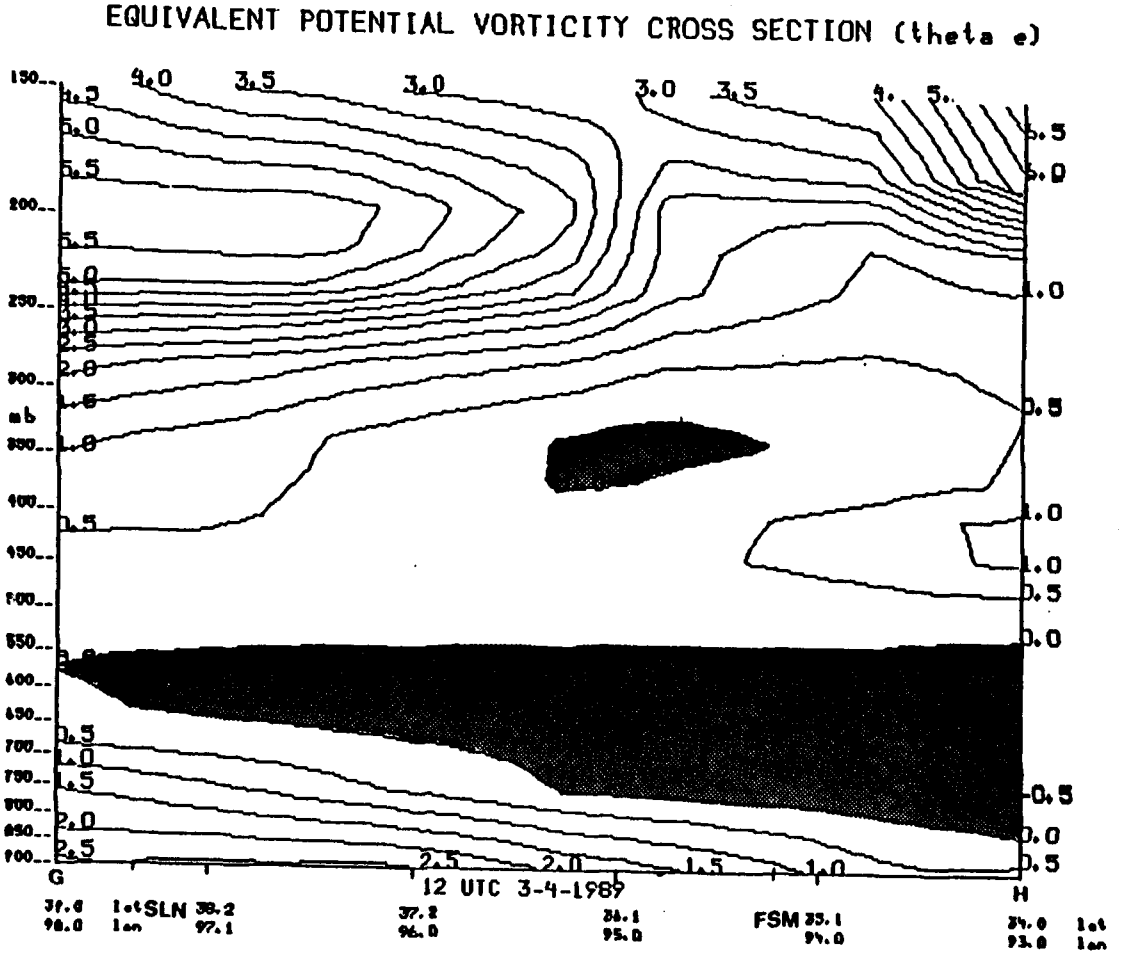

Fig. 25 Same as Fig. 23, except along line G-H.

reports of thunder and frozen precipitation in areas of CSI near the cross section. Here again there was convection confirmed by reports of thunder and frozen precipitation in an area of CSI.

4.3 Case 3: 23-24 March 1990

4.3.1 Synoptic Overview

At 0000 UTC 24 March 1990 a zonal upper air flow pattern was in place from the central plains states into the mid-Mississippi Valley (Fig. 26a). At the surface there was a stationary front extending from central Washington, to Salt Lake City, UT, through northwestern Colorado, then extending south to near El Paso, TX (Fig. 26b). A cold front extended from central North Carolina, through central Alabama and Mississippi, across northern Louisiana and down to the Big Bend area in Texas. An arctic high pressure system was centered in Montana and ridged southward into Texas and eastward to the Ohio Valley. The area of interest in this case study was the eastern two thirds of Kansas and extreme northwestern Missouri. Between 2000 UTC 23 March 1990 and 0400 UTC 24 March 1990 there were nine reports of thunder and frozen precipitation in Kansas and one in Missouri (see

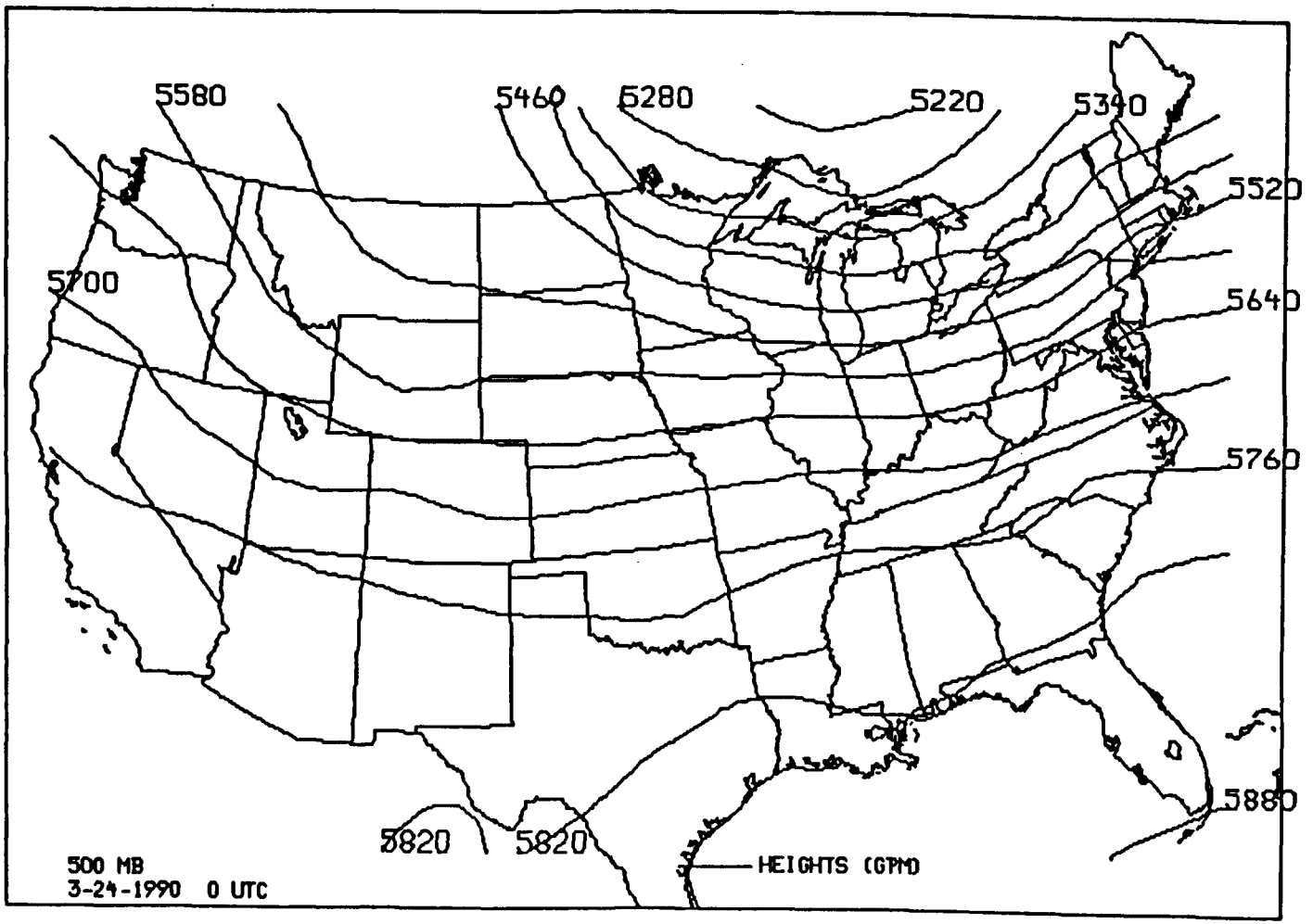

Fig. 26a Same as Fig. 2b, except for 0000 UTC 24 March 1990.

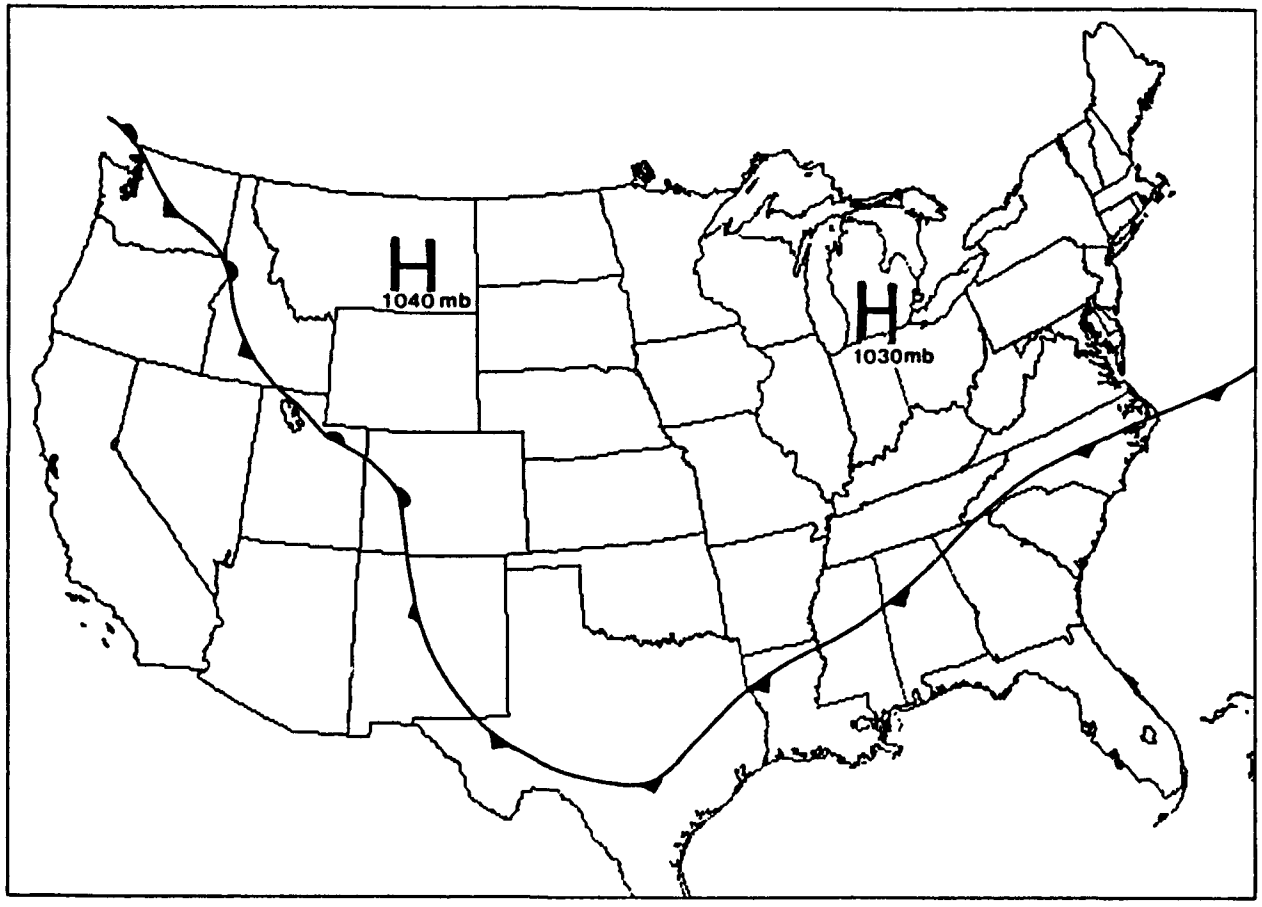

Fig. 26b Surface analysis (fronts and pressure centers) for 0000 UTC 24 March 1990.

Fig. 27). The locations of these stations and their three letter indentifiers are shown in Fig. 27. Snow accumulation between 1200 UTC 23 March 90 and 1200 UTC 24 March 90 was greater than six inches over northwestern Kansas and into Missouri (Daily Weather Maps, March 1990).

Infrared (IR) Geostationary Operational Environmental Satellite (GOES) imagery from 2201 UTC 23 March 1990 (Fig. 28a) shows an area of cold cloud tops with temperatures ranging from -42°C to -52°C over northeastern Kansas another area where thunder and frozen precipitation was reported in this case. GOES IR imagery from 0401 UTC 24 March 1990 (Fig. 28b) shows an area of cold cloud tops with temperatures ranging from -42°C to -52°C over parts of southeastern Kansas where thunder and frozen precipitation was reported. GOES IR satellite imagery from 1601 UTC 23 March 1990 to 0401 UTC 24 March 1990 (not shown) revealed that the cloud top temperatures decreased and the area of cold cloud tops (-42°C to -52°C) increased over the regions where the thunder and frozen precipitation occurred. As described in Beckman (1987), both of these parameters would have provided an indication of where the heaviest snow accumulations would occur and therefore provided information on where there was CSI and convection.

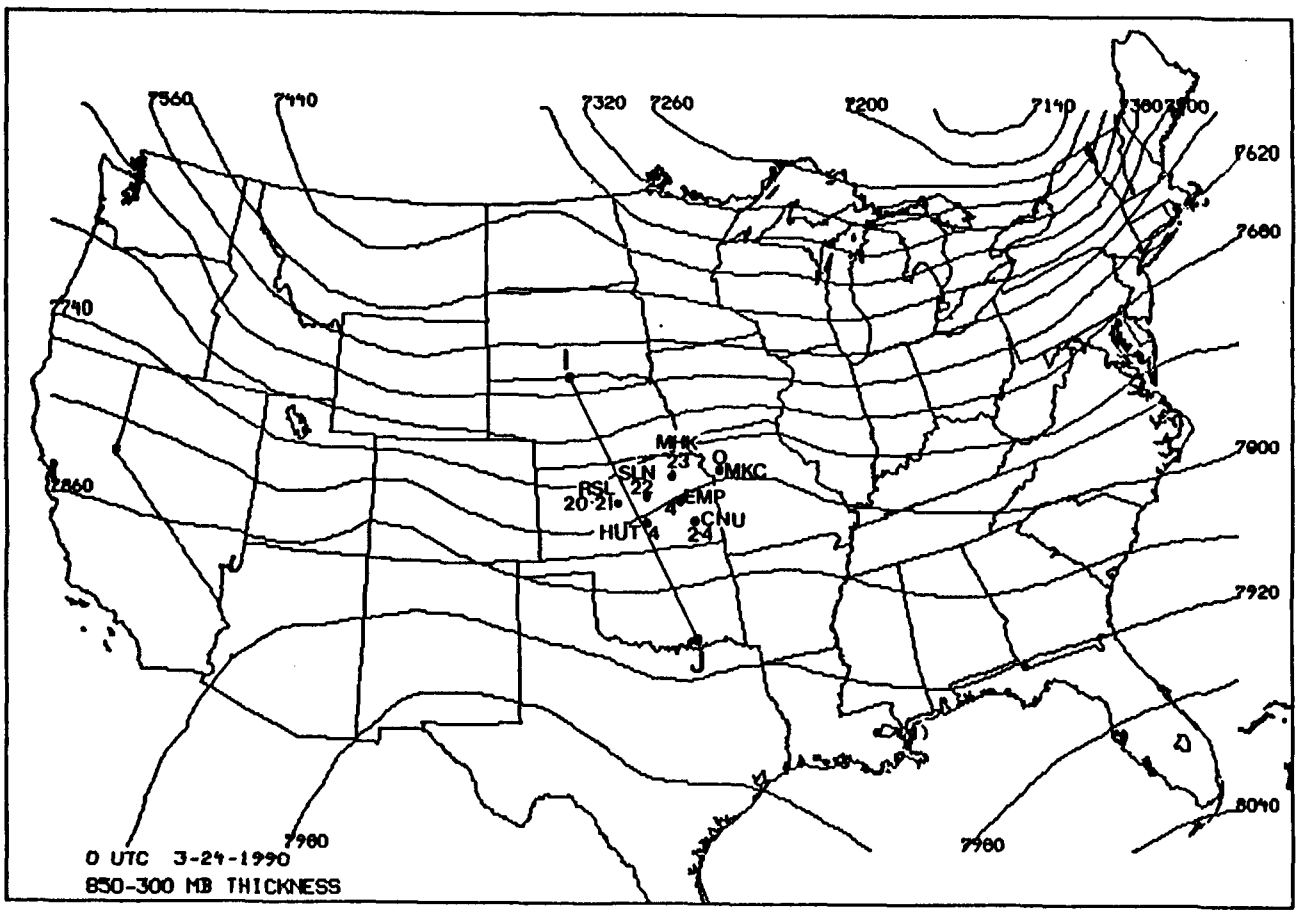

Fig. 27 Same as Fig. 10, except for 0000 UTC 24 March 1990.

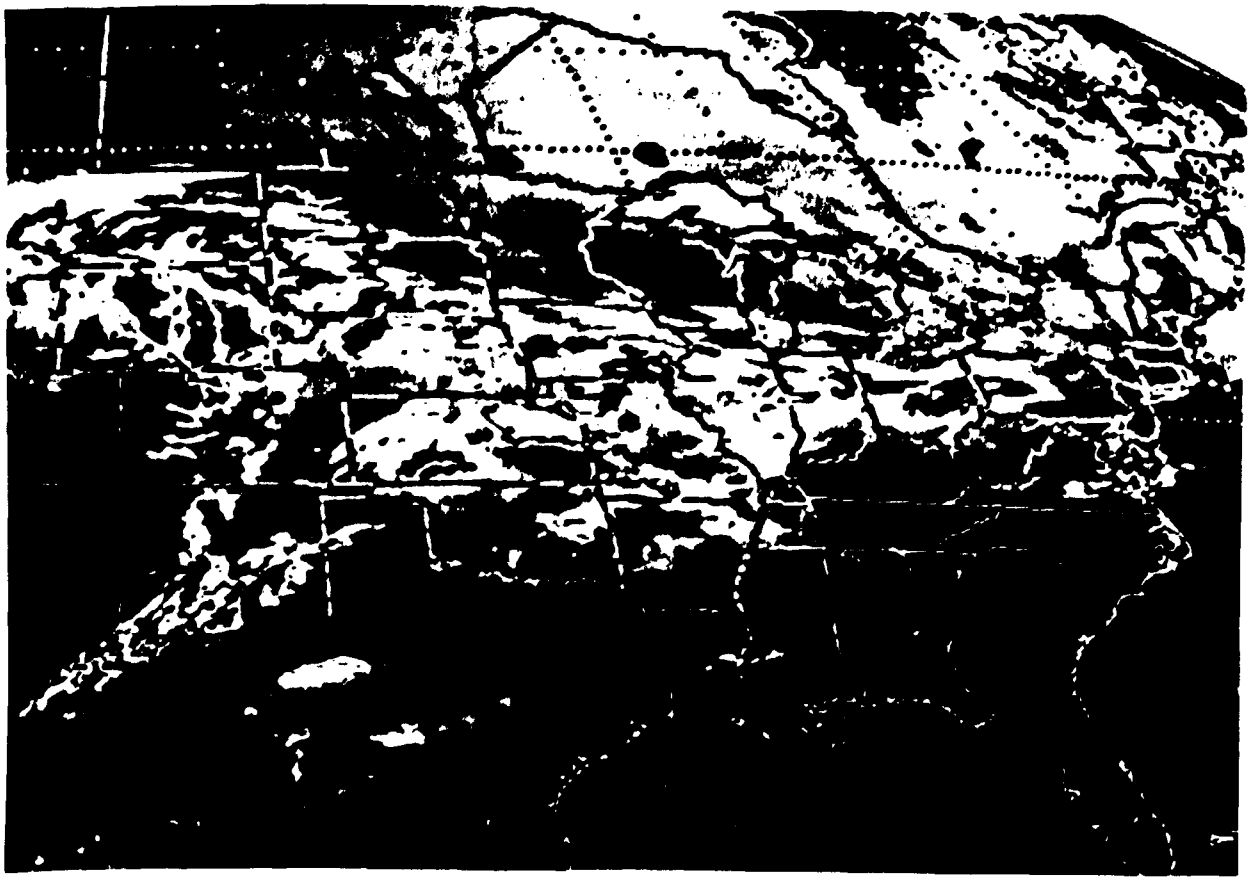

Fig. 28a Satellite imagery using the MB enhancement curve for 2201 UTC 23 March 1990.

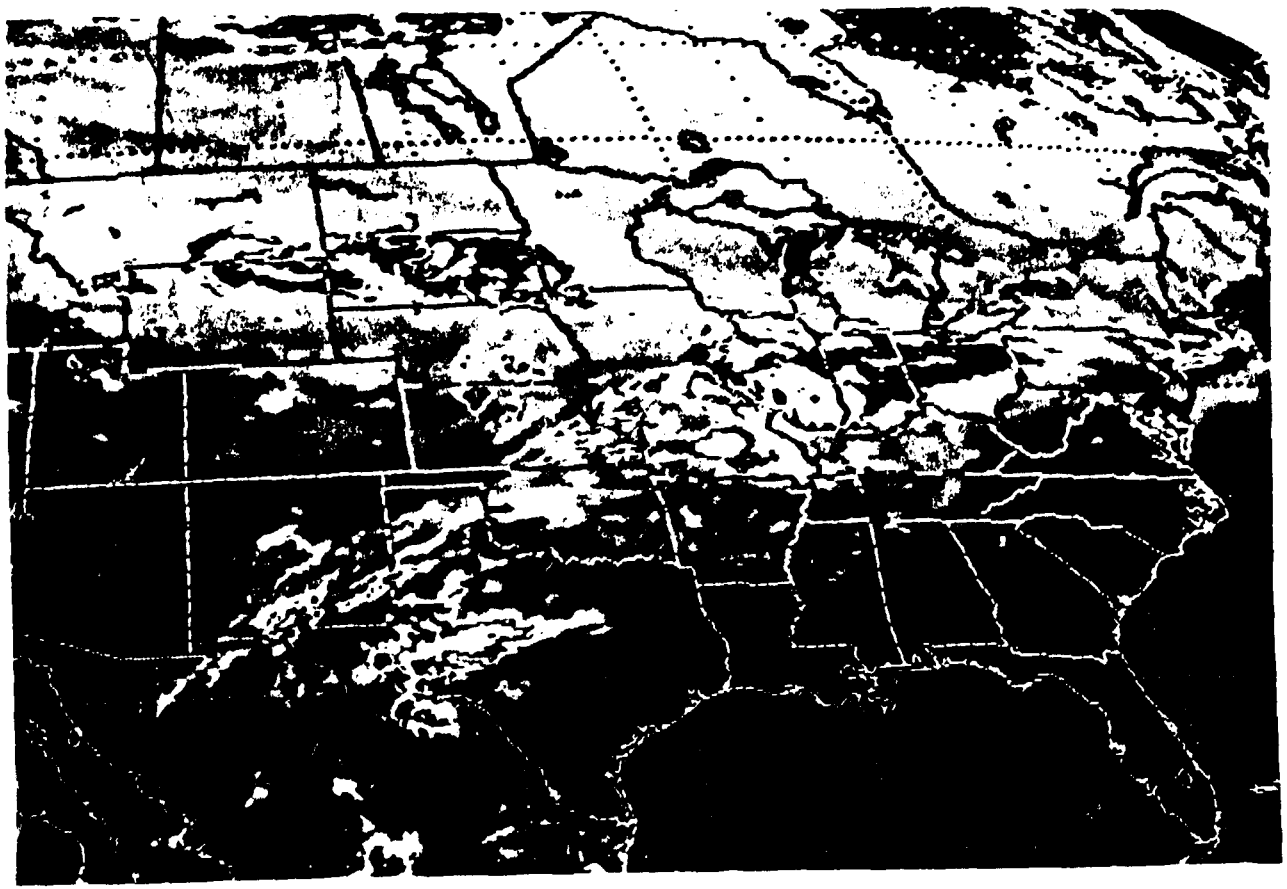

Fig. 28b Same as Fig. 19a, except for 0401 UTC 24 March 1990.

4.3.2 Vertical Motion

At 850 mb on 0000 UTC 24 March 1990 there was weak UVM over eastern Kansas with kinematic omega values near -1 microbars/s (not shown). At the 700 mb level the UVM increased over the area of interest and there was a center of UVM over eastern Kansas. As shown in Fig. 29, the values of omega ranged from -3 to -4 microbars/s over the area where thunder and frozen precipitation was reported. There was also UVM at 500 mb with kinematic omega values of -3 to -4 microbars/s over the area of interest (not shown). Several stations within this area of UVM reported thunder and frozen precipitation between 2000 UTC 23 March 1990 and 0400 UTC 24 March 1990, as shown in Fig. 27.

4.3.3 Vertical Wind Shear and Absolute Momentum

At 0000 UTC 24 March 1990 the upper level flow was primarily zonal but the vertical wind shear was strong over Kansas and western Missouri with vertical wind shear values ranging from a maximum of 7.3 m s^{-1} km^{-1} to a minimum of 5.5 m s^{-1} km^{-1}. The strong vertical wind shear is associated with a decrease in the slope of the M surfaces which increases the likelihood that the theta-e surfaces

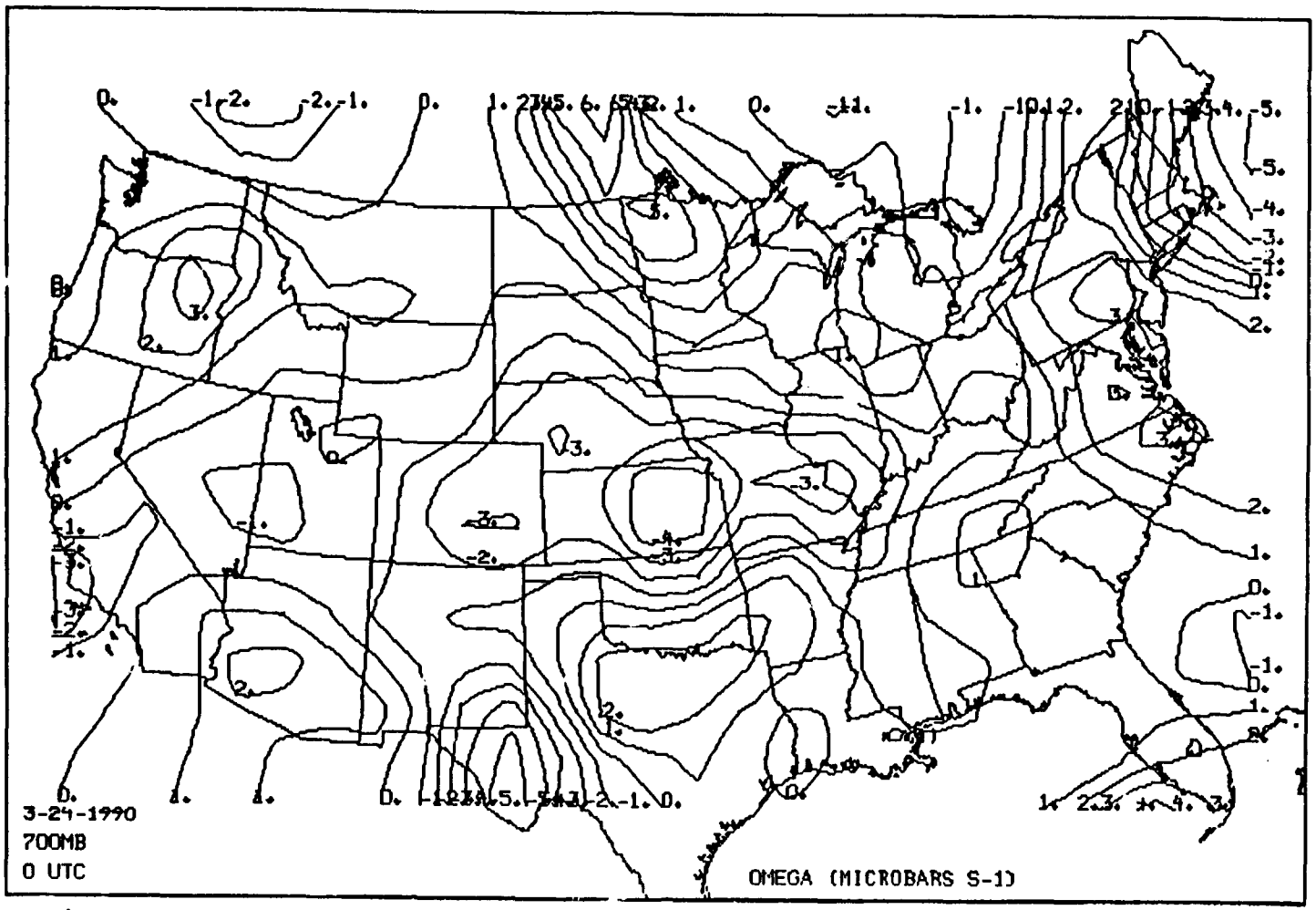

Fig. 29 Same as Fig. 6, except at 700 mb for 0000 UTC 24 March 1990.

will have a greater slope than the M surfaces which would create CSI and make the area susceptible to slantwise convection.

4.3.4 Conditional Symmetric Instability and Equivalent Potential Vorticity

To access the role of CSI, a set of vertical cross sections normal to the 850-300 mb thickness were prepared. For this case the cross section line is labeled I-J and is shown in Fig. 27. Cross section I-J begins at the South Dakota, Nebraska border, passes near Hutchinson, KS (HUT), then through the Oklahoma City, OK (OKC) area and ends near the Oklahoma, Texas border. Also shown in Fig. 27 are the location and three letter identifier for stations reporting thunder and frozen precipitation. These stations are: Russell, KS (RSL), Salina, KS (SLN), Hutchinson, KS (HUT), Manhattan, KS (MHK), Emporia, KS (EMP), Chanute, KS (CNU), and Kansas City, MO (MKC).

An analysis of the 1200 UTC 23 March 1990 850 mb theta-e advection pattern (Fig. 30) shows that the thunder and frozen precipitation occurred north of a theta-e advection ridge in an area of strong 850 mb positive theta-e advection. As described in

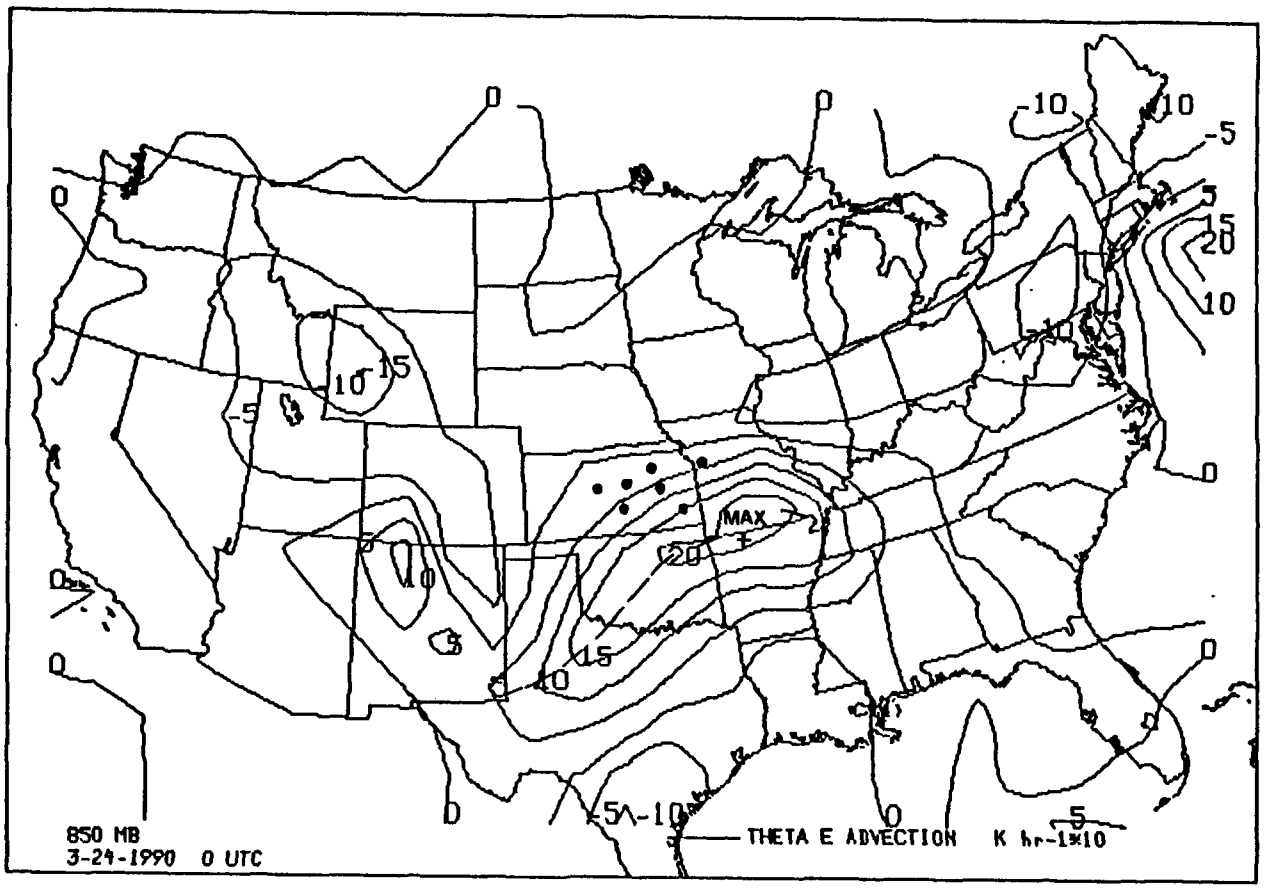

Fig. 30 Same as Fig. 12, except for 0000 UTC 24 March 1990.

Scofield and Robinson (1990) this is a tool used to forecast heavy snow.

Figure 31 shows the vertical cross section of M and theta-e along line I-J. Analysis of Fig. 31 shows that the atmosphere has strong convective stability below 750 mb and above 250 mb but there is weak convective stability with a few areas of convective instability between these layers. There are two regions of CSI shown by the shaded areas in Fig. 31. Figure 32 is a cross section of EPV, as described in (12), along line I-J. There are two areas of CSI depicted in Fig. 32 as shaded areas. The area of CSI near the 650 mb level was over the part of Kansas where convection did occur. This was verified by reports of thundersnow at five locations and thunder and frozen precipitation (freezing rain or ice pellets) at four locations in Kansas. In this case CSI was present and convection did occur indicating the possible occurrence of slantwise convection.

4.4 Case 4: 27-28 December 1990

4.4.1 Synoptic Overview

At 0000 UTC 28 December 1990, a low amplitude long wave trough was in place over the northern

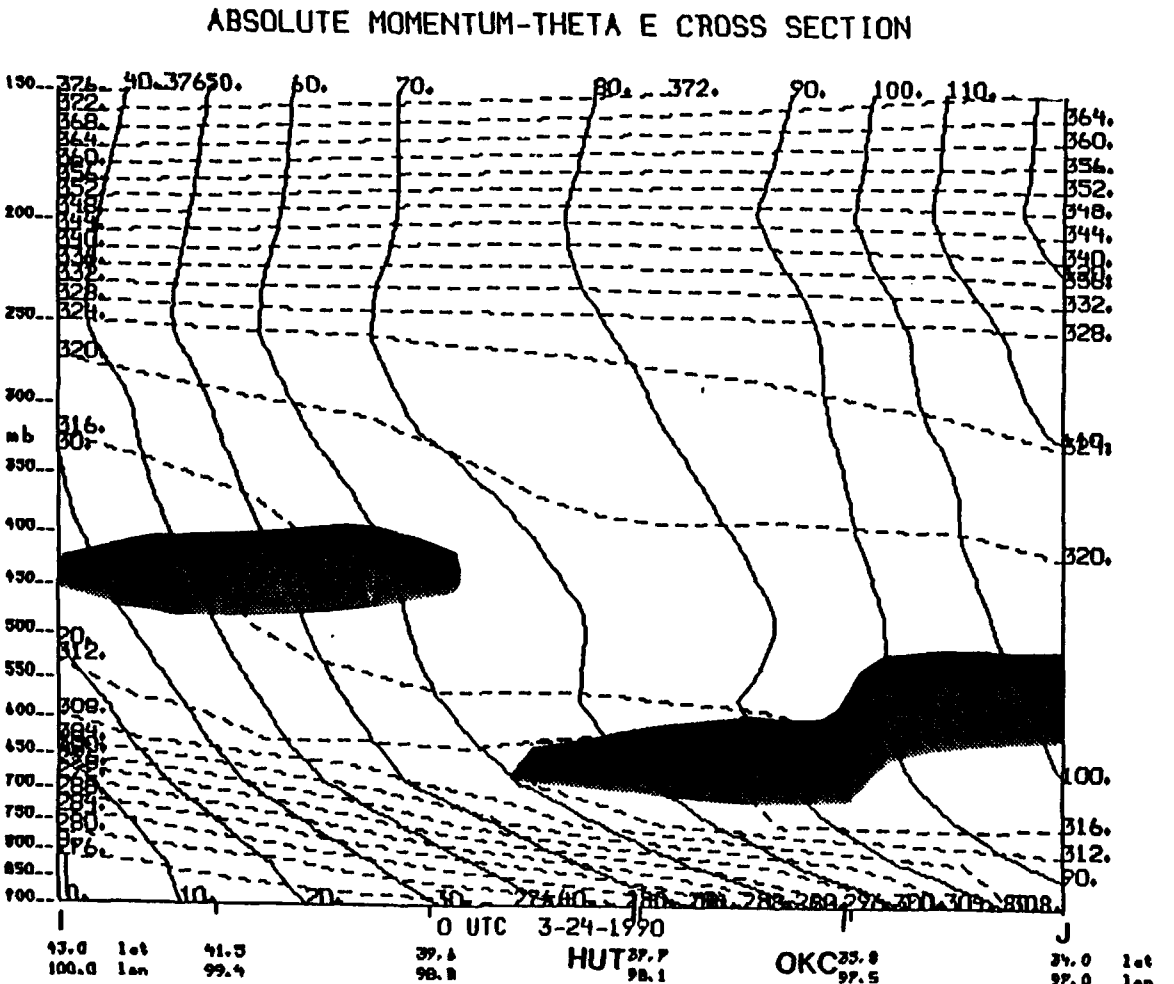

Fig. 31 Same as Fig. 11, except along line I-J for 0000 UTC 24 March 1990.

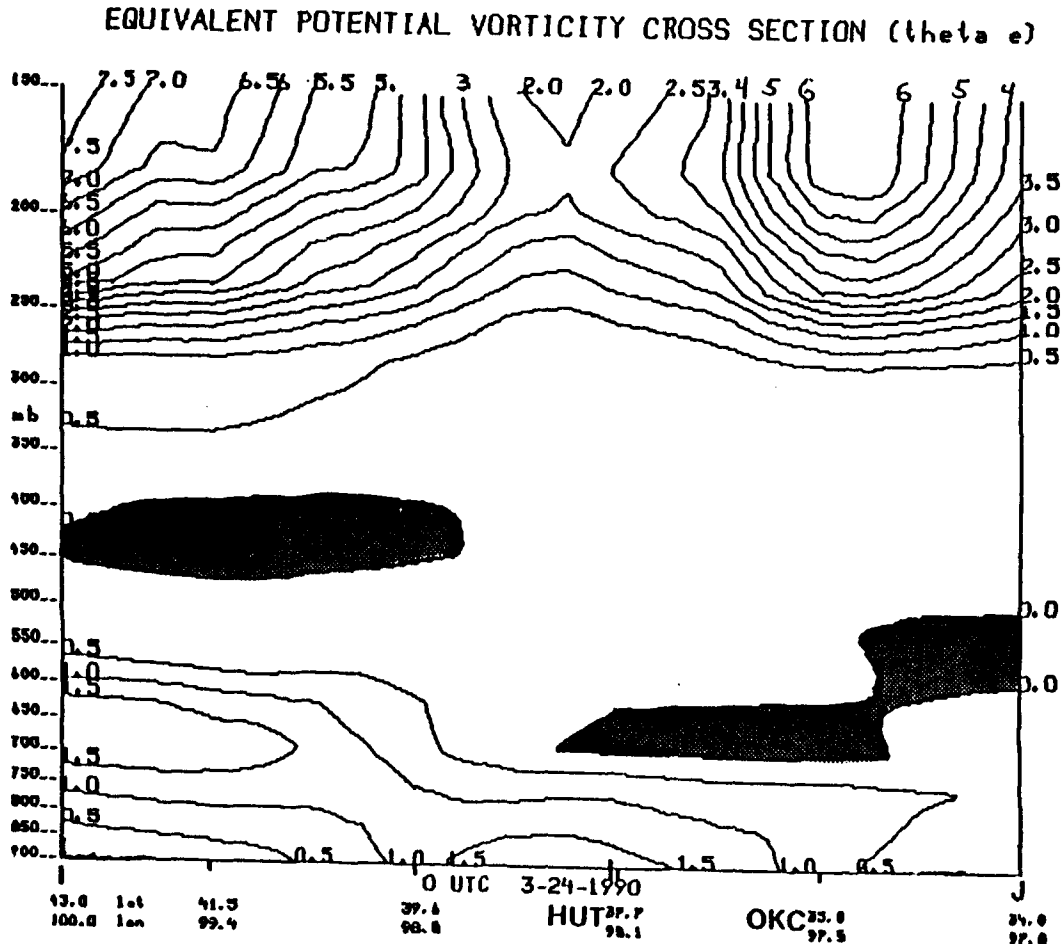

Fig. 32 Same as Fig. 13, except along line I-J for 0000 UTC 24 March 1990.

Rockies and it extended into the mid-Mississippi Valley and up over the western Great Lakes as shown in Fig. 33. At the surface there was an area of high pressure centered over northern Maine that ridged southward along the east coast. An inverted trough had developed over the previous 12 hour period and by 0000 UTC 28 December 1990 it reached from western Maryland to western Tennessee as shown in Fig. 34. During the period from 1200 UTC 27 December 1990 to 1200 UTC 28 December 1990 precipitation fell over much of the country east of the Mississippi River. The precipitation was in the form of rain from Virginia and Kentucky southward with snow to the north. Snow accumulated up to six inches from central Missouri to Ohio and over much of Pennsylvania (see Fig. 35a and Fig. 35b). No thunder and frozen precipitation was reported.

4.4.2 Vertical Motion

At 850 mb on 0000 UTC 28 December 1990 the kinematic omega values over the areas where the heaviest snowfall occurred showed weak UVM and even DVM over Pennsylvania and Illinois (Fig. 36). The 700 mb omega field (Fig. 37) shows UVM over much of the area where the heaviest snowfall occurred but it was relatively weak. In comparison to the

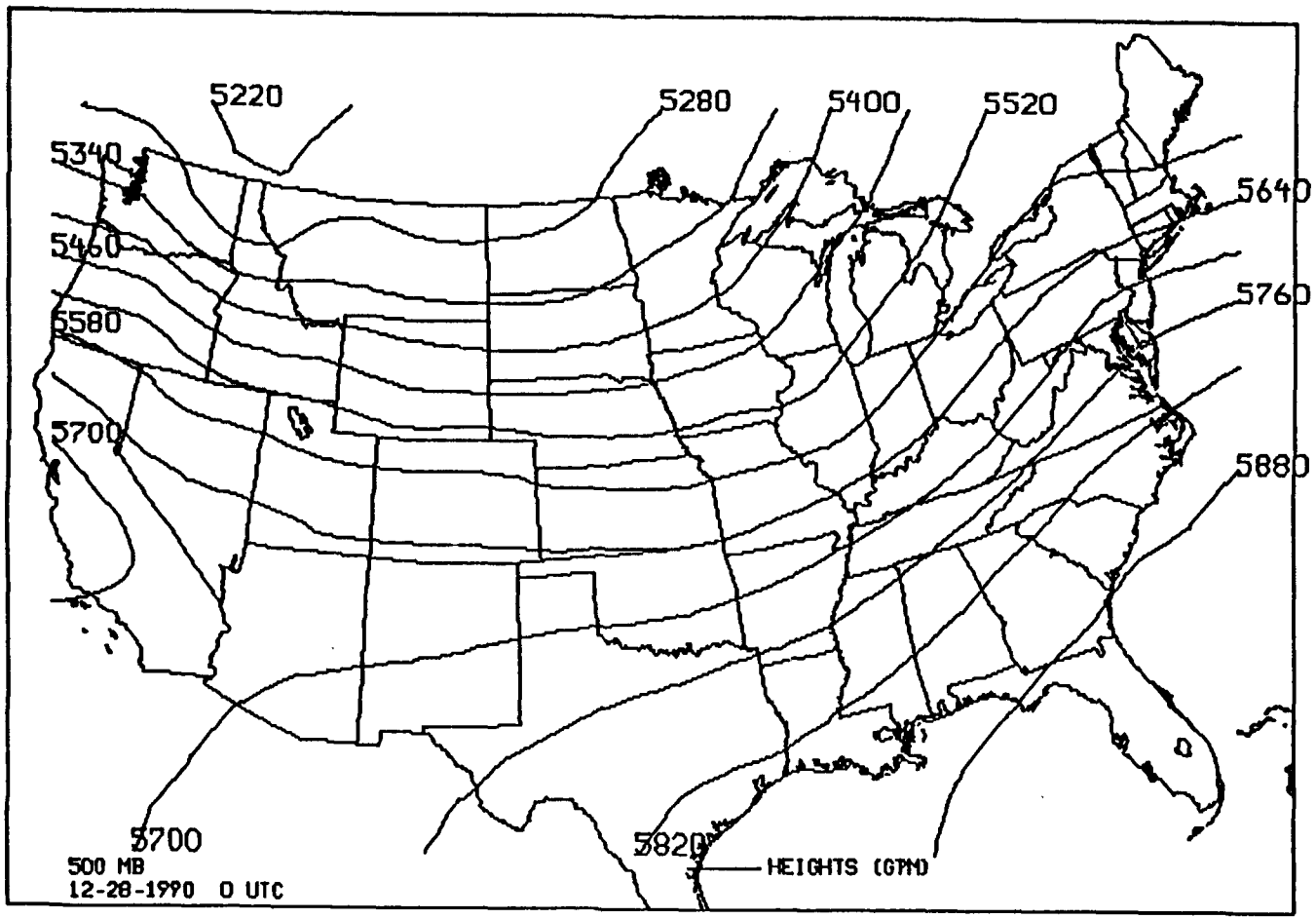

Fig. 33 Same as Fig. 2a, except for 0000 UTC 28 December 1990.

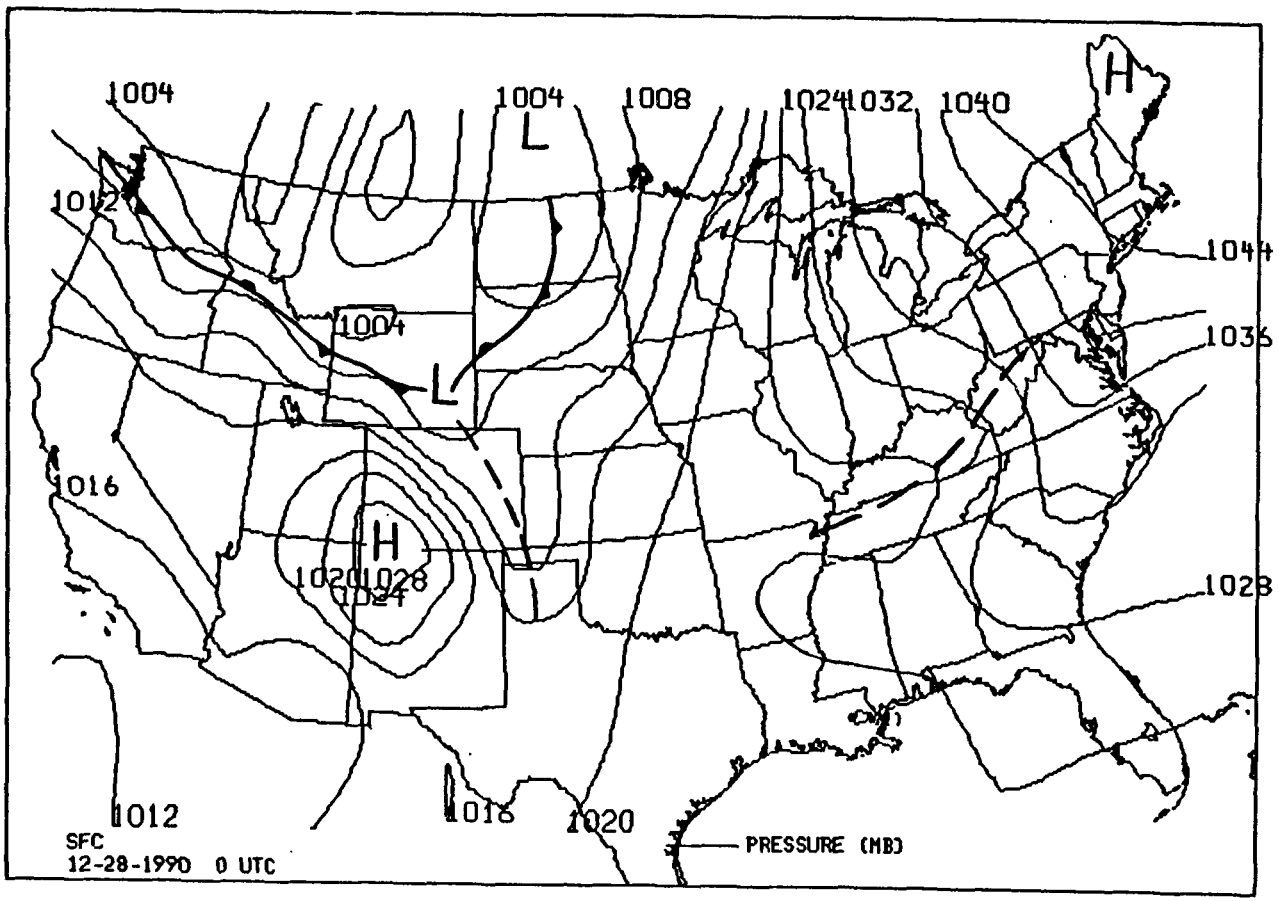

Fig. 34 Same as Fig. 3, except for 0000 UTC 28 December 1990.

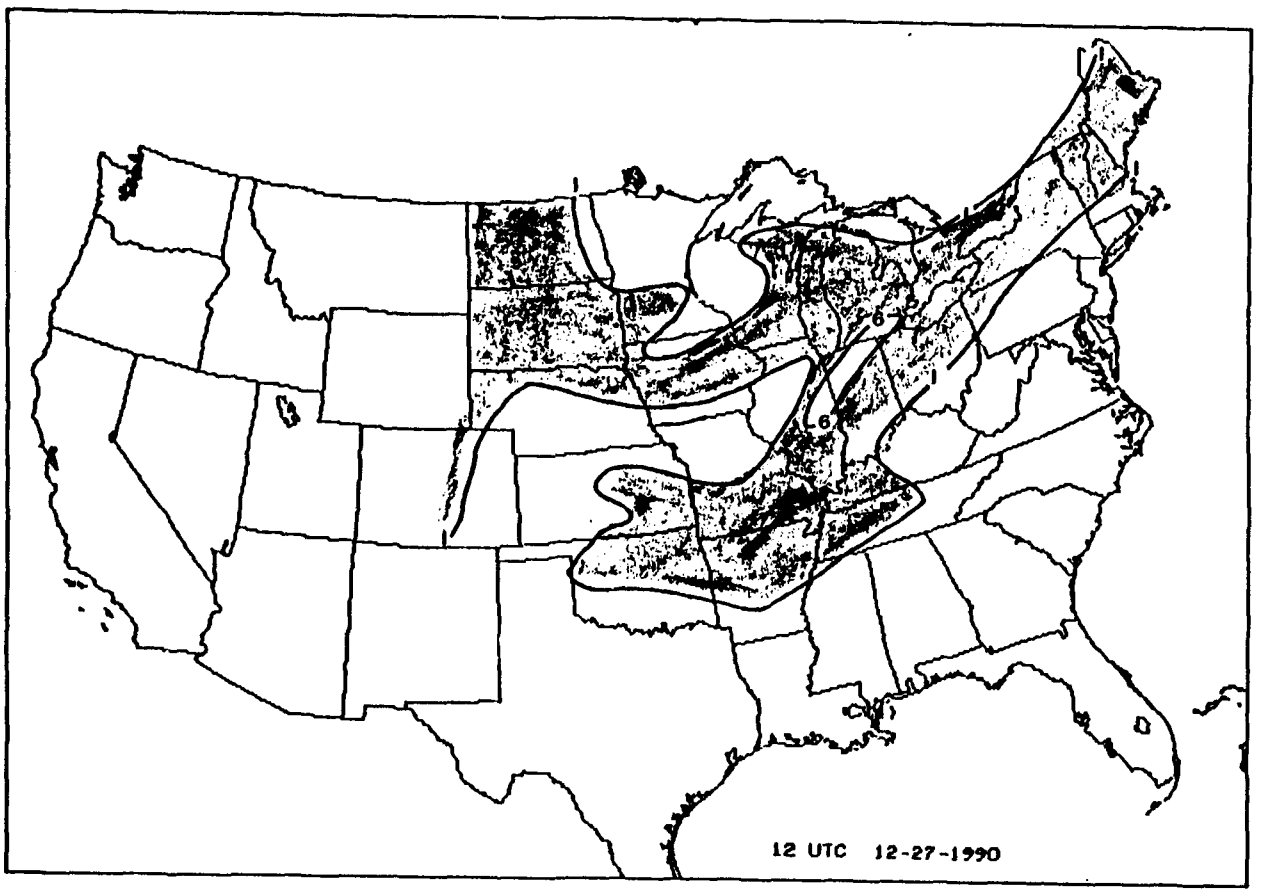

Fig. 35a Snowcover (inches) east of the Rocky Mountains for 1200 UTC 27 December 1990. Areas with 1 to < 6 inches are shown as shaded regions. Areas with > 6 inches are shown as white regions within the shaded areas.

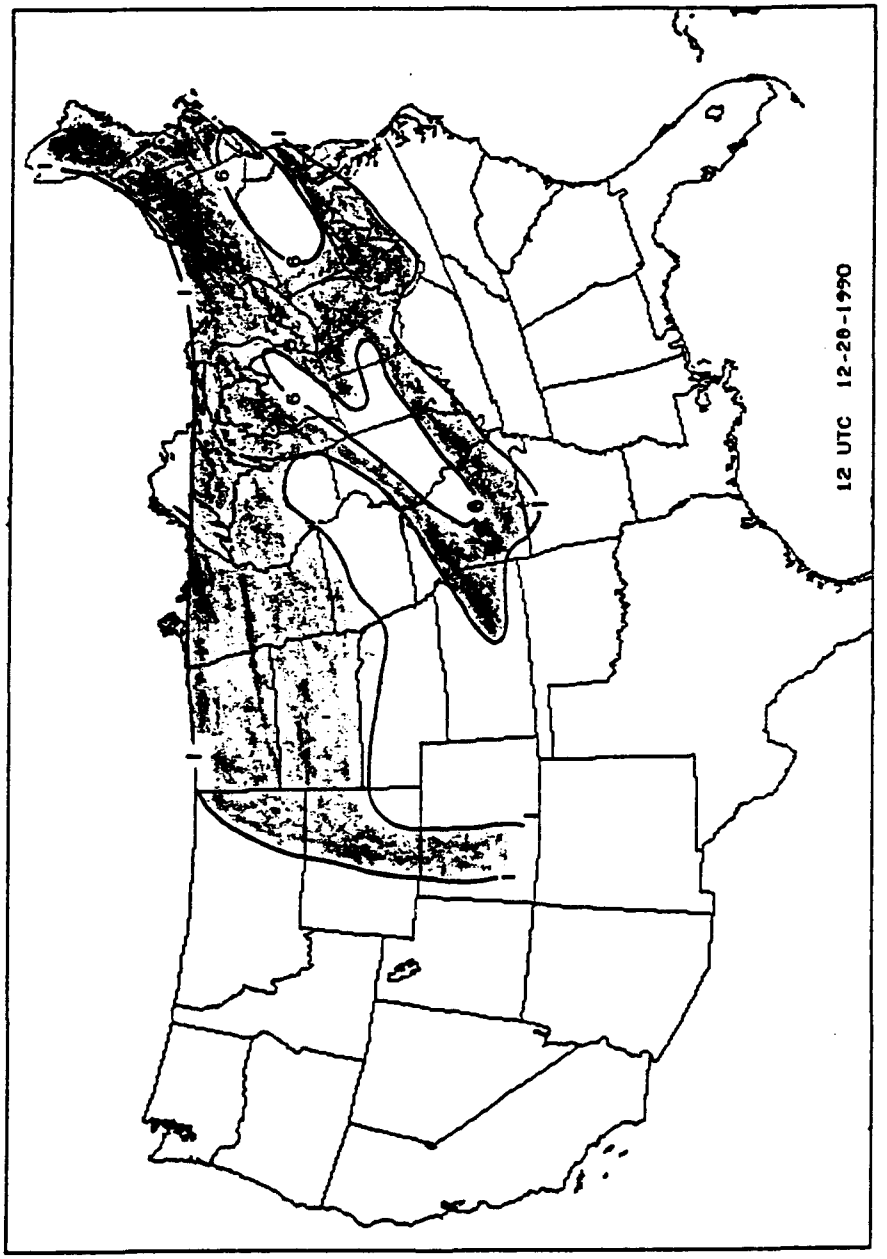

Fig. 35b Same as Fig. 35a, except for 1200 UTC 28 December 1990.

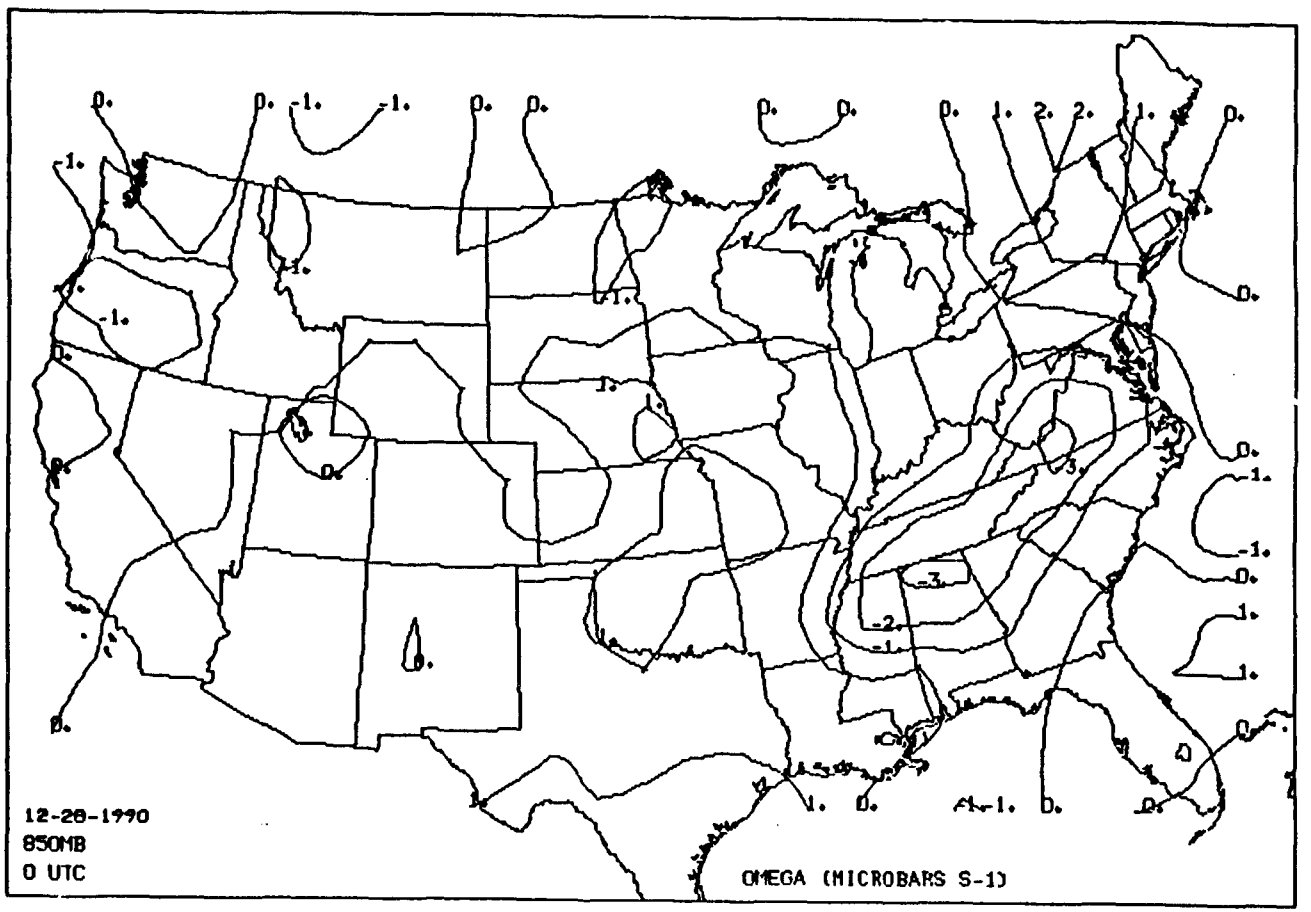

Fig. 36 Same as Fig. 6, except for 0000 UTC 28 December 1990.

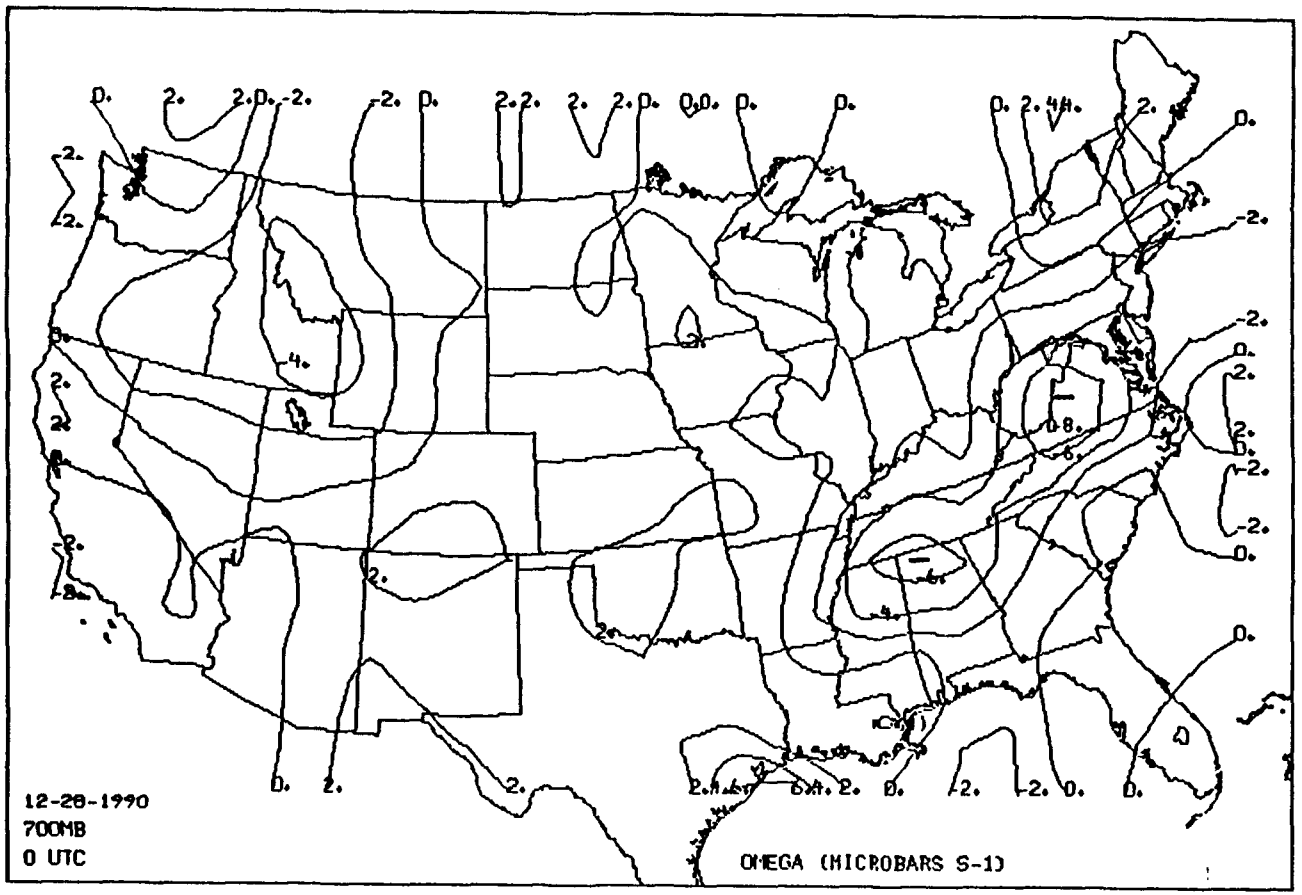

Fig. 37 Same as Fig. 36, except at 700 mb.

kinematic omega fields for the cases where there was thunder and frozen precipitation, the UVM motion field for this case was weaker.

4.4.3 Vertical Wind Shear and Absolute Momentum

At 0000 UTC 28 December 1990, the vertical wind shear values calculated from rawinsonde data were less than 5 m s^{-1} km^{-1} over the area where snow accumulation was the heaviest. In those cases where thunder and frozen precipitation was reported, the vertical wind shear values were values greater than 5.5 m s^{-1} km^{-1} (and in one case they were greater than 8 m s^{-1} km^{-1}) over the area of thundersnow and heaviest snow accumulation. This is in contrast to the present case where the vertical wind shear values for the area of heaviest snowfall were less than 5 m s^{-1} km^{-1}.

4.4.4 Conditional Symmetric Instability and Equivalent Potential Vorticity

To access the role of CSI, a set of vertical cross sections normal to the 850-300 mb thickness were prepared. Figure 38 shows the 850-300 mb thickness pattern for 0000 UTC 28 December 1990 and the two cross sections used in this case labeled K-L and M-N. Cross section K-L begins at the Illinois,

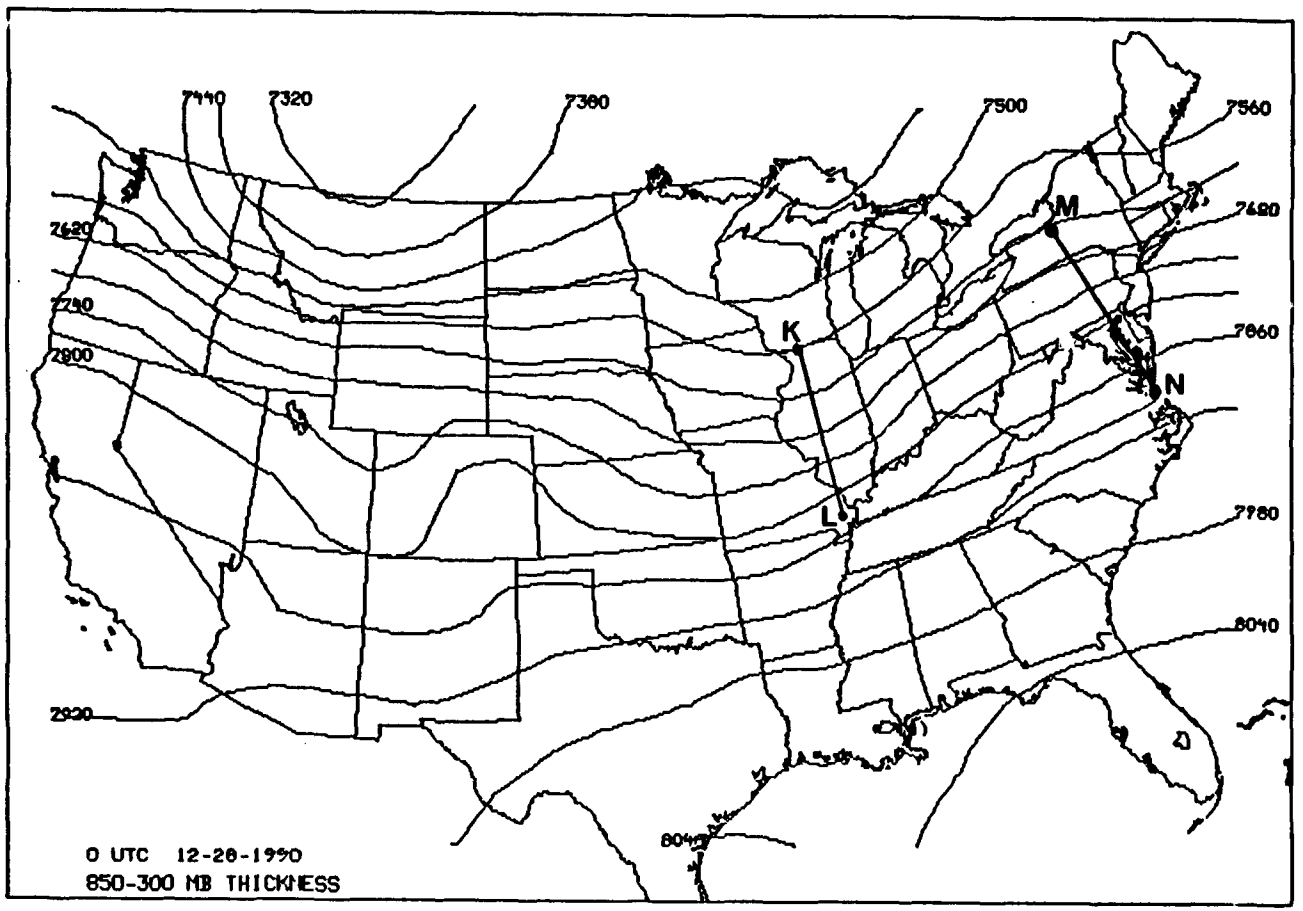

Fig. 38 Same as Fig. 10, except for 0000 UTC 28 December 1990.

Wisconsin borders and extends south passing near Peoria, IL (PIA), St. Louis, MO (STL) and ends near Cape Girardeau, MO (CGI). Cross section M-N begins near the southern shore of Lake Ontario and extends south passing near Elmira, NY (ELM), Harrisburg, PA (HAR), Baltimore, MD (BWI) and ends at Norfolk, VA (ORF).

An analysis of the 850 mb theta-e advection pattern (Fig. 39) shows that there was a moderately strong positive theta-e advection gradient over Pennsylvania and the heavier snow did occur north of the positive theta-e advection ridge axis. Further west over Illinois, Indiana, and Ohio where there was also areas of heavy snow the gradient of theta-e was weak and there was not a strong positive theta-e advection ridge. Although there was positive 850 mb theta-e advection over Pennsylvania it was not strong enough to create any areas of CSI. This is shown in Fig. 40 which is a vertical cross section of theta-e and M along line M-N. The only area of CSI is very small and located near the 350 mb level and would not have been created by 850 mb positive theta-e advection. Figure 41 is a vertical cross section of EPV along line M-N and clearly shows no CSI below the 350 mb level as EPV > 0 throughout the cross section except for the small area near 350 mb. As for the cross section line K-L a pattern of

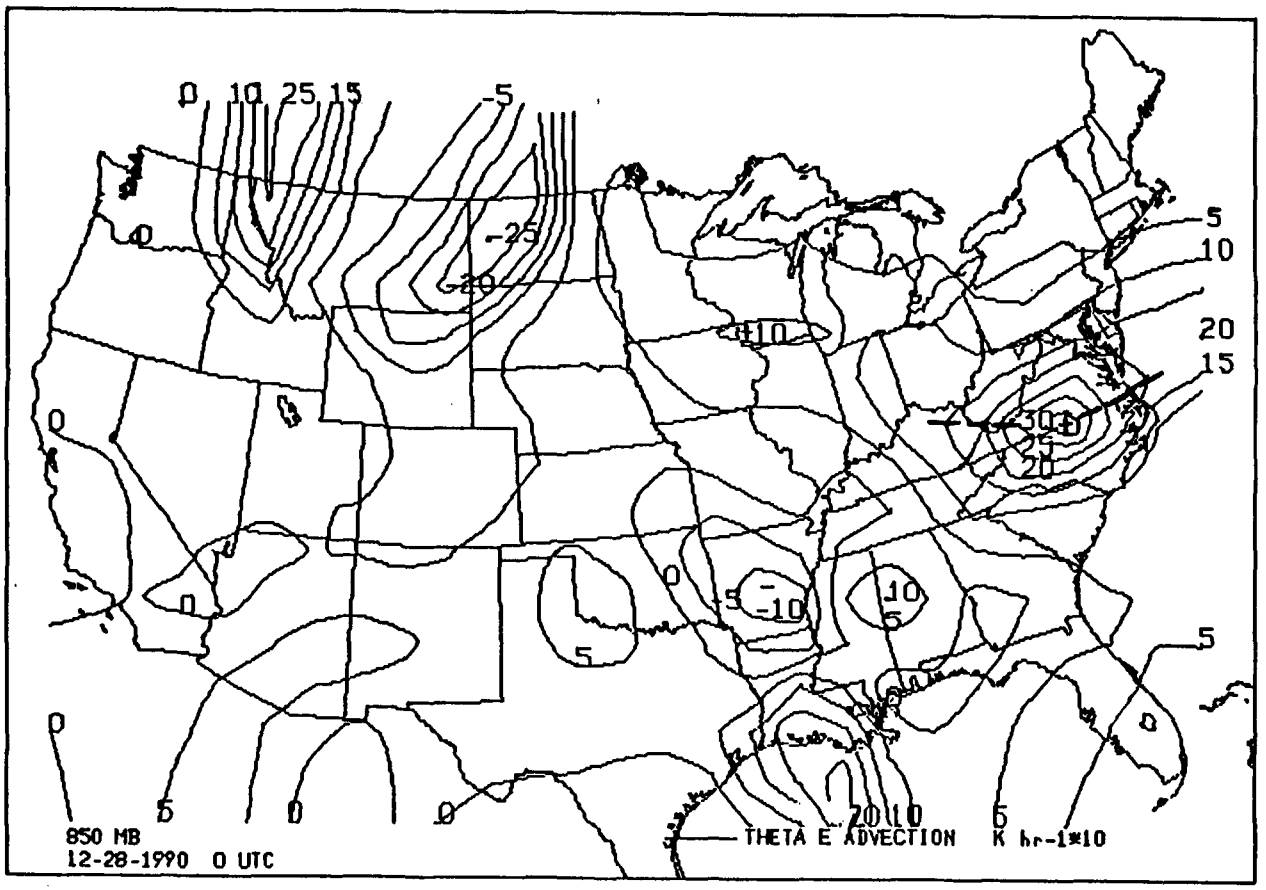

Fig. 39 Same as Fig. 12, except for 0000 UTC 28 December 1990.

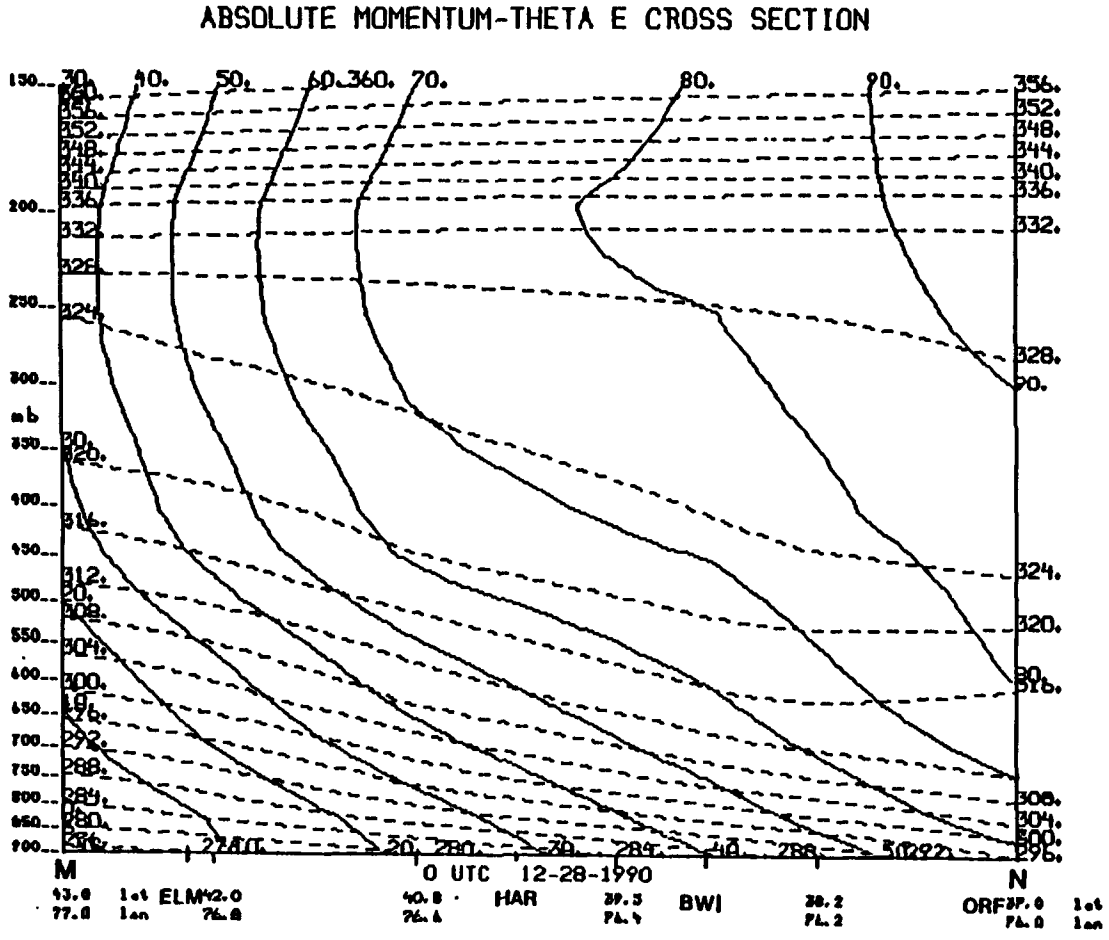

Fig. 40 Same as Fig. 11, except along line M-N for 0000 UTC 28 December 1990.

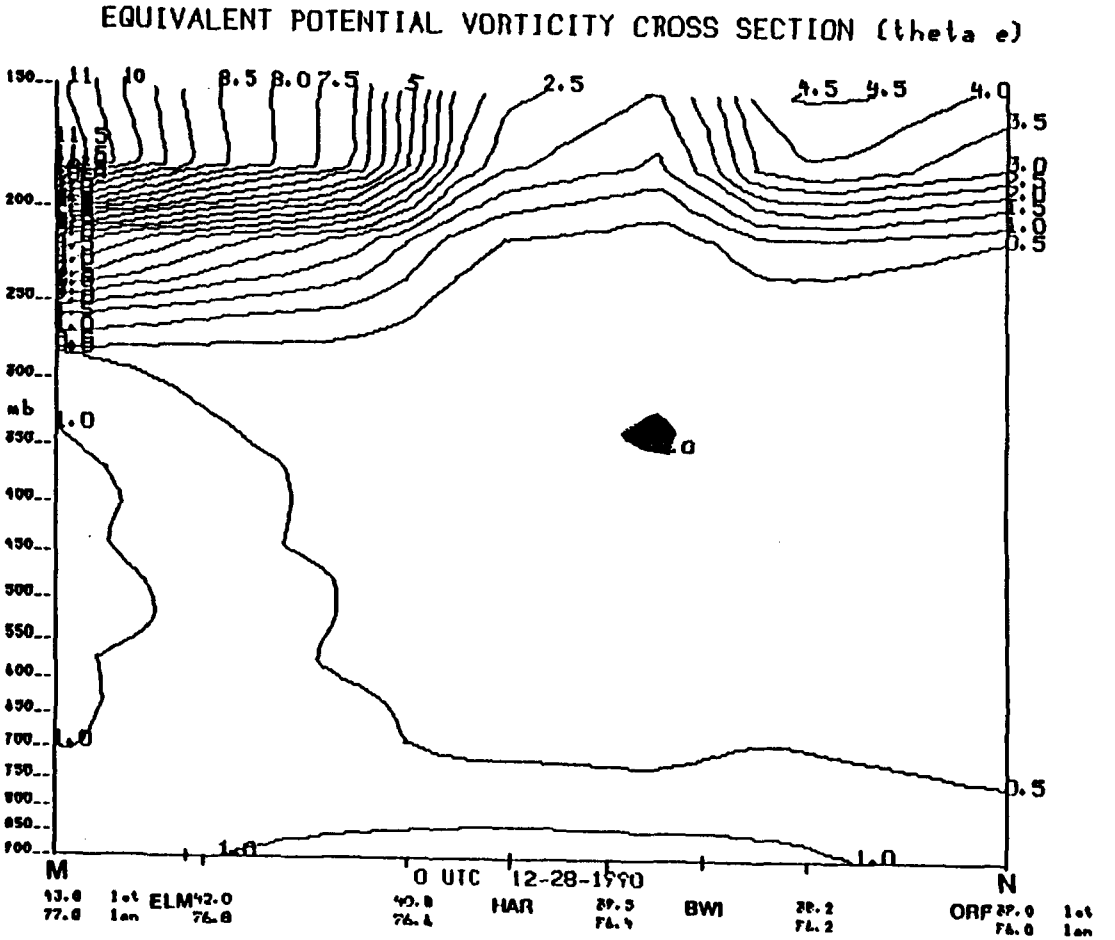

Fig. 41 Same as Fig. 13, except along line M-N for 0000 UTC 28 December 1990.

convective stability is shown in Fig. 42 as theta-e is increasing with height throughout the cross section. There were also no areas of CSI along this cross section as shown by the positive values for EPV in Fig. 43.

A significant amount of snow was produced over several areas in this case but amounts could have been much greater if the snowfall was enhanced by slantwise convection. Slantwise convection did not occur and the analysis shows that the atmosphere was not susceptible to this as there were no significant areas of CSI along either cross section. There was strong positive 850 mb theta-e advection over Pennsylvania but not strong enough to create CSI. Upward vertical motion was weak or nonexistent over both areas and the values of vertical wind shear were low. All of these factors contributed to creating conditions that did not allow CSI to develop and therefore there was also no slantwise convection in this case.

Another case where there was snow but no thunder, occurred at 1200 UTC 4 December 1990. Snow fell from eastern Illinois to Pittsburgh, PA. An analysis of the storm similar to what was done in the previous case showed weak UVM, vertical wind shear values < 5 m s^{-1} km^{-1} and no CSI associated with this storm. These conditions are very similar

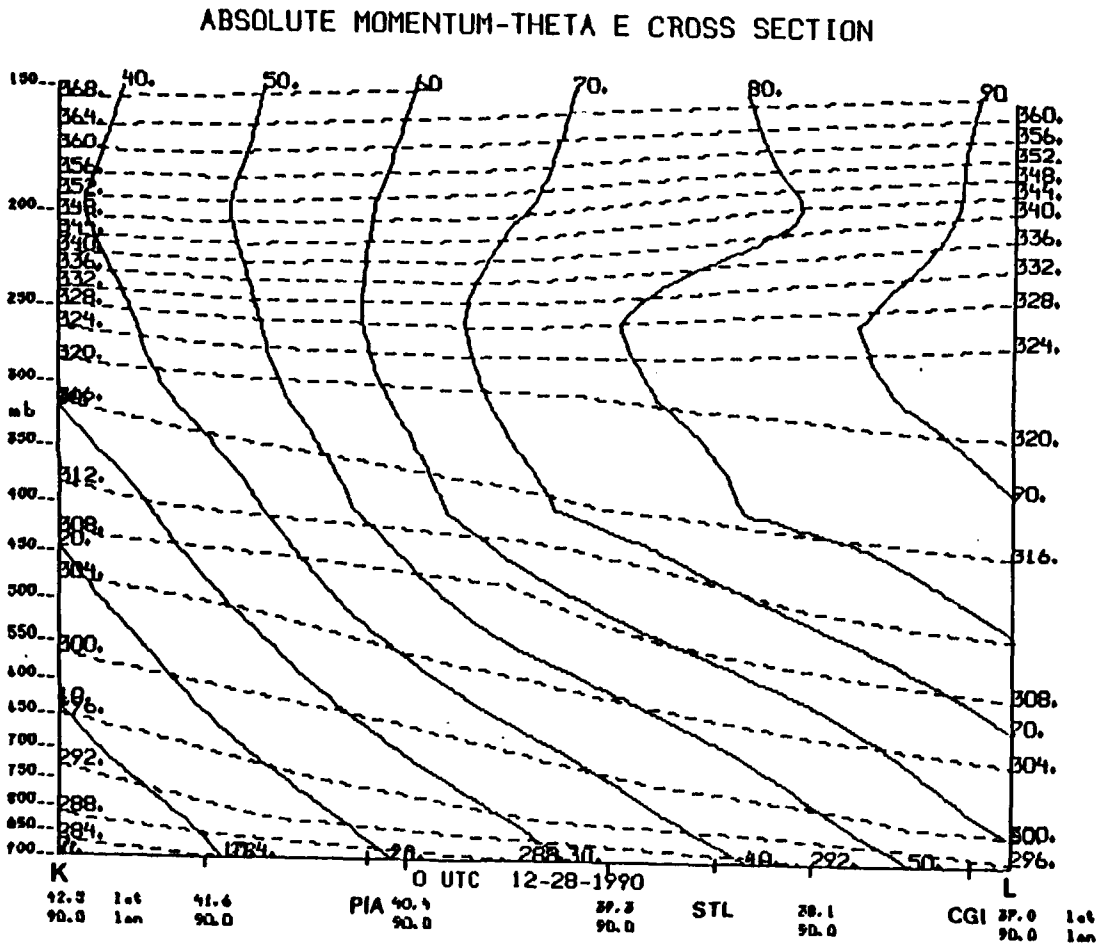

Fig. 42 Same as Fig. 40, except along line K-L.

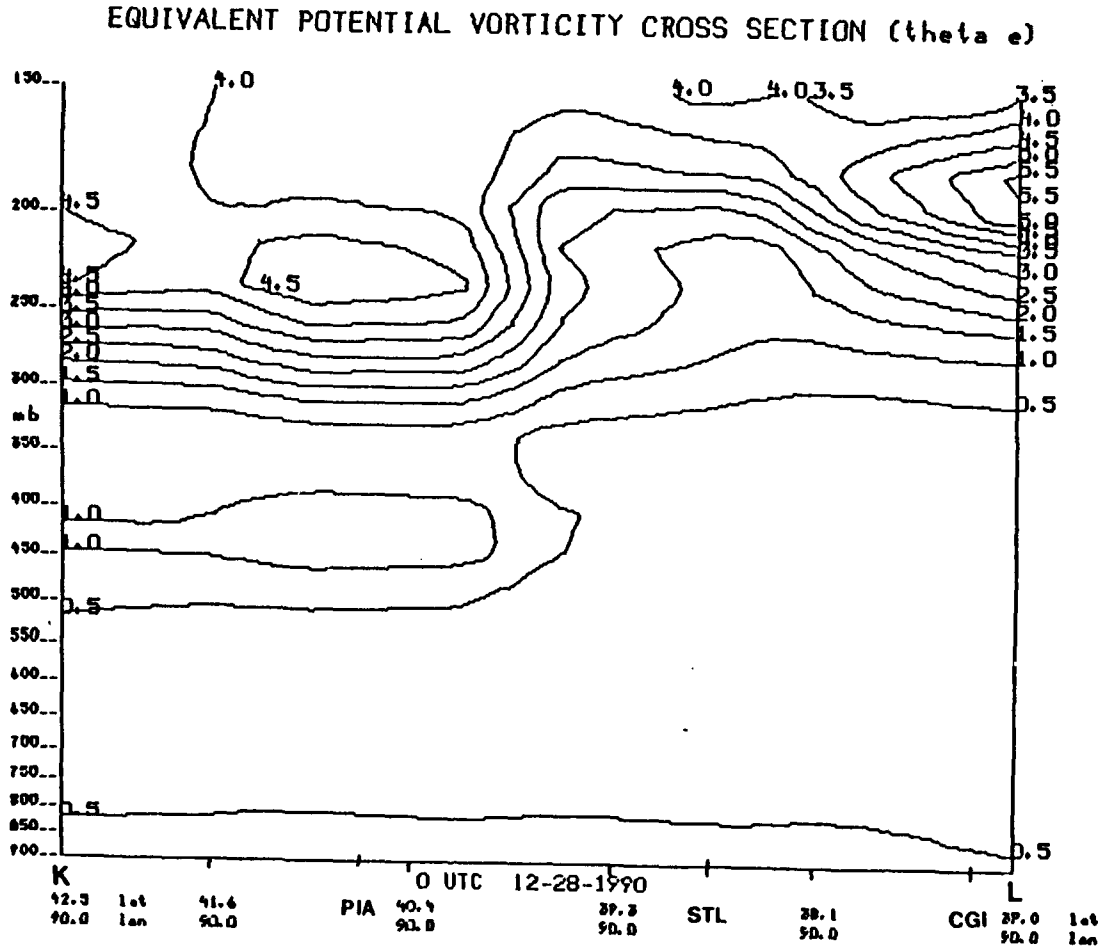

Fig. 43 Same as Fig. 41, except along line K-L.

to the previous case where there was snow but no convection (thunder was not reported).

5. SUMMARY AND CONCLUSIONS

5.1 Research Summary

The findings of this investigation support the hypothesis of this research thesis, as stated in section 1.2. The summary of the findings is as follows:

A study of four winter type ETCs that produced frozen precipitation was presented in this research thesis. Several other cases were investigated to increase the size of the data base but were not included for detailed analysis in this thesis. Surface and upper air data was used to analyze the atmosphere's vertical temperature, humidity, and wind field structure to identify if CSI was present. In all cases where there was slantwise convection, verified by reports of thunder and frozen precipitation, there were also areas of CSI. One objective of this research was to show that this relationship existed. The presence of CSI and slantwise convection over the same area shows that for the cases studied in this thesis CSI could be used to identify when and where slantwise convection was likely to occur. One case studied had no areas of CSI and no slantwise convection although there was snow. This case also supports the hypothesis

that CSI can be used to identify when and where slantwise convection is or is not likely to occur.

This research also helped to identify precursors that could be used to forecast when and where CSI, slantwise convection, and the associated thunder and heavy frozen precipitation will occur. A correlation was found between vertical motion, vertical wind shear, the theta-e field, and areas of CSI and slantwise convection. This study indicates that CSI and slantwise convection, in winter type ETCs, tends to develop in regions where there is:

- moderate to strong upward vertical motion (700 mb kinematic omegas < -2 microbars s^{-1})
- strong vertical wind shear (values > 5 m s^{-1} km^{-1})
- strong positive theta-e advection or a strong positive theta-e advection gradient at 850 mb
- decreases or even small increases in theta-e with height

There are several limitations to the results of this thesis. The poor spatial and temporal resolution of the upper air data resulted in using synoptic scale data to identify areas of CSI and slantwise convection which are mesoscale processes. Another problem was the limited number of cases. Although the cases studied indicate a direct relationship between the existence of CSI in an area

and the occurrence of slantwise convection the number of cases was far too small to allow sweeping generalizations about whether this relationship exists in all or even most cases of slantwise convection.

5.2 Future Research Recommendations

Further research is needed to increase the size of the case study data base to establish whether the relationship between CSI and slantwise convection exists in a statistically significant number of cases. Also, using data with better spatial and temporal resolution from such sources as Doppler radar and wind profilers as it becomes available will improve our ability to study mesoscale phenomena such as CSI and slantwise convection. The use of mesoscale models to diagnose the structure of the atmosphere and provide a prognosis for the mesoscale structure of the atmosphere will improve the ability to forecast areas of CSI, slantwise convection, and the resulting heavy frozen precipitation.

BIBLIOGRAPHY

Barnes, S. L., 1973: Mesoscale Objective Map Analysis Using Weighted Time-Series Observations. NOAA Tech. Memo. ERL NSSL-62, 1-9.

Beckman, S. K., 1987: Use of Enhanced IR/Visible Satellite Imagery to Determine Heavy Snow Areas. Mon. Wea. Rev., 115, 2060-2087.

Belt, C. L., and H. L. Fuelberg, 1982: The Effects of Random Errors in Rawinsonde Data on Derived Kinematic Quantities. Mon. Wea. Rev., 110, 91-101.

Bennetts, D. A., and B. J. Hoskins, 1979: Conditional Symmetric Instability - A Possible Explanation for Frontal Rainbands. Quart. J. Roy. Meteor. Soc. 105, 945-962.

Bennetts, D. A., and J. C. Sharp, 1982: The Relevance of Conditional Symmetric Instability to the Prediction of Mesoscale Frontal Rainbands. J. Roy. Meteor. Soc., 108, 595-602.

Bluestein, H., 1986: Fronts and Jet Streaks: A Theoretical Perspective. Mesoscale Meteorology and Forecasting, edited by Peter S. Ray. Amer. Meteor. Soc., MA, Chapter 9, 173-215.

Colman, B. R., 1990: Thunderstorms above Frontal Surfaces in Environments with Positive CAPE. Part I: A Climatology. Mon. Wea. Rev., 118, 1103-1121.

-----, 1990: Thunderstorms above Frontal Surfaces in Environments with Positive CAPE. Part II: Organization and Instability Mechanisms. Mon. Wea. Rev., 118, 1123-1144.

Curran, J. T., and A. D. Pearson, 1971: Proximity Soundings for Thunderstorms with Snow. Preprint: 7th Conference Severe Local Storms, Kansas City, MO., Amer. Meteor. Soc., 118-119.

Daily Weather Maps, National Oceanic and Atmospheric Administration (NOAA), Climate Analysis Center, December, 1987.

Daily Weather Maps, National Oceanic and Atmospheric Administration (NOAA), Climate Analysis Center, March 1989.

Daily Weather Maps, National Oceanic and Atmospheric Administration (NOAA), Climate Analysis Center, March 1990.

Daily Weather Maps, National Oceanic and Atmospheric Administration (NOAA), Climate Analysis Center, December, 1990.

Duquet, R. T., 1964: Data Processing for Isentropic Analysis, USAEC Report TID-21609, Pennsylvania State University, PA, 36 p.

Emanuel, K. A., 1983a: The Lagrangian Parcel Dynamics of Moist Symmetric Instability. J. Atmos. Sci., 40, 2368-2376.

-----, 1983b: On Assessing Local Conditional Symmetric Instability from Atmospheric Soundings. Mon. Wea. Rev., 111, 2016-2033.

-----, 1985: Frontal Circulations in the Presence of Small Moist Symmetric Stability. J. Atmos. Sci., 42, 1062-1071.

-----, 1988: Observational Evidence of Slantwise Convective Adjustment. Mon. Wea. Rev., 116, 1805-1816.

Emanuel, K. A., and M. Fantini, 1987: Baroclinic Instability in an Environment of Small Stability to Slantwise Moist Convection. Part I: Two Dimensional Models. J. Atmos. Sci., 44, 1559-1573.

Gyakum, J. R., 1987: Evolution of a Surprise Snowfall in the United States Midwest. Mon. Wea. Rev., 115, 2322-2345.

Herzegh, P. H., and P. V. Hobbs, 1980: The Mesoscale Clouds and Precipitation in Midlatitude Cyclones. Part II: Warm-Frontal Clouds. J. Atmos. Sci., 37, 597-611.

Holton, J. R., 1979: An Introduction to Dynamic Meteorology (Second Edition), Academic Press, New York, 391 p.

Hoskins, B. J., 1974: The Role of Potential Vorticity in Symmetric Stability and Instability. Quart. J. Roy. Meteor. Soc., 107, 480-482.

Hobbs, P. V., 1978: Organization and Structure of Clouds and Precipitation on the Mesoscale and Microscale in Cyclonic Storms. Rev. of Geophy. and Space Phy., 16, 741-755.

Houze Jr., R. A., S. A. Rutledge, T. J. Matejka, and P. V. Hobbs, 1981: The Mesoscale and Microscale Structure and Organization of Clouds and Precipitation Growth in a Warm-Frontal Rainband. J. Atmos.Sci.,38, 639-649.

Kocin, P. J., L. W. Uccellini, J. W. Zack, and M. L. Kaplan, 1985: A Mesoscale Numerical Forecast of an Intense Convective Snowburst Along the East Coast. Bull. Amer. Meteor. Soc., 66, 1412-1424.

Lilly, D. K., 1986: Instabilities. Mesoscale Meteorology and Forecasting, edited by Peter S. Ray. Amer. Meteor. Soc., Boston, MA., Chapter 11, 261-264.

Lussky, G. R., 1989: Heavy Rain and Flooding in Montana: A Case for Operational Use of Symmetric Instability Diagnosis. Wea. and Fore., 4, 186-201.

Moore, J. T., and P. D. Blakley, 1988: The Role of Frontogenetical Forcing and Conditional Symmetric Instability in the Midwest Snowstorm of 30-31 January 1982. Mon. Wea. Rev., 116, 2155-2171.

Martin, J. E., J. D. Locatelli, and P. V. Hobbs, 1991: Organization and Structure of Clouds and Precipitation on the Mid-Atlantic Coast of the United States. Part V: The Role of an Upper-Level Front in the Generation of a Rainband. Submitted to J. Atmos. Sci., Feb. 1991.

O'Brien, J. J., 1970: Alternative Solutions to the Classical Vertical Velocity Problem. J. Appl. Meteor., 9, 197-203.

Orlanski, I., 1975: A Rational Subdivision of Scales for Atmospheric Processes. Bull. Amer. Met. Soc., 56, 527-530.

Parsons, D. B., and P. V. Hobbs, 1983: The Mesoscale and Microscale Structure and Organization of Clouds and Precipitation in Midlatitude Cyclones. Part XI: Comparisons Between Observational and Theoretical Aspects of Rainbands. J. Atmos. Sci., 40, 2377-2397.

Rueter, G. W., and M. K. Yau, 1990: Observations of Slantwise Convective Instability in Winter Cyclones. Mon. Wea. Rev., 118, 447-458.

Sanders, F., and L. F. Bosart, 1985a: Mesoscale Structure in the Megalopolitan Snowstorm of 11-12 February 1983. Part I: Frontogenetical Forcing and Symmetric Instability. J. Atmos. Sci., 42, 1050-1061.

-----, 1985b: Mesoscale Structure in the Megalopolitan Snowstorm of 11-12 February 1983. Part II: Doppler Radar Study of the New England Snowband. J. Atmos. Sci., 42, 1398-1407.

Sanders, F., 1986: Frontogenesis and Symmetric Stability in a Major New England Snowstorm. Mon. Wea. Rev. 114, 1847-1862.

Scofield, R., and J. Robinson, 1990: Using Instability Bursts and Satellite Imagery to Analyze and NOWCAST Heavy Snow. Satellite Applications Information Note 90/1, NESDIS, Washington, D.C.

Seltzer, M. A., R. E. Passarelli, and K. A. Emanuel, 1985: The Possible Role of Symmetric Instability in the Formation of Precipitation Bands. J. Atmos. Sci., 42, 2207-2219.

Storm Data, December 1987: National Climatic Data Center, NOAA, Asheville, NC, 44 p.

Storm Data, March 1989: National Climatic Data Center, NOAA, Asheville, NC, 46 p.

Storm Data, March 1990: National Climatic Data Center, NOAA, Asheville, NC, 114 p.

Thorpe, A. J., and K. A. Emanuel, 1985: Frontogenesis in the Presence of Small Stability to Slantwise Convection. J. Atmos. Sci., 42, 1809-1824.

Weisman, M. L., and J. B. Klemp, 1986: Characteristics of Isolated Convective Storms. Mesoscale Meteorology and Forecasting, edited by Peter S. Ray. Amer. Meteor. Soc., Boston, MA, Chapter 15, 331-358.

Wolfsberg, D. W., K. A. Emanuel, and R. E. Passarelli, 1986: Band Formation in a New England Winter Storm. Mon. Wea. Rev., 114, 1552-1569.

BIOGRAPHY OF THE AUTHOR

Thomas E. Lambert was born in Baltimore, Maryland on August 5, 1957. He graduated from Mount Hebron High School in 1975. From the fall of 1975 until the spring of 1977 he attended Catonsville Community College and he received an Associate of Arts degree in June 1977. In the fall of 1977 he transferred to the University of Maryland and in December 1980, he received a Bachelor of Science degree in Physical Science with a speciality in meteorology.

He worked for several years in the field of air quality. In 1984 he joined the United States Air Force. He then attended Texas A+M University for six months to receive additional undergraduate meteorology training. He served as a weather of icer forecaster at Langley AFB, VA and then moved to Scott AFB, IL where he was Executive Assistant to the Commander of Air Weather Service at Headquarters Air Weather Service. In the summer of 1990 he received an Air Force assignment to complete a Master of Science degree program at Saint Louis University.